UNIVERSITÄT ZU LÜBECK

From the Institute of Systemic Inflammation Research

of the University of Lübeck

Director: Prof. Dr. Jörg Köhl

B Cell Metabolism in Autoimmunity

Dissertation

for Fulfillment of

Requirements

for the Doctoral Degree

of the University of Lübeck

from the Department of Natural Sciences

Submitted by

Timo Lindemann

from Reinbek, Germany

Lübeck 2023

First referee: Prof. Dr. rer. nat. Rudolf Manz

Second referee: PD Dr. rer. nat. Kathrin Kalies

Date of oral examination: 29.11.2024

Approved for printing: Lübeck, 09.12.2024

Statment of authenticity

I hereby declare that I have written the present thesis independently, without assistance from external parties and without use of other resources than those indicated in the text. Any concepts or quotations applicable to these sources are clearly attributed to them. This dissertation has not been submitted in the same or similar version, not even in part, to any other authority for grading.

Lübeck, January 2023 Timo Lindemann

Acknowledgement

First and foremost, I would like to express my most sincere gratitude to my supervisor Prof. Dr. Rudolf Manz for the opportunity to work on a lively and fascinating topic of immunological research. The degree of freedom and trust that I have been granted from the very start of this project has enabled me to not only make advances in the field of immunometabolism but to grow as a person. Thank you for the continuous support, guidance and the infectious enthusiasm for immunology and science in general.

Furthermore, I would like to thank my mentors Dr. Misa Hirose, Prof. Dr. Anika Wagner and Prof. Dr. Christian Sina for their support and the stimulating discussions that never failed to broaden my horizon.

A very sincere "thank you" to the entire AG Manz. To Kathleen Kurwahn, who, in addition to her consistent support in the lab, has managed to preserve the heartfelt, warm atmosphere of the group. To my partner in crime Dr. Ann-Katrin Clauder, who has set a new standard for diligent and organised work and has been an inspiration to do better. To Dr. Larissa Almeida, Dr. Christina Rau and Dr. Chinweike Christopher Udoye for their continuous support inside as well as the invaluable memories outside the lab. To all the former members of the ISEF who eased my start into research, namely: Dr. Christopher Link, Katharina Hofmann, Britta Frehse, Dr. Melanie Abram, Dr. Asmaa McGowan and Dr. Tillman Vollbrandt. To all the students who I had the privilege of supervising and who made me realise how much I love supporting others: Anna Gramalla-Schmitz, Fabienne Irrgang, Thorben Sauer, Sarah Stenger, Sandra Hilberath, Sarah-Maria Freye and Claudia Elbracht.

I would like to thank the research training group 1727 (GRK 1727) for the many opportunities to learn and grow as a scientist as well as the financial support and the valuable network it provided.

Last but most certainly not least, I need to thank the people outside university. My friends, who, even during the most unpleasant times, have managed to keep the last spark of my sanity alive. My parents, whose relentless, unwavering support has been the foundation of all my achievements. My brother, my niece and nephew and all my aunts, uncles and cousins, who have supported me in virtually anything I have ever done. It is this outstandingly supportive environment that has always enabled me to discard any ever so reasonable fear of failure and pursue the goals I am passionate about, even if they're as delusional as obtaining a doctoral degree.

Abstract

Metabolic reprogramming has been recognised as a major hallmark of immune cell activation. While researchers have gained detailed insight about this process in many different immune cells like T cells and macrophages, the B cell lineage lacks this level of understanding. In this thesis, I aimed at elucidating the metabolic profile of B cells and plasma cells to modulate their function by pharmaceutical inhibition of their respective metabolic profile.

Using flow cytometry, plasma cells and B cells were analysed with regard to the basic metabolic parameters glucose uptake and mitochondrial mass, as well as antibody synthesis and the activity of the unfolded protein response (UPR) on the single cell level. These parameters were analysed after treatment with glycolysis inhibitor 2-deoxyglucose (2-DG) *in vitro* in either isolated B cells activated with lipopolysaccharides (LPS) or whole spleen cells without stimulant. In addition, B6.NZM-Sle1$^{NZM2410/Aeg}$ Sle2$^{NZM2410/Aeg}$ Sle3$^{NZM2410/Aeg}$/Lmoj (BcN) mice, a mouse strain developing lupus-like symptoms due to the deletion of three lupus susceptibility loci, were injected with 2-DG to analyse its effect on B lineage cells in spleen and bone marrow *in vivo*.

Plasma cells from spleen showed high glucose uptake, but low mitochondrial mass. Furthermore, 2-DG treatment lead to a distinct decrease in splenic plasma cell numbers both *in vitro* and *in vivo*, indicating a preference for aerobic glycolysis. However, the number of bone marrow plasma cells was not affected by 2-DG treatment. In addition, 2-DG treatment *in vitro* resulted in a decrease in the concentration of IgM, IgG and IgA antibodies in cell culture supernatant, while only the number of IgM$^+$ plasma cells was decreased. Instead of a decrease in numbers, IgG$^+$ and IgA$^+$ plasma cells showed an increase in the amount of intracellular antibodies and UPR activity, indicating defective protein synthesis or secretion due to 2-DG. Some (but not all) of the effects of 2-DG could be prevented by adding mannose to the cell culture, an effect that could not be found when replacing 2-DG with the structurally similar glycolysis inhibitor 2-fluorodeoxyglucose (2-FDG).

In conclusion, these data show that plasma cells adopt aerobic glycolysis after differentiation, a metabolic profile similar to other mTOR-dependent immune cells like Type 1 or Type 17 T helper cells (Th1, Th17) or M1 macrophages. The dependence on aerobic glycolysis makes plasma cells susceptible to treatment with glycolysis inhibitors. While the impact of 2-DG on plasma cells is in part due to its function as a glycolysis inhibitor, it also inhibits mannose metabolism, leading to defective protein folding, flawed lysosome assembly thereby eventually inducing UPR activity. Due to its specificity towards plasma cells, 2-DG has potential to become a novel therapy approach in autoimmune diseases, reducing autoantibody production by plasma cells while simultaneously increasing the expression of the anti-inflammatory cytokine interleukin 10 (IL-10) in B cells.

Zusammenfassung

Bereits seit einigen Jahren ist bekannt, dass Immunzellen ihren Metabolismus nach der Aktivierung grundlegend verändern. Dieser Prozess ist essentiell für das Gelingen der Immunantwort. Während die Hintergründe und Auswirkungen dieses Prozesses auf verschiedene Immunzellen wie T-Zellen und Makrophagen im Detail untersucht worden sind, fehlen diese Erkenntnisse bei den Zellen der B-Zell-Familie. Diese Arbeit zielt daher darauf ab, das metabolische Profil der B-Zellen und Plasmazellen zu beschreiben. Diese Erkenntnisse sollen dann genutzt werden, um die Funktionsfähigkeit der B-Zellen und Plasmazellen über die pharmazeutische Inhibition der jeweiligen metabolischen Profile zu beeinflussen.

B-Zellen und Plasmazellen wurden mit Hilfe der Durchflusszytometrie hinsichtlich ihrer grundlegenden metabolischen Parameter wie der Glukoseaufnahme oder der mitochondrialen Masse auf Einzelzell-Level analysiert. Zusätzlich wurden die Biosynthese der Antikörper und die Aktivität der unfolded protein response (UPR) untersucht. Die Messung dieser Parameter erfolgte jeweils nach der Behandlung mit dem Glykolyseinhibitor 2-Deoxyglukose (2-DG) oder eine Kontrollsubstanz. *In vitro* wurden entweder isolierte B-Zellen durch Zugabe von Lipopolysacchariden (LPS) aktiviert oder übergreifend alle Milzzellen ohne zusätzliche Stimulation untersucht. Für die *in vivo* Versuche wurden B6.NZM-Sle1$^{NZM2410/Aeg}$ Sle2$^{NZM2410/Aeg}$ Sle3$^{NZM2410/Aeg}$/Lmoj (BcN) Mäuse verwendet, die aufgrund der Entfernung von drei Lupus-Suszeptibilitäts-Loci Lupus-ähnliche Symptome entwickeln. Den Mäusen wurde 2-DG injiziert, um die Effekte von 2-DG auf die Zellen der B-Zell-Familie in der Milz und im Knochenmark zu analysieren.

Plasmazellen aus der Milz zeigten eine hohe Glukoseaufnahme, aber eine nur geringe mitochondriale Masse. Die Behandlung dieser Zellen mit 2-DG führte zu einem deutlichen Rückgang der Zahl an Plasmazellen, sowohl *in vitro* wie auch *in vivo*. Im Gegensatz dazu wurde die Anzahl an Plasmazellen im Knochenmark *in vivo* nicht durch die 2-DG Injektion beeinflusst. *In vitro* sorgte die Behandlung der Plasmazellen mit 2-DG zu einer Reduktion der Konzentration an IgM, IgG und IgA Antikörper im Überstand der Zellkultur, obwohl lediglich die Anzahl der IgM$^+$ Plasmazellen durch die Behandlung reduziert wurde. Während ihre Anzahl gleich blieb, wiesen die IgG$^+$ und IgA$^+$ Plasmazellen erhöhte Konzentrationen an Antikörpern im Inneren der Zellen und eine verstärkte UPR Aktivität auf. Einige (aber nicht alle) dieser Effekte konnten durch die Zugabe von Mannose zur Zellkultur gelindert oder komplett verhindert werden. Diesen Effekt entfaltete Mannose nicht, wenn statt 2-DG der strukturell sehr ähnliche Glykolyseinhibitor 2-Fluorodeoxyglukose (2-FDG) verwendet wurde.

Zusammenfassend zeigen diese Daten, dass Plasmazellen nach der Differenzierung zur aeroben Glykolyse neigen, ein Profil, das auch andere mTOR-abhängige Immunzellen wie Typ 1 oder Typ 17 T-Helferzellen (Th1 und Th17) oder M1 Makrophagen aufweisen.

Ihre Abhängigkeit von der aeroben Glykolyse macht die Plasmazellen anfällig für Glykolyseinhibitoren. Obwohl ein Teil der Wirkung von 2-DG auch auf seine Funktion als Glykolyseinhibitor zurückzuführen ist, inhibiert 2-DG vor allem auch den Mannose-Metabolismus, wodurch es zu Fehlern bei der Proteinfaltung, der Lysosom-Aktivität und dadurch letztlich zum Einsetzen der UPR kommt. Durch seine Spezifität gegenüber Plasmazellen hat 2-DG das Potential als Medikament bei Autoimmunerkrankungen zum Einsatz zu kommen, da es die Produktion von Autoantikörpern verringert und die Expression des anti-entzündlichen Zytokins Interleukin-10 (IL-10) in B-Zellen steigert.

Contents

Abstract vii

Zusammenfassung ix

1 Introduction 3
- 1.1 Immunity and autoimmunity . . . 3
  - 1.1.1 Innate and adaptive immune system . . . 3
  - 1.1.2 The B cell lineage . . . 4
  - 1.1.3 Autoimmune diseases . . . 6
- 1.2 Metabolism . . . 7
  - 1.2.1 Glycolysis and oxidative phosphorylation . . . 8
  - 1.2.2 Glucose outside of energy generation . . . 11
- 1.3 Immunometabolism . . . 12
  - 1.3.1 B cell and plasma cell metabolism . . . 14
- 1.4 Aim of the study . . . 16

2 Materials and Methods 17
- 2.1 Materials . . . 17
  - 2.1.1 Consumeables . . . 17
  - 2.1.2 Chemicals and Kits . . . 17
  - 2.1.3 Buffers . . . 18
  - 2.1.4 Cell Culture . . . 19
  - 2.1.5 Cytokines, Enzymes and Standards . . . 19
  - 2.1.6 Antibodies and Fluorescent Dyes . . . 19
  - 2.1.7 Technical Equipment . . . 20
  - 2.1.8 Software . . . 21
  - 2.1.9 Mice . . . 21
- 2.2 Methods . . . 21
  - 2.2.1 Generation of Single Cell Suspensions . . . 21
  - 2.2.2 Cell counting . . . 22
  - 2.2.3 B Cell Isolation via Magnetic Cell Separation . . . 23
  - 2.2.4 Isolated B Cell Culture . . . 24
  - 2.2.5 Spleen cell culture . . . 24
  - 2.2.6 Flow cytometry . . . 25
  - 2.2.7 ELISA . . . 26
  - 2.2.8 *In vivo* administration of 2-DG and Bortezomib . . . 27
  - 2.2.9 Statistical analysis . . . 28

3 Results **29**
3.1 Plasma cells show high glucose uptake while having low mitochondrial mass 29
3.2 Glycolysis and mTORC1 inhibition drastically reduce the ability to generate plasmablasts *in vitro* . . . 31
3.3 2-DG eliminates terminally differentiated plasma cells . . . 33
3.4 Combining 2-DG and bortezomib leads to a synergistic decrease in plasma cell frequencies . . . 35
3.5 2-DG decreases the number of germinal centre B cells and plasma cells *in vivo* . . . 36
3.6 Bone marrow plasma cells survive 2-DG treatment *in vivo* but show phenotypical changes . . . 39
3.7 Combining 2-DG and bortezomib does not improve drug efficacy *in vivo* . 41
3.8 2-DG induces an unfolded protein response and reduces TACI expression 43
3.9 Mannose decreases the impact of 2-DG on plasma cell survival *in vitro* . . 45
3.10 2-DG affects the generation and secretion of different immunoglobulin classes . . . 47
3.11 2-DG affects Igκ light chain expression in plasma cells that survive treatment 48
3.12 Mannose reduces the effect of 2-DG, but not 2-FDG . . . 51
3.13 Hexokinase, but not phosphofructokinase, inhibitors hinder the generation of plasmablasts . . . 52
3.14 Glycosylation inhibition and 2-DG treatment result in similar plasma cell numbers, LAMP-1 and XBP-1s expression . . . 55

4 Discussion **57**
4.1 Plasma cells show high glucose uptake while having low mitochondrial mass 57
4.2 Glycolysis and mTORC1 inhibition drastically reduce the ability to generate plasmablasts *in vitro* . . . 58
4.3 2-DG eliminates terminally differentiated plasma cells . . . 60
4.4 Combining 2-DG and bortezomib leads to a synergistic decrease in plasma cell frequencies *in vitro* . . . 61
4.5 2-DG decreases the number of germinal centre B cells and plasma cells *in vivo* . . . 61
4.6 Bone marrow plasma cells survive 2-DG treatment *in vivo* but show phenotypical changes . . . 62
4.7 Combining 2-DG and bortezomib does not improve drug efficacy *in vivo* . 63
4.8 2-DG induces an unfolded protein response and reduces TACI expression 64
4.9 Mannose decreases the impact of 2-DG on plasma cell survival *in vitro* . . 65
4.10 2-DG affects the generation and secretion of different immunoglobulin classes . . . 66
4.11 2-DG affects Igκ light chain expression in plasma cells that survive treatment 66
4.12 Mannose reduces the effect of 2-DG, but not 2-FDG . . . 67
4.13 Hexokinase, but not phosphofructokinase, inhibitors hinder the generation of plasmablasts . . . 68

4.14 Glycosylation inhibition and 2-DG treatment result in similar plasma cell numbers, LAMP-1 and XBP-1s expression 69
4.15 Conclusion 70

5 Outlook **71**

Bibliography **73**

Abbreviations **83**

1 Introduction

1.1 Immunity and autoimmunity

The immune system is a network of cells, tissues and entire organs dedicated to the detection and elimination of pathogens. It is divided into two arms: the innate and the adaptive immune system. Both branches of the system are tightly linked and communicate constantly by secreting cytokines to defend the body from pathogens. Simultaneously, the immune system needs to be strictly regulated to avoid its activation by recognition of self-antigens leading to the development of autoimmune diseases. The discrimination between foreign pathogens to fight off and non-infectious antigens and self-antigens to ignore is the fundamental basis of immunity.

1.1.1 Innate and adaptive immune system

Evolutionary the far older of the two branches, the innate immune system encompasses all aspects of the immune defence that are encoded in their mature and fully functional form in the genetic code of the host (Chaplin, 2010). The first barrier of the immune system are physical barriers like skin and mucus membranes in the airways and intestines. These barriers block or impede the entry of pathogens into the host organism, protecting it from a vast array of foreign antigens (Castelo-Branco and Soveral, 2014). On a cellular level, the first line of defence of the innate immune system is comprised of a number of different cells like macrophages and neutrophils. While neutrophils and other granulocytes (eosinophils, basophils and mast cells) attack pathogens by secreting highly acidic granules aiming to lyse the invading cells, macrophages take up and digest living cells as well as dead debris (Parkin and Cohen, 2001). Similarly to macrophages, dendritic cells (DC) take up pathogens, digest them and present peptide fragments to T cells via the major histocompatibility complex (MHC) class II, activating the adaptive immune system. In addition, natural killer (NK) cells verify the presence of MHC class I molecules that are ubiquitously expressed on a plethora of cells. Since a lack of MHC class I is seen in tumour cells and some virus infections, these cells are lysed by the NK cells (Castelo-Branco and Soveral, 2014). To detect the presence of bacteria, viruses, fungi and parasites, immune cells are equipped with an array of pattern-recognition receptors (PRR) (Parkin and Cohen, 2001). These receptors can bind certain pathogen-associated molecular patterns (PAMPs) that are present on microbes but not host cells. The PRR Toll-like receptor 4 (TLR4) can bind to lipopolysaccheride (LPS) molecules that are present on the surface of gram-negative bacteria, thus activating the immune cell and inducing the release of cytokines (Nicholson, 2016).

Unlike the innate immune system, the adaptive branch is not in full effect at birth. One of the main functions of the adaptive immune system is to generate memory cells

that provide long-lived immunity against specific pathogens. However, these cells are only generated after contact with the pathogen therefore lacking a main function of the adaptive immune system at birth (Parkin and Cohen, 2001). The cellular side of the adaptive immune system, the so-called lymphocytes, consists of the B cell and T cells that further differentiate upon activation. While $CD4^+$ T helper cells orchestrate the immune response and recruit and activate other immune cells after contact with antigen-presenting cells (APCs) like DCs, macrophages and B cells, $CD8^+$ cytotoxic T lymphocytes detect infected cells based on their antigen presentation via their MHC class I molecules and kill them by releasing perforins and granzymes (Parkin and Cohen, 2001). The B lineage cells provide the humoral response of the adaptive branch by secreting large amounts of antibodies. In addition, B lineage cells assume regulatory functions via the secretion of a variety of different cytokines, modulating the immune response (Luu, Vazquez, and Zlotnik, 2014). What differentiates the many cells of the innate immune system from the B and T lymphocytes is their antigen recognition. While both B and T cells express PRRs, they are equipped with a distinct antigen recognition receptor called B cell receptor (BCR) and T cell receptor (TCR). Both receptors are encoded in the form of modular gene segments that are rearranged during the maturation of the cells. Each naive B and T lymphocyte is therefore equipped with a randomly arranged antigen receptor that recognises a specific target antigen (Matthews *et al.*, 2014; Chaplin, 2010). While this process enables the immune system to recognise new variations of pathogens it hasn't encountered before, it also creates the threat of autoimmune diseases caused by auto-reactive lymphocytes.

1.1.2 The B cell lineage

B lymphocytes contribute to the adaptive immune reaction by secreting cytokines (Luu, Vazquez, and Zlotnik, 2014) and presenting peptide fragments to T cells via MHC class II (Mariño *et al.*, 2008). Their main task, however, is to generate immunoglobulins (Ig) fighting of acute infections and providing long-lasting immunity.

B cell development

Along with all other immune cells, B cells descend from multipotential haematopoietic stem cells in the bone marrow. These cells differentiate into a common myeloid progenitor, the precursor of all myeloid cells of the innate immune system, and a common lymphoid progenitor, the precursor of the lymphocytes of the adaptive immune system (LeBien and Tedder, 2008; Pieper, Grimbacher, and Eibel, 2013). Deriving from the lymphoid precursor, several developmental stages of B cells can be differentiated based on the state of the heavy and light chain rearrangement of the BCR from pre-pro to pro to pre and immature B cells. First, D and J segments of the heavy chain are rearranged in pro B cells followed by recombination of the V segments of the heavy chain. After the heavy chain rearrangement is completed at the pre B cell stage, a pre B cell receptor is expressed on the cell surface (Pieper, Grimbacher, and Eibel, 2013). After final recombination of the V and J segments of the light chain, an immature B cell is formed

expressing a functional immunoglobulin M (IgM) (Ghia *et al.*, 1996). After completion of the BCR, the receptor needs to be tested for self-reactivity. In a first step, the central tolerance, a B cell that binds to self-antigens in the bone marrow undergoes receptor editing, functional anergy or clonal deletion. After egress from the bone marrow and transit to the spleen, peripheral tolerance is tested and only a weak or no reactivity to self-antigens leads to normal development of the B cell (Pieper, Grimbacher, and Eibel, 2013). In the spleen, the final steps towards fully functional, naive B cells are performed. In addition to the IgM BCR, B cells start expressing IgD BCRs as well. During their maturation in the spleen, B cells differentiate into several subsets like B-1 cells that provide natural antibodies and marginal zone B cells (MZB) as well as follicular B cells (FOB), waiting to encounter pathogens (LeBien and Tedder, 2008).

B cell activation

The IgM^{high} IgD^{low} MZBs are located in the marginal zone of the spleen. Upon antigen binding, these cells are prone to mount a T cell-independent response, forming primarily short-lived plasma cells (SLPCs) and secreting IgM antibodies into the blood (Pieper, Grimbacher, and Eibel, 2013). On the other hand, IgM^{low} IgD^{high} FOBs are more likely to initiate T cell-dependent responses, forming germinal centres and differentiating into memory B cells and more long-lived plasma cells (LLPC) secreting other immunoglobulin isotypes like IgG and IgA (Kondo *et al.*, 2002; LeBien and Tedder, 2008). For the germinal centre reaction to occur, a FOB has to be activated by antigen binding to their BCR. After internalisation of the receptor, the pathogen is lysed and digested. The processed peptide fragments are loaded onto MHC class II molecules and presented on the B cells surface (Chaplin, 2010). After activation via BCR ligation, the B cell is prone to apoptosis and requires T cell help to survive. When the B cell encounters a T cell with a TCR that binds to the presented peptide, the T cell gets activated and secretes ctyokines like IL-4, IL-6, IFN-γ or TGF-β to counteract the apoptotic signals and orchestrate the maturation of the B cell (Chaplin, 2010). After the mutual activation, both the B and T cell undergo massive clonal expansion. A germinal centre is formed consisting of circulating B cells undergoing affinity maturation and isotype switching, proliferating effector and memory T cells and follicular DCs providing constant antigen presentation (Parkin and Cohen, 2001). At the end of the reaction, B cells with enhanced receptor affinities have differentiated into memory B cells and plasma cells with different BCR isotypes, some of which are have half-lifes of several decades.

Plasma cells

Plasma cells are sometimes described as a homogeneous group of cells following the regulation imposed upon them by T cells. However, plasma cells are composed of a multitude of different subpopulations varying in the isotype and affinity of their antigen receptor, their half-life, cytokine secretion, homing and metabolism (Price *et al.*, 2019). In recent years, it has become clear that even the glycosylation pattern of the antibody influences its function, either promoting or inhibiting inflammatory responses

or complement activation (Cobb, 2020). Since plasma cells can derive from B cells activated by T cells in the follicle, extrafolliculary or even independent of T cell help via co-activation of the BCR and PRRs, the resulting plasma cells can be vastly different from one another (LeBien and Tedder, 2008; Vos *et al.*, 2000). Some plasma cells, called SLPCs, survive and secrete all kinds of antibodies for a period of days to weeks during acute immune response, while LLPCs survive for decades and secrete primarily IgG and IgA antibodies (Cenci, 2012; Ionescu and Urschel, 2019). While some argue that the longevity of the plasma cells must be an intrinsic factor caused by a certain route of maturation or activation, others support the idea of a specific survival niche in the bone marrow (Lightman, Utley, and Lee, 2019; Manz, Arce, *et al.*, 2002). Regardless of their origin, the continuous translation, folding and secretion of enormous amounts of antibodies requires remarkably stable mechanisms to deal with failure of the protein synthesis machinery and changes in nutrient availability. To support a constant flow of nutrients and deal with aggregates of unfolded proteins, plasma cells depend on a high level of autophagy (Pengo *et al.*, 2013). Simultaneously, plasma cells show constant activity of the unfolded protein response (UPR) to reduce ER stress caused by incorrectly folded proteins (Lam and Bhattacharya, 2018). The high UPR activity is so characteristic for plasma cells that the UPR transcription factor X-box binding protein 1 (XBP-1) is considered one of the main plasma cell markers with the most important markers being the master transcription factor B lymphocyte-induced maturation protein-1 (BLIMP-1) and the membrane protein Syndecan-1 (CD138) (Cossarizza *et al.*, 2019). In addition, plasma cells show high expression levels of the receptors transmembrane activator and CAML interactor (TACI) and B-cell maturation antigen (BCMA). Both receptors bind the survival factors a proliferation-inducing ligand (APRIL) and B-cell activating factor (BAFF) with different affinities.

Keeping in mind the differences between the many plasma cell subpopulations, it's important to understand the limitations of different cell culture systems. One of the most common B cell cultures uses isolated B cells from spleen and activates them by adding LPS to stimulate TLR4. Since MZBs are more prone to launch T cell-independent responses, these cultures skew the biological relevance of the results by primarily depicting the activation and differentiation of MZBs. After 5 d of culture, the cells generated in these cultures express relatively high levels of CD138 and lower levels of common B cell markers like CD19 and B220, reminiscent of plasma cells, but still proliferate and lack TACI expression almost entirely. Transcriptional profiling showed that these plasmablasts are as far from being terminally differentiated plasma cells as they are from being naive B cells (Shi *et al.*, 2015). To circumvent the limitations of these cultures, this thesis included experiments performed with whole spleen cells, including terminally differentiated plasma cells, as they can be found *in vivo*.

1.1.3 Autoimmune diseases

While the generation of randomly assembled receptors for B and T cells provides a potent weapon for the immune system, it is also a major risk for the development of autoimmune diseases. Although the tolerance mechanisms during B and T cell devel-

opment described above are able to eliminate the vast majority of autoreactive cells by inducing anergy, receptor editing or clonal deletion, autoreactive cells with low affinity receptors can sometime elude their elimination (Pillai, Mattoo, and Cariappa, 2012). Regulatory cells expressing IL-10 provide further support in suppressing the activation of these weakly reactive cells (LeBien and Tedder, 2008). Still, on rare occasions autoreactive B and T cells can come across and activate one another. Depending on the specificity of the autoreactive BCR and TCR, a variety of different symptoms can develop. Over 100 different autoimmune diseases have characterised affecting 3 % to 5 % of the human population (L. Wang, F. S. Wang, and Gershwin, 2015). Genetic and epigenetic predisposition as well as environmental factors like the microbiome contribute to the development of autoimmune diseases (Cho and Feldman, 2015). In many cases, the prevalence of autoimmune diseases is higher in women than men (L. Wang, F. S. Wang, and Gershwin, 2015). One of these diseases is systemic lupus erythematosus (SLE). SLE is caused by a global break of tolerance affecting many organs like joints, skin, the nervous system and kidneys (Choi, S. T. Kim, and Craft, 2012; Kaul *et al.*, 2016). Many factors are associated with the development of SLE including genetic as well as environmental influence like UV light exposure, Epstein-Barr virus infection or hormonal dysregulation. A variety of different treatments is applied, some focussing on the elimination of B cells with anti-CD20 antibodies or regulating cytokine interaction by blocking BAFF, IL-6 or TNF signalling (Kaul *et al.*, 2016). Unfortunately, no treatment so far has been able to restore quality of life. One of the obstacles of current therapies is the resistance of LLPCs, providing humoral memory (Hiepe *et al.*, 2011). Proteasome inhibitors like bortezomib have been proposed to eliminate LLPCs and recent case studies provide evidence for their therapeutic potential. However, at the necessary dosage, bortezomib treatment introduces the risk of severe side effects like peripheral neuropathy (Segarra *et al.*, 2020). Finding drug-sparing agents could alleviate these side effects, therefore drastically improving the therapeutic options for SLE and possibly other autoimmune diseases. With the emergence of the field of immunometabolism, metabolic pathways are now investigated for their therapeutic benefit.

1.2 Metabolism

The metabolism of an individual encompasses all chemical reactions necessary to sustain life. These reactions can be further broken down into catabolic (breaking down of substances) and anabolic (building new substances). Due to its existential nature, metabolism has not been on the forefront of research for a long time since modulating metabolic processes were believed to affect all kinds of cells to a very similar extend. Starting with Otto Warburg's discovery that tumour cells made use of a metabolic profile that was considered extremely inefficient (Warburg, Posener, and Negelein, 1924), researchers began to discover vast differences in the metabolism of different cell populations. The three main sources of energy for cells are glucose, fatty acids and amino acids. These substances are derived from the three basic nutrients taken up with diet. While metabolism is a vast network of reactions that connects all kinds of nutrients with one

another, glucose is best known as the fuel for glycolysis and subsequent phosphorylation in the mitochondrium as well as a building block for the biosynthesis of nucleotides, fatty acids and protein glycosylation. Fatty acids and amino acids contribute to the ATP generation fuelling the citric acid or Krebs cycle as well as the generation of membrane components and energy storage (Ganeshan and Chawla, 2014). While all of these components are vitally important for the function and survival of cells and the entire organism, this thesis focusses on the glucose metabolism.

1.2.1 Glycolysis and oxidative phosphorylation

To generate energy in the form of adenosine triphosphate (ATP), glucose is degraded into pyruvate in a process called glycolysis (Fig. 1). After glycolysis, pyruvate can be further degraded to CO_2 during oxidative phosphorylation. First, the cell takes up glucose using a family of 14 known glucose transporters (GLUT) (Adekola, Rosen, and Shanmugam, 2012). However, the substrate of these transporters isn't necessarily glucose and only GLUTs 1-4 have been well-established (Thorens and Mueckler, 2010). These four GLUTs are expressed in different tissues and vary in their glucose affinity. Glycolysis can be separated into three different phases: energy-investment, splitting and energy-generation phase (Akram, 2013). In the first step of glycolysis, glucose is phosphorylated at the C6-atom by the hexokinase. This rate-limiting step requires one molecule of ATP to activate the glucose for further reactions and to restrain it inside the cell (Li, Gu, and Zhou, 2015). Glucose-6-phosphate (G6P) is then converted into fructose-6-phosphate by phosphoglucose isomerase which then receives a second phosphate group by phosphofructokinase, consuming a second molecule of ATP. The resulting fructose 1,6-diphosphate constitutes the last product of the energy-investment phase of glycolysis. In the next step, the six-carbon fructose is split into two three carbon compounds, dihydroxyacetone phosphate and glyceraldehyde 3-phosphate, by the aldolase. Both products can be converted into one another by triosephosphate isomerase. providing a constant supply of glyceraldehyde 3-phosphate. In the following energy-generation phase, glyceraldehyde 3-phosphate is converted into 1,3-bisphosphoglycerate yielding two molecules of the reduced coenzyme nicotinamide adenine dinucleotide (NADH). NADH is involved in a number of cellular redox reactions and provides electrons for the oxidative phosphorylation, providing the possibility to generate energy later on. In the next step, phosphoglycerate kinase uses its substrate to phosphorylate two adenosine diphosphate (ADP) molecules to generate two ATP and 3-phosphoglycerate. Afterwards, the phosphate group is transferred to the C2 atom by phosphoglycerate mutase generating 2-phosphoglycerate which is then converted into phosphoenolpyruvate by the enzyme enolase. In the last step of glycolysis, pyruvate kinase transfers the remaining phosphate group to ADP generating ATP and pyruvate, the end product of glycolysis. In total, two molecules of ATP are invested in the first phase of glycolysis to yield four molecules of ATP and 2 molecules of NADH per glucose. Glycolysis itself is oxygen-independent. However, under anaerobic conditions, the pyruvate cannot be further degraded in the Krebs cycle which depends on oxygen. In this case, lack of NAD^+ to be reduced to NADH by GAPDH can lead to the termination of the glycolytic pathway. To sustain

glycolysis even under anaerobic conditions, pyruvate can be reduced to lactate by lactate dehydrogenase, oxidising two NADH to NAD^+ in the process. The excess lactate is then secreted to the extracellular space using monocarboxylate transporters.

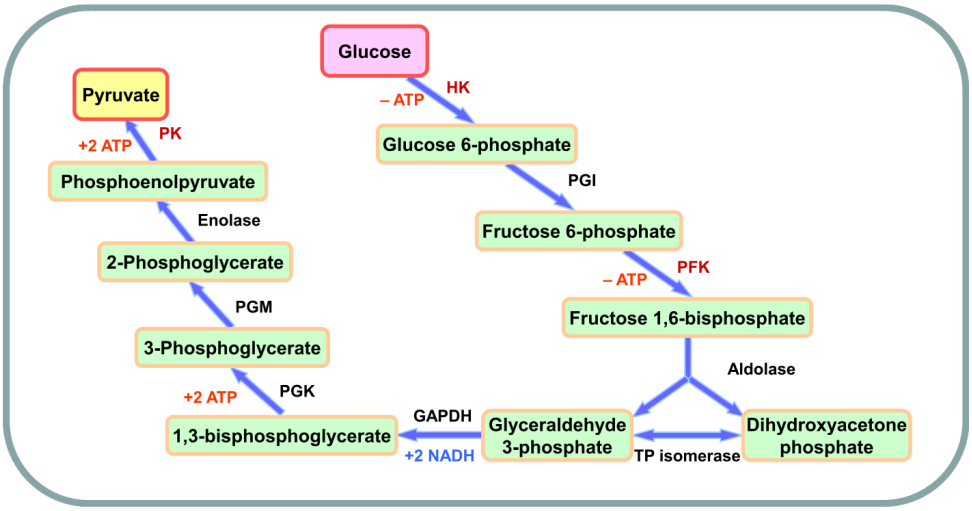

Figure 1: Schematic overview of glycolysis. Depiction of the sequence of chemical reactions during glycolysis. ATP: adenosine triphosphate, HK: hexokinase, PGI: phosphoglucose isomerase, PFK: phosphofructokinase, TP isomerase: triosephosphate isomerase, GAPDH: glyceraldehyde 3 phosphate dehydrogenase, PGK: phosphoglycerate kinase, PGM: phosphoglycerate mutase, PK: pyruvate kinase. Figure created by Li, Gu, and Zhou (2015).

Under aerobic conditions, pyruvate can be used to fuel the Krebs cycle, also known as citric acid or tricarboxylic acid cycle (Fig. 2. For that purpose, pyruvate is converted to acetyl coenzyme A (acetyl-CoA) and enters the Krebs cycle. Acetyl-CoA can also be gained from other sources like β-oxidation of fatty acids or degradation of some amino acids. Within the Krebs cycle, four molecules of NADH and one molecule of reduced falvin adenine dinucelotide (FADH) are generated. These coenzymes act as electron donors in a variety of reactions but also fuel the generation of a proton gradient by the complexes I and II of the electron transport chain (ETC) (Donnelly and Finlay, 2015). Using oxidative phosphorylation (oxphos) to breakdown glucose entirely yields around 36 ATP while using anaerobic glycolysis yields only two ATP. Due to its superior efficiency, using glucose and other nutrients like fatty acids to fuel oxphos was recognised as the main pathway for energy generation of most cells. However, both glycolysis and oxhphos are not only used for energy generation but for providing building blocks for biosynthesis. Glyceralde-3-phosphate is used to form triglycerides and phospholipids while intermediates of the Krebs cycle are used to synthesise amino acids. One of the most versatile intermediates, glucose-6-phosphate is used for the generation of glycogen to store energy, nucleotides via the pentose phosphate pathway and other sugars like mannose and fructose. Together with those other monosaccherides, glucose is used to form complex sugar structures that are required for post-translational modifications called glycosylation.

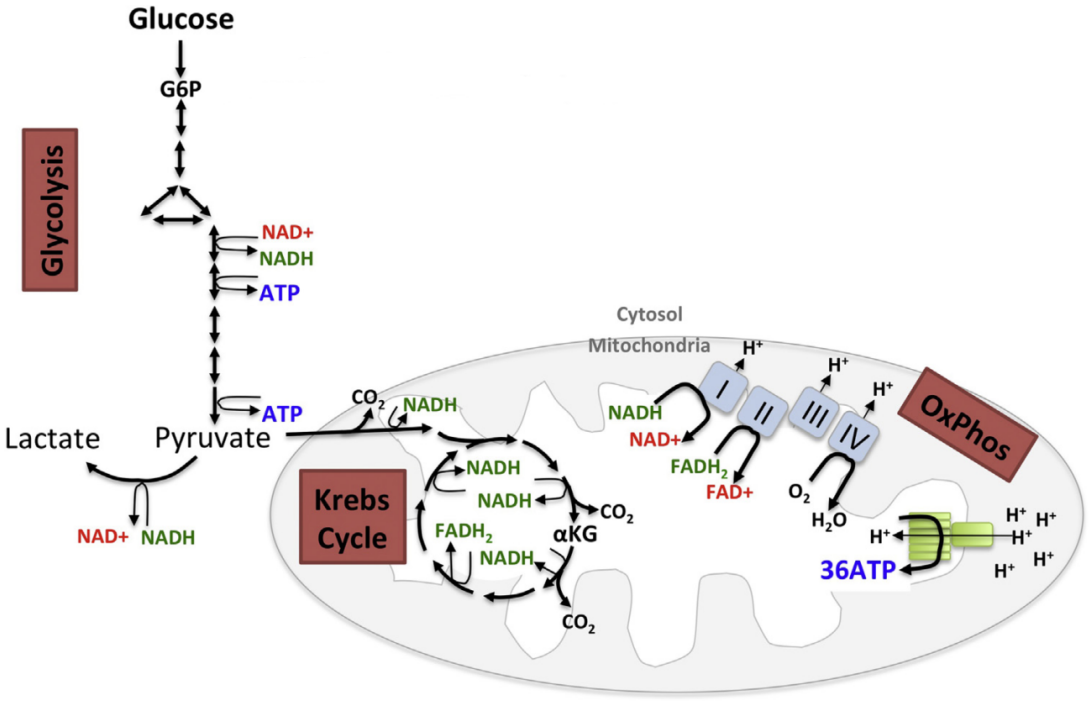

Figure 2: Complete breakdown of glucose from glycolysis to oxidative phosphorylation. After the conversion of glucose to pyruvate during glycolysis, pyruvate can be oxidised to acetyl-CoA and to enter the Krebs cycle (also known as citric acid cycle or tricarboxylic acid cycle). The Krebs cycle yields the electron donors NADH and $FADH_2$ to fuel the electron transport chain (ETC) and generate a proton gradient across the inner membrane of the mitochondrium. The proton gradient fuels the ATP-synthase (complex V) to generate ATP. α-KG: α-ketoglutarate, ATP: adenosine triphosphate, FAD^+/FADH: oxidised/reduced flavin adenine dinucleotide, G6P: glucose-6-phosphate, NAD^+/NADH: oxidised/reduced nicotinamide adenine dinucelotide. Figure adapted from Donnelly and Finlay (2015).

1.2.2 Glucose outside of energy generation

The conversion of glucose into glucose-6-phosphate is the steppingstone for a vast array of chemical reactions. While the diet provides many kinds of monosaccherides, cellular glucose metabolism is of major importance for the generation of sugars like mannose as well (Sharma and Freeze, 2011). Therefore, modulating glucose metabolism affects catabolic and anabolic reactions of other, seemingly unrelated saccharides as well (Fig. 3). The impact these changes can have can be illustrated nicely using the process of glycosylation. Glycosylation is a most diverse network of post-translational modifications that, among others, alter protein folding, half-life and function (Schjoldager *et al.*, 2020). Glycosylations can be categorised into N-linked, O-linked and C-linked glycosylation and glycosylphosphatidylinositol (GPI)-anchors. While a variety of different saccharides-derived structures can be linked to the oxygen atom of serine, threonine and in some cases tyrosine, the initial steps of N-glycosylation are very similar (Schjoldager *et al.*, 2020). In a first step, a lipid-linked oligosaccharide (LLO) is generated consisting of two molecules of N-acetylglucosamine (GlcNAc), nine mannose and three glucose molecules bound to a dolichol-phosphate anchor. In the second step, the LLO is linked to a protein and the structure is truncated and transported from the endoplasmatic reticulum to the Golgi apparatus. There, it is further processed to a variety of different glycans consisting of mannose, glucose, galactose and sialic acids, concluding the third step (Schjoldager *et al.*, 2020). Glucose is at the heart of this process as it is necessary to create the activated sugars uracil-diphosphate (UDP)-glucose and guanosine-diphosphate (GDP)-mannose as well as the glucosamine necessary for the synthesis of GlcNAc (Sharma, Ichikawa, and Freeze, 2014). In addition, mannose is used to synthesise GPI-anchors. These anchors are bound to the C-terminus of proteins to retain them in the plasma membrane, ensuring the function of a variety of different proteins involved, among others, in cell-cell interactions and complement regulation. Defects in the synthesis of GPI anchors have been shown to be lethal at the embryonic stage (Paulick and Bertozzi, 2008). In addition to the use as an anchor, mannose is also used as a signalling molecule. Enzymes like hydrolases destined for lysosomes are labelled with mannose-6-phosphate (M6P) (Kornfeld and Mellman, 1989). The M6P is bound by a mannose-6-phosphate receptor (MPR) in the Golgi and transferred to late endosomes. Due to their lower pH, the M6P-labelled protein is released in the endosome and maturation continues (Coutinho, Prata, and Alves, 2012). Dysfunction of the MPRs or the pathways generating M6P can lead to lysosomal storage disease and is even associated with stuttering (Coutinho, Prata, and Alves, 2012).

The diversity of these pathways nicely illustrates how broad the impact of glucose on a single cell is. Whether it is used to generate energy or provide metabolites for post-translational modifications, localisation or signalling, glucose is at the heart of many metabolic processes. Interfering with glucose metabolism seems to force consequences that can hardly be foreseen. Only with the emergence of the field of immunometabolism has it become clearer that targeting metabolism might provide new therapeutic options for a plethora of diseases.

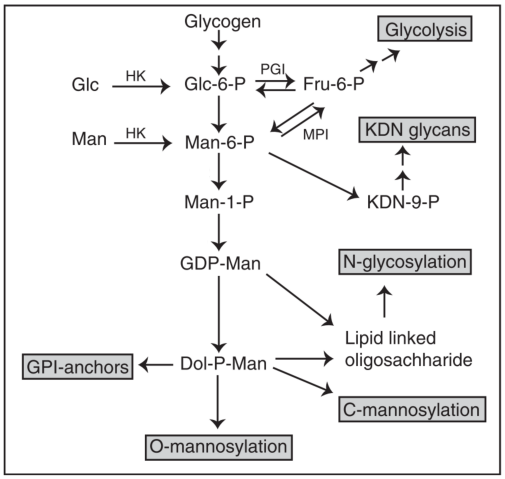

Figure 3: Metabolic pathways of mannose. Mannose-6-phosphate can be gained by taking up mannose from the blood or by converting glucose-6-phosphate or fructose-6-phosphate. After transferring the phosphate to C1, mannose-1-phosphate can be converted to its activated form GDP-mannose. GDP-mannose is used in a variety of different pathways, including N-, O-, and C-glycosylation as well as the synthesis of GPI-anchors. Glc: glucose, Man: mannose, Glc-6-P: glucose-6-phosphate, Man-6-P: mannose-6-phosphate, Fru-6-P: fructose-6-phosphate, Dol-P-Man: dolichol phosphate mannose, KDN-9-P: KDN-9-phosphate, HK: hexokinase, PGI: phosphoglucose isomerase, MPI: phosphomannose isomerase. Figure adapted from Sharma, Ichikawa, and Freeze (2014).

1.3 Immunometabolism

Almost a century ago, Otto Warburg discovered that tumour cells converted glucose to lactate but neglected to use it to fuel the Krebs cycle and oxidative phosphorylation (Warburg, Posener, and Negelein, 1924). While it was first believed that the lack of oxidative metabolism had to be caused by a lack of oxygen in the tumour's environment, it became clear that tumour cells adopted this metabolic profile even under aerobic conditions. This profile was therefore termed "aerobic glycolysis" (anaerobic glycolysis even under aerobic conditions) or the "warburg effect". While the warburg effect was discussed in the context of other cells as well, it was only at the beginning of this century that immunology took keen interest in metabolism (Calder, Dimitriadis, and Newsholme, 2007). During the course of the immune reaction, immune cells are subject to massive changes in their function and morphology. Starting with research done on T cells, it became clear that metabolism had to adjust to these changes accordingly (Windt and Pearce, 2012). While $CD8^+$ effector T cells relied on glycolysis to support their proliferation, memory T cells shifted towards a more mitochondrial-based metabolism, becoming more efficient and less susceptible to variations in the nutrient availability. Interestingly, similar patterns could be found in macrophages with regard to their pro- or anti-inflammatory potential. Macrophages with a deletion of the *Interleukin-10* gene (*IL-10*) showed higher levels of glycolysis after LPS treatment compared to wildtype

control. Inversely, treatment with the anti-inflammatory IL-10 resulted in a shift towards oxidative metabolism instead of glycolysis (Ip *et al.*, 2017). Over the years, similar patterns were found in neutrophils, mast cells and DCs, where rapidly differentiating, activated cells often promoting inflammation were more glycolytic while resting cells favoured pathways fuelling the Krebs cycle and oxphos (Ganeshan and Chawla, 2014; Soto-Heredero *et al.*, 2020) (Fig. 4).

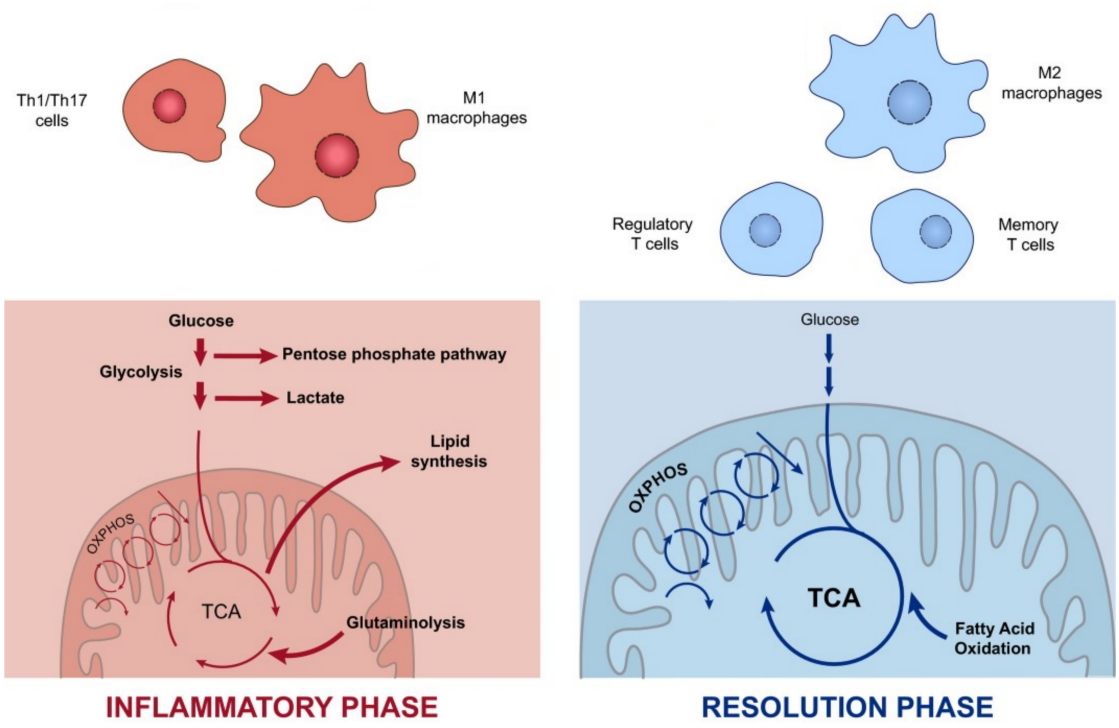

Figure 4: Role of metabolism during inflammation and resolution. Immune cells promoting inflammation like Th1/Th17 or classically activated M1 macrophages make use of aerobic glycolysis to fuel the pentose phosphate pathway and synthesise nucelotides. Glutamine is used as the carbon source for the tricaboxylic acid cycle (TCA) and fuels lipid synthesis. During the resolution phase, anti-inflammatory and resting cells like M2 macrophages, regulatory and memory T cells favour oxphos fuelled from glycolysis and fatty acid oxidation. Figure adapted from Soto-Heredero *et al.* (2020).

One of the major signalling hubs integrating nutrient levels and cell fate are the mammalian target of rapamycin (mTOR) and its counterpart adenosine monophosphate-activated protein kinase (AMPK). The so-called "nutrient sensor" mTOR complex 1 (mTORC1) is activated when glucose and a variety of amino acids and growth factors are abundant resulting in nucleotide, lipid and protein synthesis, preparing the cell for growth and proliferation (S. G. Kim, Buel, and Blenis, 2013). AMPK, on the other hand, is able to sense shifts in the ration of ATP to AMP, monitoring the energy homoeostasis of the cell. When energy levels decrease, AMPK inhibits mTORC1 activity and induces glucose uptake as well as catabolic processes like fatty acid oxidation to counteract the

lack of ATP. Since its purpose is to monitor whether the metabolic prerequisites to support high levels of cellular activity are met, mTOR activity is of major importance for many activated immune cells (Xu *et al.*, 2012). Unsurprisingly, high mTOR activity is found in immune cells that favour aerobic glycolysis over oxphos like CTLs, activated NK cells and several T helper subsets. Simultaneously, resting or anti-inflammatory immune cells are driven by oxidative metabolism (Donnelly and Finlay, 2015).

1.3.1 B cell and plasma cell metabolism

While more and more researchers focussed on immunometabolism, research on the B cell metabolism was lacking. In a review from 2014, the knowledge on B cell metabolism could be summarised in six sentences, suggesting that B cells may or may not behave similarly to their T cell relatives (Ganeshan and Chawla, 2014). In the same year, one of the earlier studies tackling B cell metabolism could show that, unlike T cells, B cells upregulated both glycolysis and oxphos after LPS stimulation (Caro-Maldonado *et al.*, 2014). However, this study focussed on the first 24 h of the B cell reaction and had no implications on the variety of other stages and subpopulations of B cells described above. Only in recent years, in parallel to this work, has research started to gain a broader view of the metabolism of B cells and plasma cells, not least due to the work of Julia Jellusova.

In one of the first compelling articles about B cell metabolism, Jang *et al.* (2015) dissected the mitochondrial status of B cells during activation. Tracking the mitochondria of B cells after activation with LPS and IL-4 *in vitro*, the data revealed a sharp increase in mitochondrial mass after 1 d followed by a steady decrease during the next 3 d. Further analysis showed that the MitoTracker^{high} population consisted of around 25 % class-switched B cells but only few CD138^{+} plasmablasts, while the MitoTracker^{low} population was made up of over 50 % of CD138^{+} plasmablasts but only few class-switched B cells (Jang *et al.*, 2015). Looking into the germinal centre reactions after immunisation, an even clearer correlation was found *in vivo*. The group provided evidence that the higher concentration of reactive oxygen species (ROS) found in MitoTracker^{high} cells led to the activation of the transcriptional regulator Bach2, which then inhibited the activation of Blimp-1, one of the master regulators for plasma cells. Interestingly, treating the B cells with the glycolysis inhibitor 2-deoxy-glucose (2-DG) *in vitro* led to a sharp decrease in the frequency of CD138^{+} plasmablasts and kept the B cells at high mitochondrial mass (Jang *et al.*, 2015). The importance of mitochondrial ROS was further supported by Akkaya *et al.* (2018), showing that the sharp increase in ROS production after BCR ligation led to potentially lethal intracellular calcium levels that could only be rescued by second signals via T cell help or TLR signalling.

The impact of one of the crucial pathways in B cell signalling, the phosphoinositide 3-kinases (PI3K) pathway, on B cell metabolism was nicely reviewed by Jellusova and Rickert (2016). The article shows how the stimulation of several receptors like the BCR, CD40, IL-4 receptor or BAFF receptor regulate metabolism either directly by activating glycolytic enzymes like HK and PFK or indirectly via activation of mTOR signalling pathways. However, glucose is not only used to fuel glycolysis. During proliferation,

glucose is used for lipogenesis, providing metabolites for the expansion of the membrane network (Dufort *et al.*, 2014). Interfering with glucose metabolism using 2-DG was shown to affect B cells during the germinal centre reaction, but had little effect on the overall frequency of B cells or follicular helper T cells (Jellusova, Cato, *et al.*, 2017). This finding further supports the notion that, while B cells upregulate both glucose uptake as well as oxphos shortly after activation (Caro-Maldonado *et al.*, 2014; Akkaya *et al.*, 2018), the ability to use glucose to support proliferation and plasma cell differentiation is vital for the function of activated B cells.

Surpassing even activated B cells, plasma cells were shown to take up massive amounts of glucose (Lam, Becker, *et al.*, 2016). However, around 90 % of the glucose taken up by plasma cells is used for glycosylation instead of energy generation, coupling the glucose uptake with the biosynthesis and modification of proteins like antibodies. Interestingly, plasma cells can be dissected into two subpopulations based on their glucose uptake (Lam, Jash, *et al.*, 2018). Plasma cells with high glucose uptake show a 5-fold increase in antibody production but appear to be longer lived as well. Using BrdU feeding experiments, Lam, Jash, *et al.* (2018) could show that high glucose uptake correlated with longer half life. In addition, the retention of these cells after immunisation was longer compared to plasma cells with lower glucose uptake. One of the reasons for the longevity of this subpopulation seems to be their increased use of glucose for mitochondrial metabolism, making them more robust in comparison to their shorter-lived counterparts (Lam, Becker, *et al.*, 2016). In addition to the high glucose levels, LLPCs also show higher expression of amino acid transporters like CD98 and higher levels of autophagy (Lam, Jash, *et al.*, 2018). As mentioned before, autophagy enables plasma cells to deal with aggregates of unfolded proteins and supports a constant flow of nutrients from the breakdown of cellular compartments (Pengo *et al.*, 2013). Both of these actions are most important in LLPCs, making autophagy an essential factor in these cells (Cenci, 2014). In conclusion, plasma cells depend on massive glucose uptake to support protein production and modification as well as energy generation. Similar to B cells, plasma cells also make use of oxphos despite having rather low mitochondrial mass. Both of these factor are especially important for LLPCs to provide for a robust metabolism.

1.4 Aim of the study

Due to the striking evidence for the importance of metabolism in other immune cells, this thesis aims to investigate the metabolic changes during the differentiation of B cells towards plasma cells. Focussing on glucose metabolism and taking into account the vast heterogeneity of B cells and plasma cells described above, glucose uptake and mitochondrial mass were assessed in different *in vitro* settings and in an autoimmune mouse model. Using inhibitors of glycolysis, the metabolic profile as well as the therapeutic potential of the inhibitors were evaluated. More detailed insights into the glucose metabolism of plasma cells were obtained trying to elucidate the mechanism of the inhibitors.

2 Materials and Methods

2.1 Materials

2.1.1 Consumeables

Material	Source
Cell culture flasks	Greiner bio-one
Cell culture plates, flat bottom, 6/24/48-well	Greiner bio-one
Cell culture plate, round bottom, 96-well	Greiner bio-one
Cell strainer 70 µm	Greiner bio-one
Disposable Reagent Reservoir	Corning
ELISA plate 96-well plate, flat bottom	Corning
ELISA plate sealers	R&D Systems
FACS tubes 5 mL	Becton Dickinson
Falcon tube 15 mL and 50 mL	Greiner bio-one
Filter tips (10 µL, 20 µL, 100 µL, 1000 µL)	Sarstedt
Glass sildes faint edge	Carl Roth
Gloves Nitra-Tex	Ansell
MACS LS, LD, MS columns	Miltenyi Biotec
Petri dish	Greiner bio-one
Reaction tube (500 µL, 1.5 mL and 2 mL)	Sarstedt
Serological pitettes (5 mL, 10 mL, 25 mL)	Sarstedt
Syringe 10 mL plastic	Becton Dickinson

2.1.2 Chemicals and Kits

Chemicals/Kits	Source
Annexin V binding buffer	Biolegend
B Cell Isolation Kit, mouse	Miltenyi Biotec
Bovine Serum Albumin (BSA)	Sigma-Aldrich
Dimethyl sulfoxide (DMSO)	Sigma-Aldrich
Ethylenediaminetetraacetic acid (EDTA)	Sigma-Aldrich
EasySep B cell isolation kit, mouse	Stemcell Technologies
KCl	Sigma-Aldrich
KH_2PO_4	Sigma-Aldrich
NaCl	Merck Millipore

Na_2HPO4	Sigma-Aldrich
NaOH	Merck Millipore
Penicillin streptomycin	Thermo Fisher Scientific
2-Propanol (70 %)	Otto Fischer
Super Block	Thermo Fisher Scientific
Tris Base	Sigma-Aldrich
True-Nuclear Transcription Factor Buffer Set	Biolegend
Tween 20	Sigma-Aldrich

2.1.3 Buffers

Solution	**Composition**
Dilution buffer (DB)	45 mL ELISA washing buffer 5 mL Super Block solution
ELISA washing buffer (WB)	100 mL 10x Tris-buffered Saline 900 mL nanopure H_2O 500 µL Tween 20
MACS buffer	1 L PBS/BSA (0.5 %) 2 mM EDTA
PBS	8 g NaCl 0.2 g KCl 1.44 g Na_2HPO_4 0.24 g KH_2PO_4 pH 7,4 1 L nanopure H_2O
PBS/BSA 0.5 %	1 L PBS 5 g BSA
Tris-buffered saline, 10x	15.125 g Tris Base 43.8 g NaCl 1 L nanopure H_2O pH 7,2

2.1.4 Cell Culture

Component	Source
β-Mercaptoethanol	Thermo Fisher Scientific
Fetal calf serum (FCS)	Thermo Fisher Scientific
Glucose solution	Thermo Fisher Scientific
Lipopolysaccherides (LPS)	Sigma-Aldrich
Roswell Park Memorial Institute (RPMI) 1640 with 11 mM glucose or glucose free	Thermo Fisher Scientific

2.1.5 Cytokines, Enzymes and Standards

Component	Source
Interleukin-4 (IL-4)	Biolegend
Interleukin-6 (IL-6)	Biolegend
Horseradish Peroxidase	Thermo Fisher Scientific
Mouse Reference Serum	Bethyl

2.1.6 Antibodies and Fluorescent Dyes

Unless stated otherwise, all antibodies used were targeted against mouse antigens.

Antibody or Dye	Conjugate	Conc. [µg/100 µL]	Clone	Source
2-NBDG	dye	342		Thermo Fisher Scientific
B220	A405	1	RA3-6HB2	generated at ISEF
B220	BV711	0.5	RA3-6HB2	Biolegend
B220	A647	0.625	RA3.B2	generated at ISEF
CD138	BV421	0.5	281-2	Biolegend
CD138	PE	1	281-2	Biolegend
CD138	APC	1	281-2	Biolegend
CD16 / CD32	unlabelled	1.6	2.4.G2	Becton Dickinson
CD19	APC	0.2	6D5	Biolegend
CD19	BV785	0.5	6D5	Biolegend
CD43	APC Fire 750	1	S11	Biolegend
CD95	BV605	1	SA367H8	Biolegend
Fixable Viability Dye	dye	1:1600		Thermo Fisher Scientific
GL7	PE-Cy7	2	GL7	Biolegend
IgA	biotin	0.1	polyclonal	Southern Biotech
IgA	unlabelled	10	polyclonal	Southern Biotech
IgA	FITC	1	mA-6E1	Thermo Fisher Scientific

IgD	A405	2.2	11.26.c.2a	generated at ISEF
IgD	Pacific Blue	2.5	11.26.c.2a	Biolegend
IgG	PE-Cy7	1	polyclonal	Biolegend
IgG1	biotin	0.1	polyclonal	Southern Biotech
IgG1	unlabelled	10	polyclonal	Southern Biotech
IgG1	PE-Cy7	0.5	RMG1-1	Biolegend
Igκ	PE	1	RMK-45	Biolegend
IgM	biotin	0.1	polyclonal	Southern Biotech
IgM	unlabelled	10	polyclonal	Southern Biotech
IgM	BV510	4	RMM-1	Biolegend
IgM	A647	2	M41	Biolegend
LAMP-1	A488	1.25	1D4B	Biolegend
MitoTracker	dye	0.00067		Thermo Fisher Scientific
TACI	APC	0.5	ebio17B7	Biolegend
Ubiquitin	A647	2.5	P4G7	Biolegend
XBP-1s	BV421	0.5	Q3-695	Becton Dickinson

2.1.7 Technical Equipment

Equipment	**Source**
CASY cell counter	OMNI Life Science
Centrifuge 58105	Eppendorf
Centrifuge Allegra X-22R	Beckman Coultier
Centrifuge Microfuge 22R	Beckman Coultier
EasyEights Magnet	Stemcell Technologies
EasySep Magnet	Stemcell Technologies
ELISA Immuno Wash	Capp ApS
ELISA reader FLUOstar Omega	BMG Labtech
Flow cytometer LSR II	Becton Dickinson
Freezer −80 °C	Sanyo
Fume cupboard	Waldner
Incubator	Integra Bioscience
Labgard Biological Safety Bench Class II	Nuaire
MACS Multistand	Miltenyi Biotec
Magnet MACS Midi	Miltenyi Biotec
Magnets Easy Sep and Easy Eights	Stemcell Technologies
Microcentrifuge	Carl Roth
Microscope EC3	Leica
Neubauer Chamber Assistent	Karl Hecht
Ultrasonic Bath Sonorex TK-20	Bandelin
pH meter Toledo	Mettler
Pipette filler Pipetus	Hirschmann

Pipettes Research Plus	Eppendorf
Scale	Satorius
Water Bath SW-20-c	Julabo
Vortex Genie	Scientific Industries

2.1.8 Software

Software	**Source**
FACSDIVA	Becton Dickinson
FlowJo 10	FlowJo LLC
MARS Data Analysis Software	BMG Labtech
Prism 6	Graph Pad

2.1.9 Mice

Organs for cell cultures were mainly taken from female C57BL/6 (BL6) mice 3-4 months of age. Mice were purchased from Charles River Laboratory (Sulzfeld, Germany) and kept under special-pathogen-free (SPF) conditions until sacrifice. B6(Cg)-IL10$^{tm1.1Karp}$/J mice (VertX mice / IL-10 reporter mice) were used to determine IL-10 expression in cells. In these mice, the enhanced green fluorescent protein (eGFP) gene is integrated downstream of the IL-10 gene resulting in eGFP expression upon transcription of the IL-10 gene. For *in vivo* studies, B6.NZM-Sle1$^{NZM2410/Aeg}$ Sle2$^{NZM2410/Aeg}$ Sle3$^{NZM2410/Aeg}$/Lmoj (BcN) mice were used. These mice were bred under SPF conditions and used at 3-4 months of age. Due to the three lupus susceptibility quantitative trait loci (QTL) *Sle1*, *Sle2* and *Sle3*, BcN mice develop lupus-like symptoms like the production of anti-dsDNA antibodies and fatal glomerulonephritis (Morel *et al.*, 2000). The breeding and experiments with BcN mice were approved by the Ministry of Energy, Agriculture, the Environment, Nature and Digitalization (numbers V122-39 (84-8/19) and (31-3/19)).

2.2 Methods

2.2.1 Generation of Single Cell Suspensions

To generate single cell suspensions used for subsequent flow cytometric staining and cell culture experiments, mouse spleen and bone marrow were used. If the cells were supposed to be used for cell culture experiments, all steps were carried out in a sterile biological safety cabinet. In case of spleen and lymph nodes, the organs were mashed on ice in a petri dish containing cold PBS/BSA 0.5 % between two glass slides. The suspension was then filtered using a 70 µm cell strainer, filled up to 50 mL (spleen) with PBS/BSA 0.5 % and centrifuged at 400 g for 10 min at 4 °C. Afterwards, the supernatant was discarded and the remaining cell pellet resuspended in an appropriate buffer for further experiments. Cells were then counted with a Neubauer chamber.

For bone marrow cells, surrounding tissue was removed from tibia, fibula and femur. The bones were cut open at the ankle or hip joint, respectively. The bones were bent with the openings pointing downwards and placed in 1000 µL pipette tips. The tips were placed in 15 mL tubes and centrifuged at 1800 g for 5 min at 4 °C. Afterwards, the tips were discarded and the cell pellet resuspended and counted with a Neubauer chamber or CASY cell counter.

2.2.2 Cell counting

To determine the number of cells in a suspension to either prepare a new experiment or analyse a finished one, two different methods were used - trypan blue viability assay in a Neubauer chamber and the CASY cell counter. While both methods produced reliable results, the two techniques were not used interchangeably. Either one of the methods was used from generating a single cell suspension to the final analysis of an experiment to avoid systemic errors.

Neubauer chamber

For the Neubauer chamber, an aliquot of the cell suspension was taken and diluted with trypan blue. For spleen and bone marrow cell suspensions, 1:10 dilutions were performed. Samples from cell culture were diluted 1:2. Due to their intact membrane, trypan blue is unable to infiltrate live cells but stains the intracellular proteins of dead and apoptotic cells. Under a light microscope, only the living, white cells are counted. The cell concentration is calculated using the mean number of cells in each square:

$$\text{Dilution factor} * \text{mean cell number} * \text{chamber factor} = \text{cell concentration [cells/mL]}$$

CASY cell counter

To improve the reproducibility and speed of cell counting, a CASY cell counter was used. The CASY uses a capillary with a small opening through which the cell suspension can be sucked in. An electric field is created by placing on electrode within the capillary and one on the outside. When cells enter the capillary, deviations in the electric filed can be detected. Due to their intact membrane, live cells pose a big electric resistance while dead cells lose the resistance of their cytoplasmic membrane. Only the small nucleus can still be detected. Using the volume of the cell suspension that was sucked in the capillary and the number of cells that have passed the electric field, the concentration of cells in a cell suspension is calculated. Due to the automated process, counting cells with the CASY is less susceptible to different handling and therefore increases the reproducibility of the counting. For spleen and bone marrow, 30 µL of cell suspensions were diluted in 10 mL of the CASYton buffer. For the analysis of cell culture experiments, 100 µL of cell suspensions were used.

2.2.3 B Cell Isolation via Magnetic Cell Separation

Magnetic Activated Cell Sorting (MACS) is a method to isolate cells by labelling them with antibodies coupled to magnetic beads and retaining the labelled cells within a magnetic field. For positive isolation, cells of interest are labelled with magnetic beads, retained in the magnetic field and later eluted. For negative isolation, all cells except the population of interest are labelled and retained in the magnet. While the magnet retains all irrelevant cells, the untouched cells of interest pass the magnetic field and can be collected and used for further experiments. All cell isolation used for this thesis was done by negative selection to avoid signalling induced by the labelled antibodies. B cell isolation kits from two different suppliers were used with identical results.

Column-based - Miltenyi Biotec

The B cell isolation with the kit from Miltenyi Biotec was performed at 4 °C. The number of live cells in a freshly prepared single cell suspension (see section 2.2.1) was determined as described in section 2.2.2 and centrifuged at 300 g for 10 min at 4 °C. The supernatant was discarded and the pellet resuspended in 40 µL of pre-cooled and degassed MACS buffer per 1×10^7 cells. 10 µL of the Biotin-Antibody Cocktail per 1×10^7 cells were added to label unwanted cells. The antibody cocktail consists of antibodies against CD43 (expressed on plasma cells, activated B cells and several other non-B lineage cells like granulocytes and NK cells), CD4 (expressed on T cells and some monocytes and macrophages) and Ter-119 (expressed on erythrocytes). The suspension was then mixed and incubated for 5 min at 4 °C. After the incubation, 30 µL of MACS buffer were added per 1×10^7 cells to dilute the antibody-cocktail. 20 µL of Anti-Biotin MicroBeads per 1×10^7 cells were then added to the suspension to mark the undesired, labelled cells with magnetic beads. After mixing, the suspension was incubated for 10 min at 4 °C. LS columns were placed in the magnet and flushed with 3 mL of MACS buffer. The cell suspension was adjusted to a minimum volume of 500 µL and up to 1×10^8 labelled cells were applied onto each column. The flow-through was collected in a 15 mL tube. After the cell suspension had passed the column in its entirety, the column was washed three times with 2 mL MACS buffer each. The flow-through was collected as well and pooled with the other suspensions. The cell concentration was determined and suspension centrifuged at 300 g for 10 min at 4 °C. The supernatant was discarded and the pellet stored for subsequent use in cell culture or staining.

Tube-based - Stemcell Technologies

The B cell isolation with the kit from Stemcell Technologies follows a similar procedure but is performed at RT. The number of cells in a fresh single cell suspension (see section 2.2.1) was determined and the suspension adjusted to a concentration of 1×10^8 cells/mL. 50 µL/mL rat serum was added to the suspension to block unspecific binding of the antibody-cocktail. The required sample volume was transferred into a 5 mL tube and 50 µL/mL Isolation Cocktail added. The suspension was mixed and incubated for

10 min at RT. After mixing for 30 s, 75 µL/mL of sample of RapidSpheres were added to the suspension and incubated for 2.5 min at RT to add magnetic beads to the antibody-labelled cells. The suspension in the tube was then topped up to a volume of 2.5 mL and placed in the EasySep magnet where the suspension was left to rest for another 2.5 min. After the bead-labelled cells had moved to the tube wall, the cell suspension was poured into another tube in a continuous motion. To increase the yield of the isolation system, the last two steps were repeated twice with fresh MACS buffer. After isolation, the cell concentration was determined and the suspension centrifuged at 300 g for 10 min at 4 °C. The supernatant was then discarded and the cell pellet used for subsequent cell culture experiments.

2.2.4 Isolated B Cell Culture

To understand longer-term effects on the differentiation of B cells towards plasmablasts, isolated B cells were cultured for 5 d. All cell culture work was carried out using a biological safety bench. RPMI 1640 medium was supplemented with 10 % fetal calf serum (FCS), 1 % penicillin/streptamycin and 50 µM β-mercaptoethanol. The mixture was warmed up to 37 °C in a water bath. In a 48-well plate, 400 µL of warm RPMI 1640 medium per well was supplemented with 10 µg/mL LPS and different inhibitors like 200 µM 2-DG or 10 nM rapamycin. Doublets were used for all experimental conditions to minimise variation arising in the cell culture. After the treatment master mix was added to the plate, a pellet of isolated B cells (see section 2.2.3) was resuspended in warm RPMI 1640 medium to a concentration of 5×10^6 cells/mL. 100 µL of the cell suspension was added to each well resulting in 5×10^5 cells/well. The plate was then mixed carefully by pivoting the plate and incubated at 37 °C for 5 d in 5 % CO_2. In the B cell culture data provided by Sandra Hilberath, only 2.5×10^5 cells/well were used, increasing the differentiation of B cells to plasmablasts. During the incubation, the cell growth was regularly checked via microscope. After the incubation, cells were resuspended in the medium by mixing with a pipette. The cell suspension was transferred into 1.5 mL tubes and centrifuged at 300 g for 10 min. The supernatant was transferred into another tube and stored for ELISA while the cell pellet was used for flow cytometric staining.

2.2.5 Spleen cell culture

To assess the impact of metabolites and metabolic inhibitors on terminally differentiated plasma cells generated *in vivo*, a 48 h spleen cell culture was established. All cell culture work was carried out using a biological safety bench. Similar to the long-term LPS culture, RPMI 1640 medium was supplemented with 10 % FCS, 1 % penicillin/streptamycin and 50 µM β-mercaptoethanol and kept warm at 37 °C in a water bath. Depending on the experimental setup, glucose-free RPMI 1640 was used and supplemented with glucose and mannose according to the setup. Unlike the long-term culture, no stimulant was used to activate the cells. In a 48-well plate, 250 µL of warm RPMI 1640 medium was supplemented with 10 ng/mL IL-6 to prolong the half-life of the plasma cells. Depending on the hypothesis, different metabolites (glucose, mannose and non-essential

amino acids) or inhibitors (2-DG, 2-FDG, bortezomib and tunicamycin) were added to the master mix. Doublets were used for all experimental conditions to minimise the variation in the cell culture. After the master mix was added to the plate, a pellet of spleen cells (see section 2.2.1) was resuspended in warm RPMI 1640 medium at a concentration of 1×10^7 cells/mL. 250 µL of the cell suspension was then added to the master mix resulting in a cell number of 2.5×10^6 cells/well. The cells were then distributed evenly by pivoting the plate and incubated for 24 h at 37 °C and 5 % CO_2. In experiments where glucose-free medium was supplemented with glucose or mannose, cells were left to rest for 24 h at 37 °C to adapt to the new sugar concentrations. After the resting phase, treatments were applied and incubated for another 24 h before they were analysed. After the treatment, cells were resuspended in the plate by mixing with a pipette. The cell suspension was transferred into 1.5 mL tubes and centrifuged at 300 g for 10 min. The supernatant was transferred into another tube and stored for ELISA while the cell pellet was used for flow cytometric staining.

2.2.6 Flow cytometry

Flow cytometry is a method used to characterise cells based on their size, granularity and expression of different surface proteins and intracellular molecules. Cells are labelled with fluorophore-coupled antibodies or compartment-specific dyes and which emit light after excitation via a laser. The emitted light is measured in a flow cytometer, compensated in case of spectral overlap and analysed using software (FlowJo).

Metabolic staining

To assess the glucose uptake and the mitochondrial mass of the B cell and plasma cell populations in flow cytometry, two metabolic dyes were used. The fluorescent glucose analogue 2-(N-(7-Nitrobenz-2-oxa-1,3-diazol-4-yl)Amino)-2-deoxyglucose (2-NBDG) was used to determine the glucose uptake while a group of dyes called MitoTracker was used to stain mitochondria. Both dyes were on the live cells before surface staining. To stain cells with 2-NBDG and/or MitoTracker, a cell pellet of whole spleen cells (see section 2.2.1) or cells from a cell culture experiment (see section 2.1.4) was resuspended in 200 µL warm RPMI 1640 medium with 11 mM glucose. 100 µM 2-NBDG and 10 nM MitoTracker were added to the warm suspension and incubated at 37 °C for 20 min. After the incubation, the dyes were washed by adding 1 mL of PBS/BSA 0.5 % and centrifuged at 300 g for 10 min at 4 °C. After centrifugation, the supernatant was discarded. While the cells could already be used for analysis, subsequent surface staining multiplies the information generated from the staining. Unfortunately, the signal of 2-NBDG or the MitoTracker Green is not stable after fixation and is therefore lost if an intracellular staining is performed afterwards.

Surface staining

Starting with a cell pellet after metabolic staining or fresh cells from spleen or bone marrow (see section 2.2.1) or cells from a cell culture experiment (see section 2.1.4), Fcγ-receptors were blocked by resuspending the cells in 50 µL (1.6 µg) of anti-CD16/anti-CD32 antibodies. After mixing, cells were incubated at 4 °C for 5 min. In the meantime, a master mix of all relevant staining antibodies was generated in PBS/BSA 0.5 % to reduce variances in handling. After the incubation, 50 µL of the master mix was added to each tube. For unstained samples, FMO and isotype matched FMO controls, 50 µL PBS/BSA 0.5 % was added and antibodies pipetted individually. The cells were then incubated for 10 min at 4 °C in the dark. The cells were then washed by adding 1 mL PBS/BSA 0.5 % and centrifuged at 300 g for 10 min at 4 °C. After centrifugation, the supernatant was discarded and the cells resuspended in a reasonable amount of PBS/BSA 0.5 % (200 µL to 400 µL) for measurement at the LSR II flow cytometer.

Intracellular staining

In case intracelluar proteins were targeted for staining, further steps had to be performed. For this thesis, staining the transcription factor XBP-1s required an intranuclear staining. For intranuclear stainings, the True-Nuclear Transcription Factor Buffer Set from Biolegend was used. Instead of resuspending the cell pellet in PBS/BSA 0.5 % as the last step of the surface staining, cells were fixed using 300 µL of a formaldehyde solution called True-Nuclear Fix Buffer. The suspension was mixed and incubated in the dark for 45 min at RT. After incubation, 1 mL of True-Nuclear Perm Buffer was added and centrifuged 300 g for 10 min at RT. In the meantime, a master mix of all staining antibodies was generated by diluting the antibodies in perm buffer. After centrifugation, the supernatant was discarded and the pellet resuspended in 100 µL of master mix. For staining controls (isotype matched FMO, single stainings and unstained), the pellet was resuspended in 100 µL of perm buffer and antibodies were added individually. Treatment with the saponin-containing perm buffer results in small ruptures in the plasma membrane as well as the nuclear membrane through which antibodies can enter the cell. After incubation for 30 min at RT, 1 mL of perm buffer was added and centrifuged at 300 g for 10 min at RT. The supernatant was discarded and the cell pellet resuspended in an appropriate amount of PBS (200 µL to 400 µL) for measurement at the LSR II flow cytometer.

2.2.7 ELISA

To quantify the amount of different antibody classes in cell culture supernatant, a sandwich luminescence enzyme-linked immunosorbent assay (ELISA) was applied. The protocol was designed to detect mouse IgM, IgG and IgA antibodies. First, the capture antibody was diluted in tris saline to a contraction of 10 µg/mL. 50 µL/well of the antibody solution was added to a white, high binding 96-well plate and incubated overnight at 4 °C. After incubation, the plate was washed six times with a tris saline based wash-

ing buffer containing 0.5 % Tween 20. Afterwards, each well was filled with 100 µL of blocking buffer and incubated for 60 min at RT on a tumbling shaker. In the meantime, the sample and standard dilutions were prepared in a separate round well plate. After blocking, the buffer was discarded and 30 µL of the samples and standard dilution were transferred to the white plate. Doublets were used to minimise variation. After incubation for 30 min on a tumbling shaker at RT, the plate was washed six times with washing buffer. The biotinylated detection antibody was diluted to a concentration of 100 ng/mL. 30 µL of the detection antibody solution was added to each well and incubated for 20 min on a tumbling shaker at RT. After incubation, the plate was washed six times with washing buffer. To detect the biotinylated antibodies, a solution of stretavidin-labelled horseradish peroxidase (HRP) with a concentration of 50 ng/mL was generated. 30 µL/well of the solution was applied onto the plate and incubated for 25 min on a tumbling shaker at RT. After incubation, the plate was washed ten times and filled up with 200 µL of tris saline to stop the plate from drying. The luminol-based substrate solution was then prepared (Super Signal ELISA Substrate, Thermo Fischer). After discarding the tris saline solution, 150 µL of substrate solution was applied per well and the plate measured on a plate reader. The data was then analysed with the MARS analysis software using a 5-parameter fit to correlate the luminescence signal and the concentration.

2.2.8 *In vivo* administration of 2-DG and Bortezomib

Treatment with 2-DG

To evaluate the impact of 2-DG treatment *in vivo*, an autoimmune mouse model was employed. Due to their genetic modification, BcN mice develop lupus-like symptoms like plasmacytosis and glomerulonephritis. At an early age of three to four months, BcN already show a severe increase in plasma cell numbers. Since the disease progression is different in males and females, only females were used for the *in vivo* experiments. For the treatment, mice were injected intraperitoneally (i.p.) with a 2-DG solution or PBS as vehicle control. The concentration of 500 mg/kg bodyweight of 2-DG as well as the treatment interval were chosen based on a recent paper (Jellusova, Cato, *et al.*, 2017). 2-DG was solved in PBS at a concentration of 50 mg/mL resulting in an injection volume of 10 µL/g bodyweight. 3-4 months old BcN mice were weighted on day 0 and i.p. injected with 2-DG or PBS daily for three consecutive days. On day four, the mice were anaesthetised and killed by cervical dislocation. Spleen and bone marrow were taken and stored on ice for subsequent analysis.

Treatment with 2-DG and bortezomib

In a second experiment, the drug-sparing capacity of 2-DG was assessed. As in the treatment with only 2-DG, mice were i.p. injected on three consecutive days. However, mice were injected with either bortezomib or a combination of bortezomib and 500 mg/kg 2-DG. For the bortezomib treatment, a rather low concentration of 0.2 mg/kg was chosen

to avoid elimination of the plasma cells by bortezomib alone. A bortezomib solution with a concentration of 0.02 mg/mL was generated and either used on its own or after adding 50 mg/mL 2-DG to create a co-treatment. As before, 10 µL/g bodyweight were injected on three consecutive days. On day four, the mice were anaesthetised and killed by cervical dislocation. Spleen and bone marrow were taken and stored on ice for subsequent analysis.

2.2.9 Statistical analysis

Figures and graphs were created using the FlowJo software for FACS plots and GraphPad Prism 6 for the statistical analysis of the data. Data are presented as mean ± SEM (standard error of the mean). Cell culture experiments were designed to generate paired data, increasing the statistical power of the experiments. Therefore, paired student T-tests were used to compare two groups and one-way repeated measures ANOVA to compare more than two groups. The data provided in the *in vivo* animal experiments are not paired. Therefore, unpaired student T-test and one-way ANOVA were used. Statistical significance was marked as: *: $p < 0.05$; **: $p < 0.01$; ***: $p < 0.001$ and ****: $p < 0.0001$.

3 Results

3.1 Plasma cells show high glucose uptake while having low mitochondrial mass

To obtain a first overview of the glucose uptake and the mitochondrial metabolism in plasma cells, cells from spleen and bone marrow from C57BL/6J mice were incubated with the fluorescent glucose analogue 2-NBDG and the mitochondrial dye MitoTracker (Fig 5). The 2-NBDG uptake is a measure for the glucose demand (Teslaa and Teitell, 2014; O'Neil, Wu, and Mullani, 2005), while the MitoTracker staining reveals the mitochondrial mass of the cells (Agnello, Morici, and Rinaldi, 2008; Chazotte, 2011).

The 2-NBDG staining revealed two distinct populations of $CD138^{high}$ plasma cells in both spleen (Fig. 5A) and bone marrow (Fig. 5C). In spleen, plasma cell populations of roughly equal size were found showing either intermediate (2-$NBDG^{int}$) or high (2-$NBDG^{high}$) glucose uptake. Similar populations were found in bone marrow where the 2-$NBDG^{high}$ plasma cells were dominant, making up around 75 % of all plasma cells in the tissue (Fig. 5B and D). It is likely that 2-$NBDG^{high}$ plasma cells resemble LLPCs, since the bone marrow is known to be rich in LLPCs. This idea was supported in a recent paper, correlating glucose uptake and longevity (Lam, Jash, *et al.*, 2018).

Comparing plasma cells with $CD19^{+}$ B cells, the glucose uptake of plasma cells clearly exceeded that of the B cells (Fig. 5F). Simultaneously, the plasma cells showed a more than 10-fold lower mitochondrial staining than the B cells (Fig. 5E). While the MitoTracker staining does not show mitochondrial activity but only mitochondrial mass or volume, this was a first indication that plasma cells might utilise mitochondrial metabolism to a much lower extend than the naive B cells.

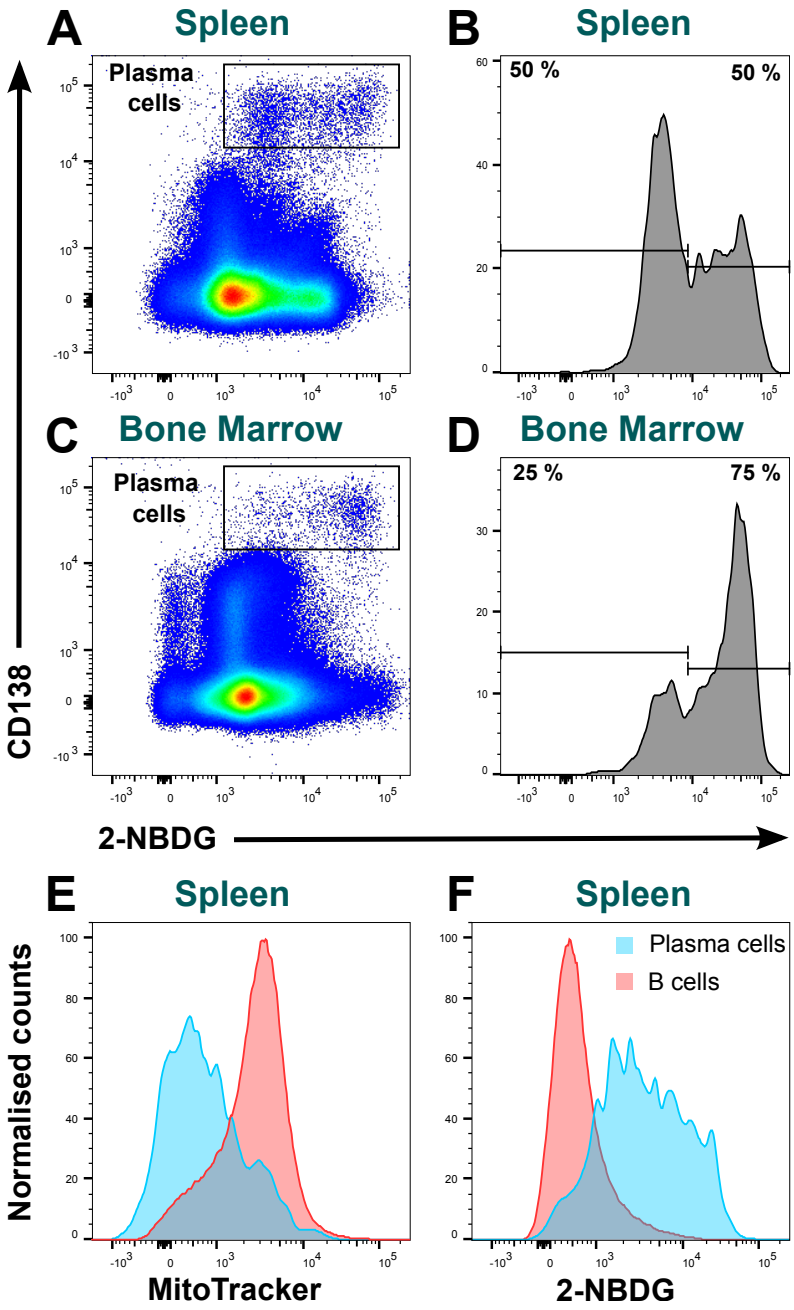

Figure 5: Glucose uptake and mitochondrial mass of spleen and bone marrow cells. Leukocytes were isolated from spleen and bone marrow, stained with anti-CD138 antibodies and incubated for 20 min with fluorescent glucose-analogue 2-NBDG and MitoTracker Deep Red to determine the glucose uptake and mitochondrial mass. Subsequently, cells were analysed by flow cytometry. Dead cells, debris and doublets were excluded from analysis using a life/dead staining and the forward/sideward scatter. Gating for $CD138^{high}$ plasma cells is indicated. Glucose-uptake of splenic plasma cells is shown in A) 2-D Plot and B) histogram. Glucose uptake of bone marrow plasma cells is shown in C) 2-D plot and D) histogram. Splenic plasma cells and B cells were compared regarding their respective E) mitochondrial mass and F) glucose uptake. Graphs shown are representative examples of 3 independent experiments using 6 mice total.

3.2 Glycolysis and mTORC1 inhibition drastically reduce the ability to generate plasmablasts *in vitro*

Since the first experiment hinted at the importance of the glucose metabolism, an LPS stimulated 5 d B cell culture was established to assess the importance of glycolysis on the generation of plasmablasts. Due to its nutrient sensing capability and involvement in catabolic processes like glycolysis, the impact of mammalian target of rapamycin complex 1 (mTORC1) inhibition was analysed as well. 2-DG was used to inhibit glycolysis at an early stage and rapamycin was added to block mTORC1 activity and simulate nutrient deprivation. To enable the analysis of the anti-inflammatory IL-10 response, spleen B cells were isolated from VertX IL-10 reporter^{egfp} mice and stimulated and treated for 5 d.

Both 2-DG and rapamycin were used at concentrations that did not affect the overall number of live cells (consisting of B cells and plasmablasts) (Fig. 6A). However, both inhibitors severely decreased the number of plasmablasts generated in the culture at day 5 compared to control (Fig. 6B). Since the treatments started at day 0, this experimental setup can not differentiate between the inhibitors acting on B cells, limiting their ability to differentiate into plasmablasts, and the inhibitors acting on the plasmablasts, limiting their survival or proliferation.

In addition to the plasmablast generation, the expression of the transcriptional reporter for IL-10 was analysed. Again, both inhibitors had a similar effect, increasing the frequency of IL-10$^+$ cells among B cells from 32 % to 39 % for 2-DG and to 48 % for rapamycin (Fig. 6C). In contrast, 2-DG reduced the frequency of IL-10$^+$ cells among plasmablasts from 45 % to 32 %. Rapamycin on the other hand consistently increased the frequency of IL-10$^+$ cells among plasmablasts to 58 %.

This experiment provided further indication that gylcolysis is of major importance for plasmablasts and plasma cells. Blocking glycolysis hampers with either survival or generation of plasmablasts. B cell survival appears to be less affected by glycolysis inhibition, but IL-10 expression is increased in B cells. IL-10 expression seems to be linked to low mTORC1 activity across plasmablasts and B cells alike, contrasting the distinct impact of glycolysis inhibition on IL-10 expression in these cells.

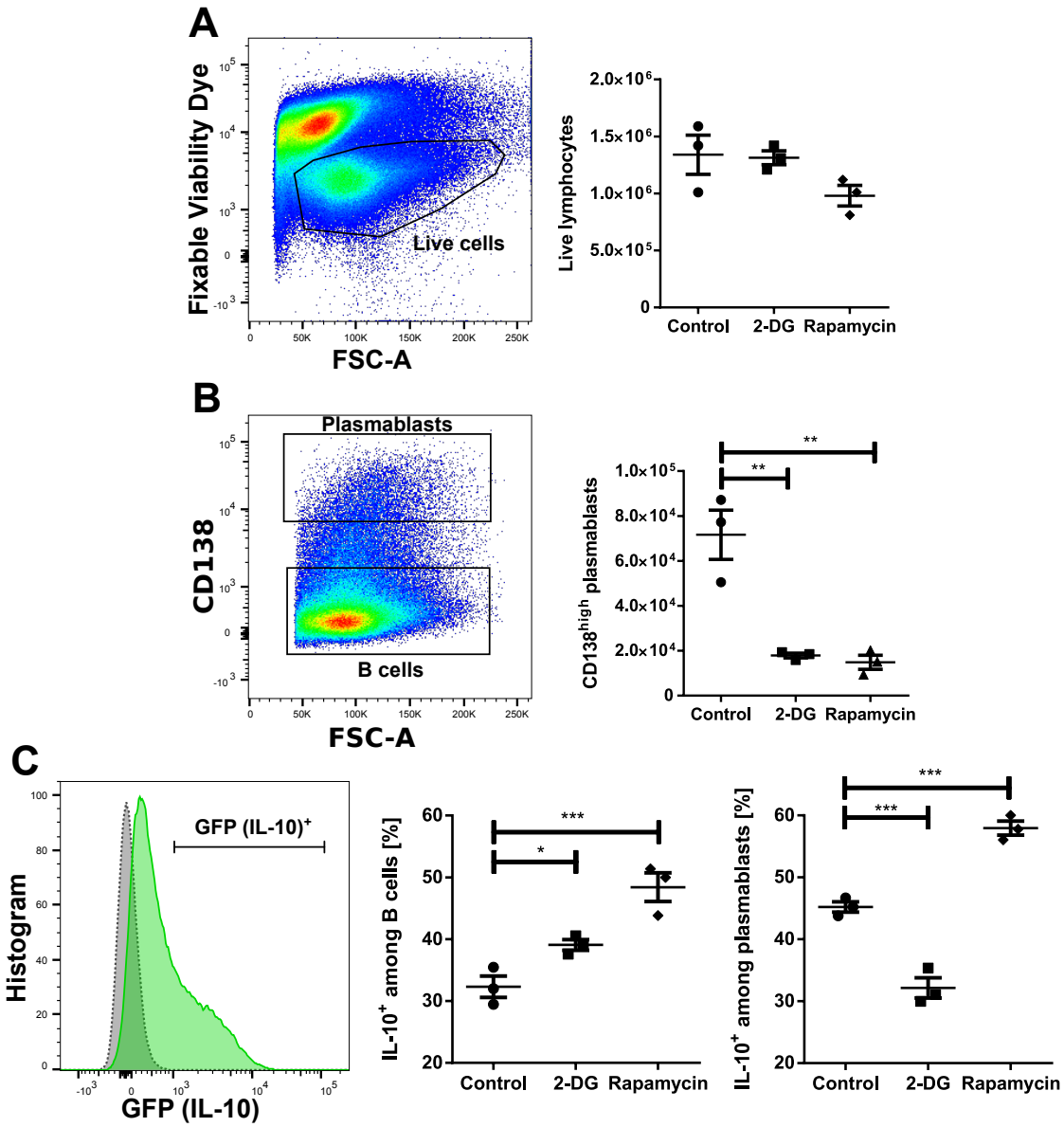

Figure 6: Glycolysis and mTOR inhibition in LPS stimulated B cell culture. B cells from VertX IL-10 reporter^{egfp} mice were isolated and cultured in RPMI 1640 medium containing 10 µg/mL LPS for 5 days. At the start of the culture, 200 µM 2-DG, 10 nM rapamycin or PBS was added. At the end, cells were analysed by flow cytometry. A) Dead cells were excluded from analysis using a viability dye for flow cytometry or trypan blue for counting. B) CD138-expression was used to differentiate plasmablasts from B cells. C) IL-10-expression was analysed measuring the GFP signal of the IL-10 reporter mice. One-way repeated measures ANOVA followed by Dunnett's multiple comparison post test was used to check for statistical significance. *: $p < 0.05$; **: $p < 0.01$; ***: $p < 0.001$. Mean values and SEM are shown ($n = 3$).

3.3 2-DG eliminates terminally differentiated plasma cells

To specify the impact of glycolysis inhibition, whole spleen cells were incubated with 2-DG, a glucose analogue that competes with glucose for uptake and subsequent metabolisation (Xi, Kurtoglu, and Lampidis, 2014; Kurtoglu, Maher, and Lampidis, 2007). The freshly isolated cells were varying doses of 2-DG for only 24 h. To improve the survival of plasma cells, 10 ng/mL of IL-6 was added to the culture. No further stimulant was used.

2-DG treatment led to minor drop in live cells at 1 mM and a major decrease at 5 mM after 24 h treatment (Fig. 7A). B cells were affected only at high concentrations showing a similar drop in frequency compared to all live cells by approximately factor two at 5 mM (Fig. 7B). This result is in line with the observation that 2-DG inhibits the formation of plasmablasts in an LPS culture, but affects B cell survival at relatively low concentrations of 0.2 mM 2-DG only to a minor extend. Primary plasma cells, however, were affected even at 0.2 mM 2-DG suggesting a higher susceptibility compared to B cells (Fig. 7C). Accordingly, 1 mM 2-DG led to a drop in plasma cell frequency of approximately factor 2 (0.2 % to 0.1 %), compared to an only minor impact on B cells (59 % to 54 %. The decrease in plasma cell frequency showed a clear dose-dependency (Fig. 7D).

Carrying on with the observation that 2-DG is able to prevent the formation of plasmablasts in an LPS culture, this experiment shows that 2-DG is able to kill primary plasma cells. Compared with other immune cells of the spleen, like B cells, plasma cells appear to be more susceptible to the treatment. While proliferation of and differentiation to plasma cells would skew the results, these processes are expected to have little influence in this culture system due to the short time span of 24 h and the lack of external stimulants like LPS.

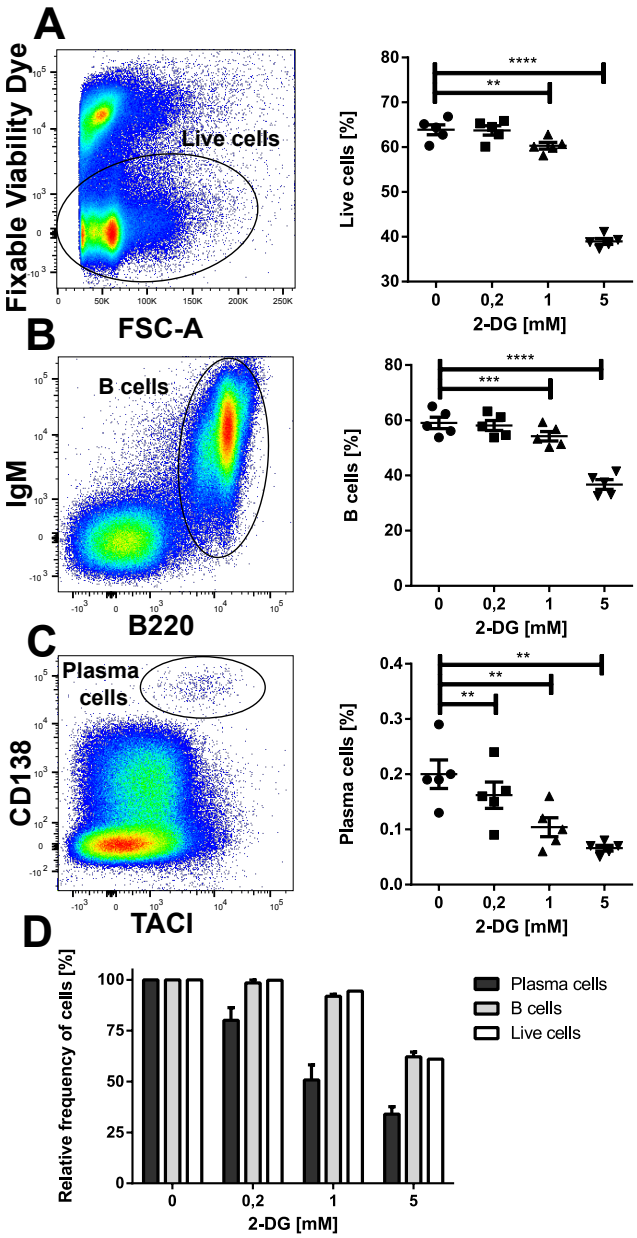

Figure 7: Impact of 2-DG on terminally differentiated plasma cells. Spleen cells were cultivated in RPMI 1640 medium for 24 h in the presence of 10 ng/mL IL-6 to increase survival of plasma cells. Cells were treated with different doses of 2-DG and stained for flow cytometric analysis. Dead cells were excluded from analysis using a viability dye A) Left plot: gating for live cells. Right plot: percentage of live cells. B) Left plot: gating for B cells using B220. Right plot: percentage of B cells among living cells. C) Left plot: gating for $CD138^{high}$ $TACI^{high}$ plasma cells. Right plot: percentage of plasma cells among live cells. D) Impact of 2-DG on plasma cells, B cells and overall viability. One-way repeated measures ANOVA followed by Dunnett's multiple comparison post test was used to check for statistical significance. **: $p < 0.01$; ***: $p < 0.001$; ****: $p < 0.0001$. Mean values and SEM are shown ($n = 5$).

3.4 Combining 2-DG and bortezomib leads to a synergistic decrease in plasma cell frequencies

Since 2-DG was able to reduce the number of plasma cells with little effect on other cell types, the question arose whether 2-DG could be used in combination with other drugs to deplete plasma cells more effectively or with lower side effects. Due to its high efficacy in eliminating plasma cells but severe side effects at high dosages, the proteasome inhibitor bortezomib was chosen as an example to test the drug-sparing capacity of 2-DG. Again, total spleen cells were cultured for 24 h in the presence of IL-6. Cells were then treated with either 1 mM 2-DG, 1.5 ng/mL bortezomib, a combination of both drugs or the vehicle control. At the end of the culture period, plasma cells were quantified using flow cytometry (Fig. 8A and B).

Both drugs were titrated before to use them at concentrations were each drug killed around 50 % of the plasma cells on its own (data not shown). This experiment reproduced the findings from the previous experiment in that both 2-DG and bortezomib decreased the frequency of plasma cells from around 0.2 % to 0.1 % in total (Fig. 8C). Combining both drugs led to a further decrease in plasma cell frequency by 65 % on top of the 50 % each drug induced when used separately. This finding suggested that 2-DG could improve the efficacy of bortezomib *in vitro* and therefore have a possible therapeutic use to increase efficacy or decrease side effects of other drugs.

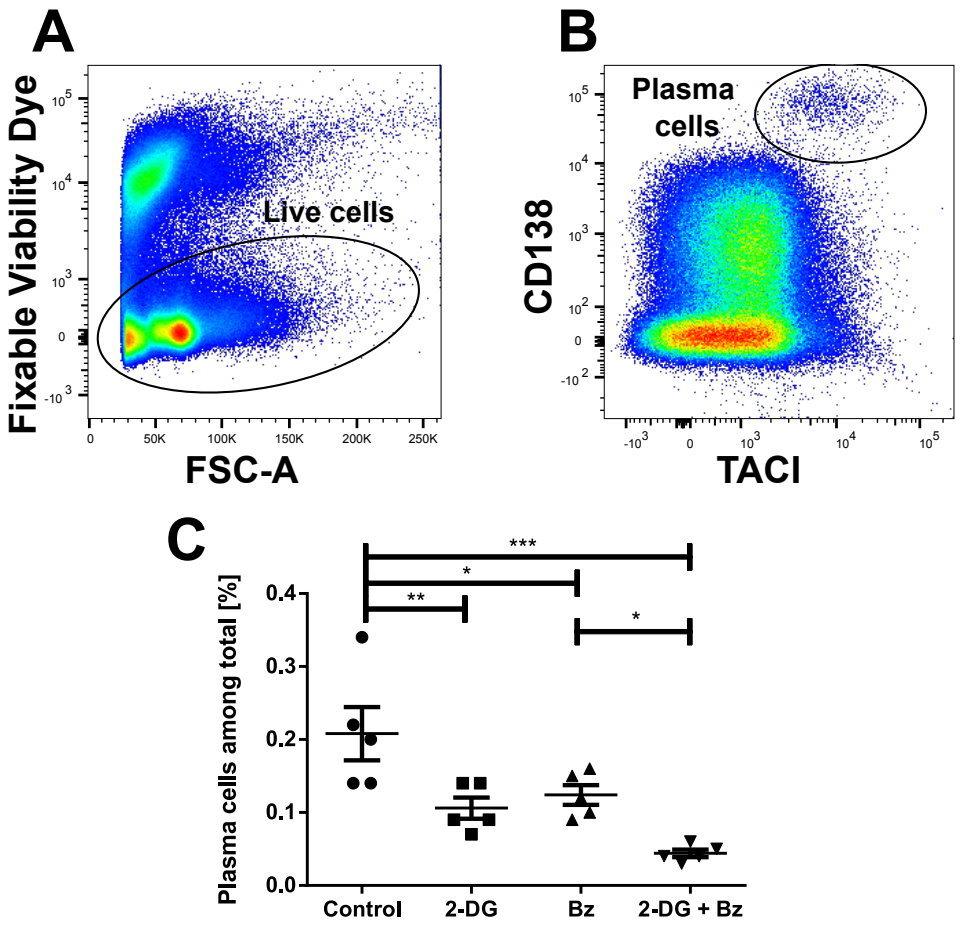

Figure 8: Synergistic effect of 2-DG and bortezomib on splenic plasma cells. Spleen cells were cultivated for 24 h in the presence of 10 ng/mL and treated with 1 mM 2-DG, 1.5 ng/mL bortezomib (Bz), a combination of both drugs or a vehicle control. Subsequently, cells were analysed by flow cytometry. A) For analysis, dead cells were excluded using a viability staining. B) Plasma cells were identified as $CD138^{high}$ $TACI^{high}$. C) Plasma cell frequencies of all groups, as indicated. One-way repeated measures ANOVA followed by Dunnett's multiple comparison test was used to check for statistical significance. *: $p < 0.05$; **: $p < 0.01$; ***: $p < 0.001$. Mean values and SEM are shown. Cells from five mice were used and split into the four groups ($n = 5$). Each dot represents a measurement based on one mouse. The experiment was reproduced once with identical results.

3.5 2-DG decreases the number of germinal centre B cells and plasma cells *in vivo*

To determine the therapeutic potential of 2-DG *in vivo*, 3-4 months old mice of the lupus-prone BcN were treated with this drug, either alone or in combination with bortezomib. Due to the modification of three loci, these mice develop lupus-like symptoms like plasmacytosis and subsequent kidney failure. In a first experiment, 500 mg/kg 2-DG

or the same volume of PBS was injected i.p. on three consecutive days. At day 4, mice were killed and spleen and bone marrow analysed by flow cytometry. The staining was designed to encompass a broad spectrum of the B cell lineage based on a recent guideline for the use of flow cytometry (Cossarizza *et al.*, 2019).

For spleen, cells were gated on lymphocytes, overall $B220^+$ B cells, IgM^{high} IgD^{low} marginal zone B cells (MZB), IgM^{low} IgD^{high} follicular B cells (FOB), IgM^- IgD^- class-switched B cells, $GL7^+$ $CD95^+$ germinal centre B cells (GCB) and $CD138^{high}$ $TACI^{high}$ plasma cells (Fig. 9A). Plasma cells were further divided based on their IgM and CD19 expression. The glucose uptake of all populations was analysed using 2-NBDG.

While the number of lymphocytes did not show a significant difference ($p = 0.07$), the number of all B cells (Fig. 9B), MZB and FOB (data not shown) decreased significantly by 30 %. The difference in the number of B cells (~4.5×10^7 cells) is close to the difference in lymphocyte numbers (~6×10^7 cells), suggesting that 2-DG impacts the cell numbers of other populations less than the B cell lineage. While 2-DG led to a 1.4-fold reduction in B cells, MZB and FOB, the number of class-switched B cells was reduced by a factor of 2.5 (Fig. 9C). An even stronger reduction could be seen in GCB and plasma cells, where 2-DG treatment induced a 3.5-fold decrease (Fig. 9D and E). Focussing on the plasma cells, 2-DG treatment shifted the IgM expression in this population to more IgM^+ cells (Fig. 9F) and led to an increase in CD19 expression (Fig. 9G). Both parameters indicate a less mature state of these plasma cells. The repression of the germinal centre reaction, which generates fully mature plasma cells, might therefore also cause the shift in the plasma cell phenotype. Although 2-DG acts as a glycolysis inhibitor, only class-switched B cells showed a significant decrease in glucose uptake after treatment with 2-DG (data not shown).

Taken together, 2-DG treatment led to minor reductions in the number of B cells, MZB and FOB (factor 1.4). More pronounced reductions were found in class switched B cells (factor 2.5) and GCB and plasma cells (factor 3.5). Furthermore, the IgM and CD19 expression of the plasma cells indicated a lower degree of maturity compared to plasma cells in the control group. Glucose-uptake, while suspected to be broadly affected by glycolysis inhibition, was only decreased in class-switched B cells.

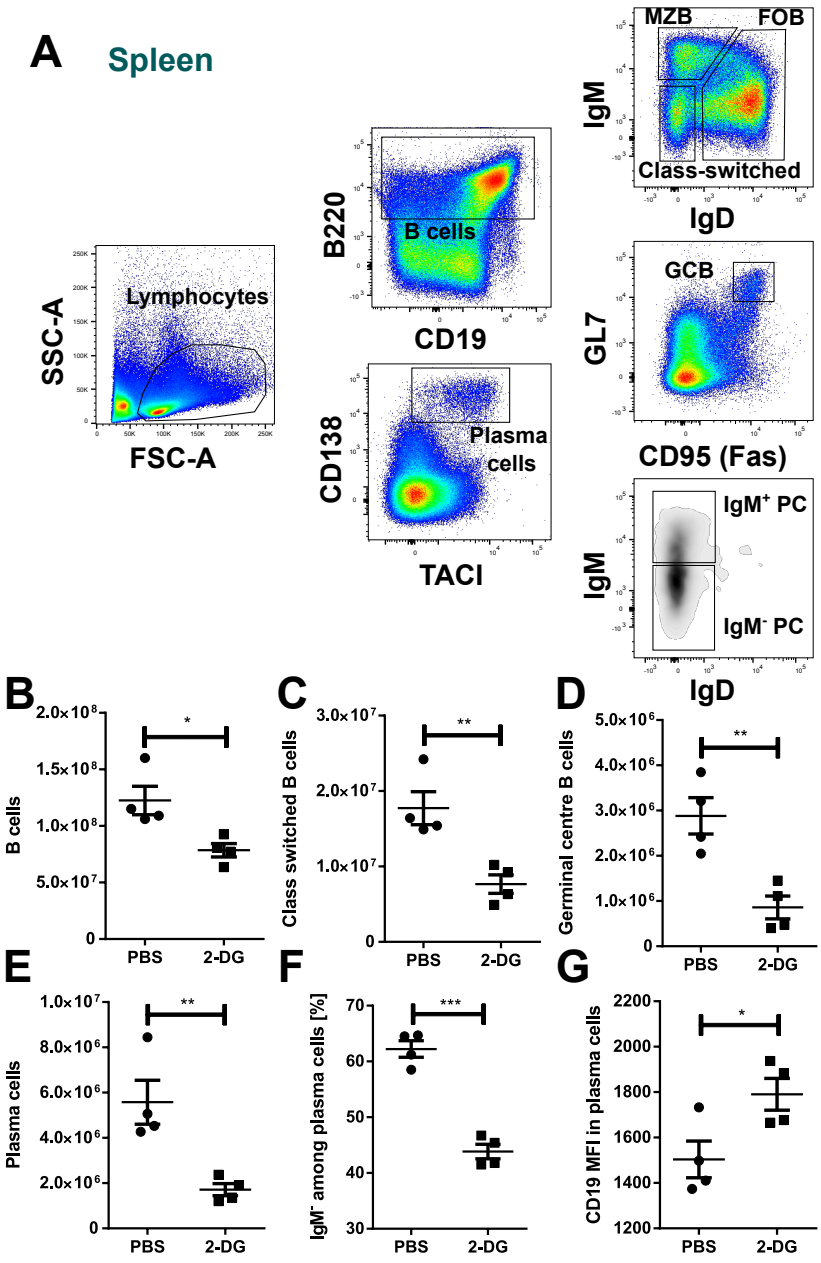

Figure 9: Impact of 2-DG treatment on B lineage cells in the spleen of BcN mice. Female BcN mice aged 3-4 months were injected daily with 500 mg/kg 2-DG or an equal volume of PBS on three consecutive days. At day 4, the mice were killed and cells from spleen were analysed by flow cytometry. A) Gating strategy. B) Number of B cells. C) Number of IgM$^-$ IgD$^-$ (class-swichted) B cells. D) Number of germinal centre B cells (GCB). E) Number of plasma cells. F) Frequency of IgM expression among plasma cells. G) CD19 expression in plasma cells. Paired t-tests were used to check for statistical significance. *: $p < 0.05$ **: $p < 0.01$; ***: $p < 0.001$. Mean values and SEM are shown. This experiment was only performed ones using 4 mice per group ($n = 4$).

3.6 Bone marrow plasma cells survive 2-DG treatment *in vivo* but show phenotypical changes

Similar to the analysis in spleen, a broad staining was used to check the impact of 2-DG on a variety of different B lineage cells (Cossarizza *et al.*, 2019). Cells were gated for lymphocytes and $B220^+$ $CD19^+$ B cells that were further categorised into IgM^{high} IgD^- immature and IgM^{int} IgD^{high} mature B cells (Fig. 10A). Pre, pro and pre-pro B cells were characterised by their low CD43 and intermediate to high B200 expression and further refined as IgM^- IgD^-. Last, $CD138^{high}$ $TACI^{high}$ plasma cells were gated and analysed regarding to their IgM and CD19 expression (Fig. 10A). The glucose uptake was measured for all populations using a 2-NBDG staining.

Unlike in the spleen, the number of B lineage cells appeared to be unaffected by 2-DG treatment. Neither the number of overall B cells (Fig. 10B) nor immature, mature, pre, pro or pre-pro B cells showed any difference after 2-DG treatment (data not shown). Even plasma cells, which were among the most affected cells in spleen, were present in similar numbers in both groups (Fig. 10C). However, both the glucose uptake (Fig. 10D) and CD19 expression (Fig. 10E) of plasma cells were altered showing that 2-DG did affect the bone marrow cells. Although the pattern of CD19 expression in plasma cells was similar in bone marrow and spleen, the relative difference was much more pronounced in the bone marrow starting on a lower CD19 level. Unlike in spleen, the glucose uptake of the bone marrow plasma cells decreased significantly after treatment but was much higher overall compared to splenic plasma cells (bone marrow: MFI 20000 vs. spleen: MFI 6000). This finding is in line with the data showing that the bone marrow is enriched with a plasma cell subpopulation with massive glucose uptake.

To understand why IgM^- plasma cells in the spleen were more affected by 2-DG than IgM^+ ones and why bone marrow-residing plasma cells showed no change in survival at all, all measured parameters were checked for correlating expression patterns. In fact, TACI expression was highest in plasma cell populations that were not or only mildly affected by 2-DG treatment (Fig. 10F). While the highly affected splenic IgM^- plasma cells showed a distinctly lower level of TACI expression than the less affected splenic IgM^+ plasma cells, TACI expression was approximately 2-fold higher in all bone marrow plasma cells which survived the 2-DG treatment. Although this finding is a correlation and not necessary causative, it seems reasonable that a receptor like TACI, that integrates survival signals, would be able to counteract apoptotic signals induced by 2-DG.

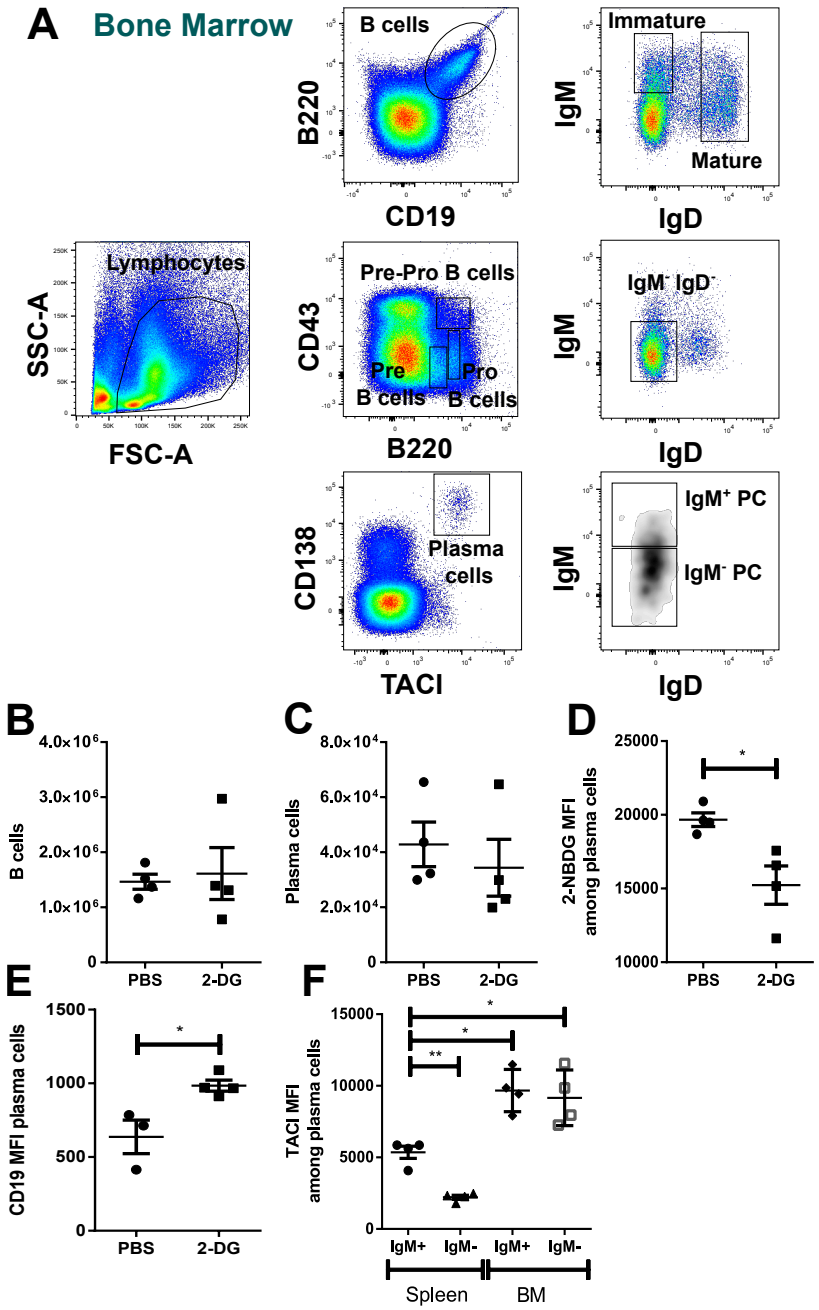

Figure 10: Impact of 2-DG treatment on B lineage cells in the bone marrow of BcN mice. Female BcN mice aged 3-4 months were injected daily with 500 mg/kg 2-DG or an equal volume of PBS on three consecutive days. At day 4, the mice were killed and analysed with flow cytometry. A) Gating strategy for bone marrow (BM) cells. B) Number of B cells in BM, C) number of plasma cells in BM, D) glucose uptake of BM cells, E) CD19 expression of BM cells. F) TACI expression in plasma cells from BM and spleen. Paired t-tests and a repeated measures one-way ANOVA were used to check for statistical significance. *: $p < 0.05$; **: $p < 0.01$. Mean values and SEM are shown ($n = 4$). The experiment was performed once.

3.7 Combining 2-DG and bortezomib does not improve drug efficacy *in vivo*

To confirm the promising synergistic effect of 2-DG and bortezomib seen *in vitro*, the combined treatment was applied *in vivo* to see if the combination of both drugs could improve on the impact of 2-DG alone. The procedure was identical to the 2-DG treatment. 3 to 4 months old BcN mice were injected with 0.2 mg/kg bortezomib or a combination of bortezomib and 500 mg/kg 2-DG daily for three consecutive days. On day 4, mice were killed and analysed with the same staining panel as before (Fig. 9 and 10).

In contrast to what was observed *in vitro*, combining bortezomib and 2-DG did not lead to an increased efficacy over bortezomib alone. While class-switched B cells, germinal centre B cells and plasma cells were affected the most by 2-DG alone in spleen, the combination of 2-DG and bortezomib did not increase the efficacy (Fig. 11A, B and C). The same was found in bone marrow, where neither the number of plasma cells (Fig. 11D) nor the CD19 expression (Fig. 11E) or glucose uptake (Fig. 11F) were any different between bortezomib or combined treatment. Although a low concentration of bortezomib (0.2 mg/kg) was chosen to avoid overshadowing the impact of 2-DG, the number of plasma cells after treatment with bortezomib was similar to that after treatment with 2-DG, suggesting that both drugs had a similar impact.

In conclusion, with the experimental protocol used, no synergistic effect of a combined treatment of 2-DG and bortezomib was found in this mouse model *in vivo*. While optimising the concentrations of both drugs might yield favourable results, the concentrations used in this experiment were sufficient to induce clear changes when used separately.

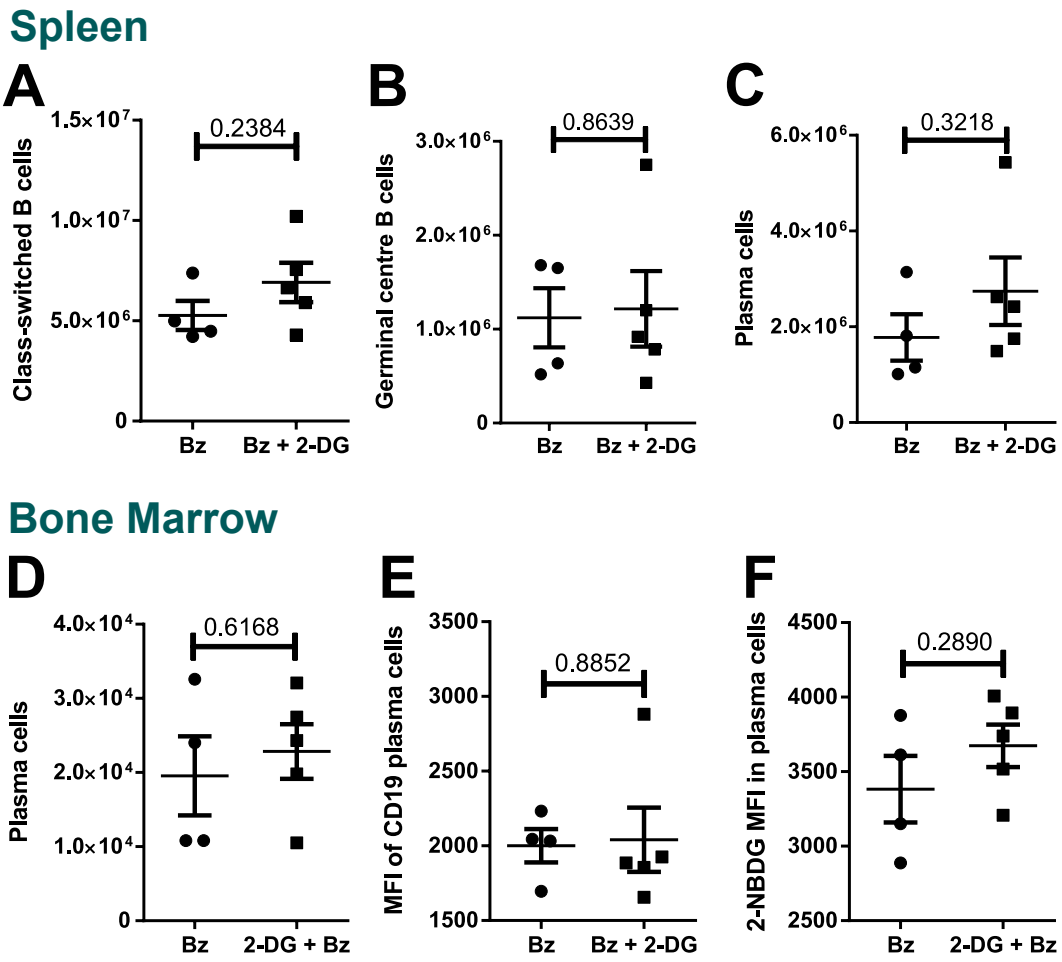

Figure 11: Combination of 2-DG and bortezomib on B lineage cells in spleen and bone marrow of BcN mice. Female BcN mice aged 3-4 months were injected daily with 500 mg/kg 2-DG or a combination of 500 mg/kg 2-DG and 0.2 mg/kg bortezomib on three consecutive days. At day 4, the mice were killed and analysed with flow cytometry. The gating was performed identical to figures 9A and 10A. For spleen, the numbers of A) IgM^- IgD^- class-switched B cells, B) germinal centre B cells (GCB) and C) plasma cells are depicted. For bone marrow, D) the number of plasma cells as well as their E) CD19 expression and F) glucose uptake are shown. Paired t-tests were used to check for statistical significance. p-values, means and SEM are shown ($n = 4 - 5$).

3.8 2-DG induces an unfolded protein response and reduces TACI expression

In order to elucidate the mechanism behind the 2-DG-induced reduction in plasma cell numbers, the short-term plasma cell culture was utilised again. Whole spleen cells were cultivated in different concentrations of 2-DG for 4 h or 24 h and analysed with flow cytometry. $CD138^{high}$ $TACI^{high}$ plasma cells, $B220^{+}$ $CD138^{-}$ B cells and $B220^{-}$ $CD138^{-}$ non-B cells were analysed (Fig. 12A). Since a recent paper suggested that plasma cells used glucose mainly for glycosylation and not for energy consumption (Lam, Becker, *et al.*, 2016), the transcription factor XBP-1s was stained to check the activity of the unfolded protein response (UPR).

After 4 h incubation with 5 mM 2-DG, plasma cells showed a significant increase in XBP-1s expression (Fig. 12B). Other cell types like B cells and $B220^{-}$ cells showed an overall lower level of XBP-1s, which was not affected by 2-DG treatment. Simultaneously, TACI expression declined with increasing 2-DG concentrations in plasma cells, but not in B cells or $B220^{-}$ cells (Fig. 12C). After 24 h, XBP-1s levels were increased not only at 5 mM 2-DG, but already at 0.2 mM (Fig. 12C). Unlike the 4 h time point, no difference in TACI expression was observed in any of the cell types after 24 h treatment (Fig. 12E). However, the TACI levels in plasma cells dropped from an MFI or 4000 at 4 h to around 2000 at 24 h treatment indicating a major change in these cells regardless of the 2-DG treatment (Fig. 12C and E). The TACI levels in B cells and $B220^{-}$ cells remained stable at an MFI of 500 and 100, respectively.

In conclusion, plasma cells, which are exposed to severe stress from protein synthesis even under homeostatic conditions, showed an increase in the UPR transcription factor XBP-1s as early as 4 h after 2-DG treatment. Simultaneously, the TACI expression in plasma cells dropped early on due to 2-DG treatment but plateaued after 24 h regardless of 2-DG concentration. Whether these cells downregulated the TACI expression or the $TACI^{high}$ plasma cells died during the experiment, could not be differentiated in this experiment. 2-DG, however, could be shown to influence not only glycolysis, but also induce UPR activation.

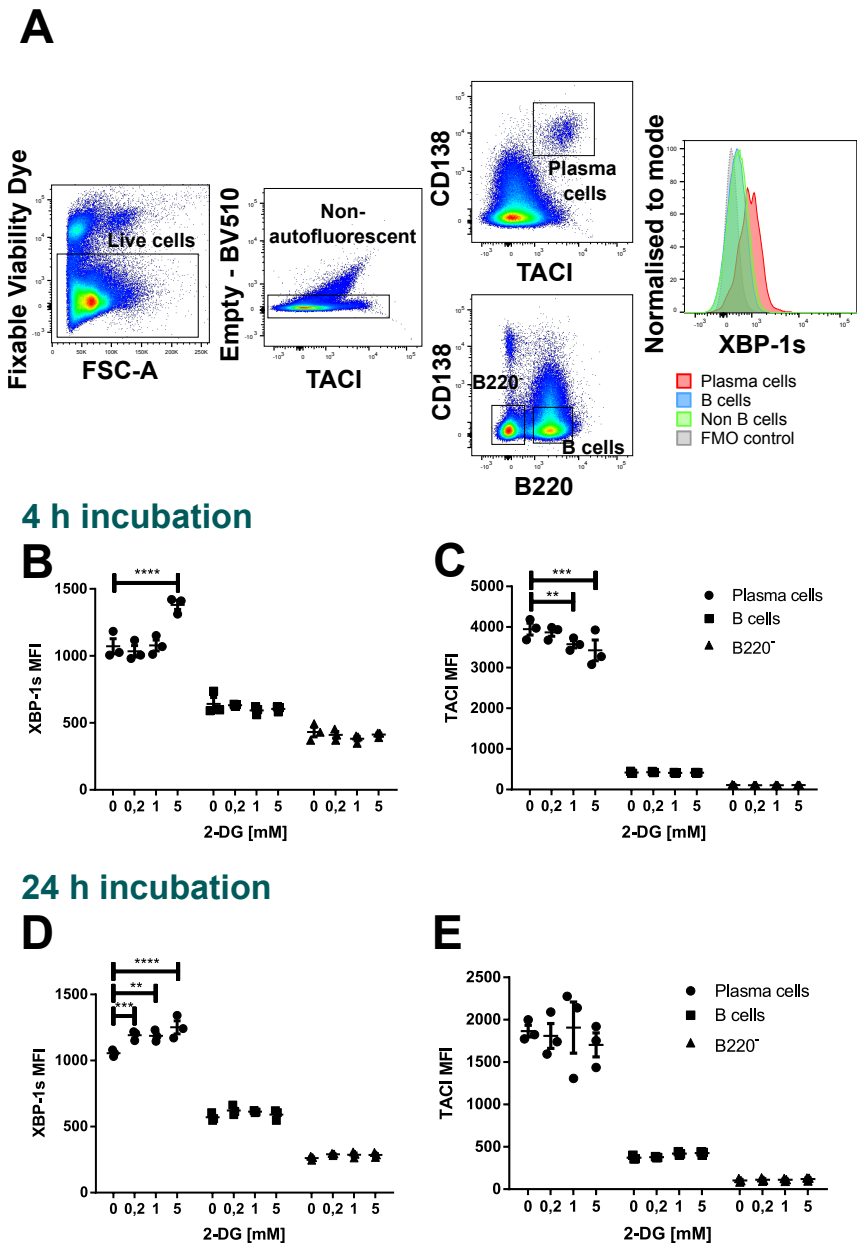

Figure 12: Impact of 4 h and 24 h 2-DG treatment on plasma cells, B cells and non-B lineage cells. Cells from spleen from C57BL/6 mice were cultivated in the presence of 10 ng/mL IL-6 to increase survival. Cells were treated with different doses of 2-DG for 4 h or 24 h, respectively. Afterwards, cells were analysed by flow cytometry. A) Gating strategy for the analysis. B) XBP-1s expression after 4 h 2-DG treatment. C) TACI expression after 4 h 2-DG treatment. D) XBP-1s expression after 24 h 2-DG treatment. E) TACI expression after 24 h 2-DG treatment. Matched two-way ANOVA followed by Dunnett's multiple comparison post test was used to check for statistical significance within populations. **: $p < 0.01$; ***: $p < 0.001$; ****: $p < 0.0001$. Mean values and SEM are shown ($n = 3$). The experiment was performed once.

3.9 Mannose decreases the impact of 2-DG on plasma cell survival *in vitro*

Since we speculated that 2-DG activated the UPR, further experiments were aimed at elucidating its impact on protein synthesis and glycosylation. A paper from 2007 showed that mannose, but not glucose, was able to counteract 2-DG in different tumour cell lines (Kurtoglu, Gao, *et al.*, 2007). Cells from spleen were pre-treated with either 5 mM glucose (control), 10 mM glucose (glucose), 5 mM glucose and 5 mM mannose (mannose) or 5 mM glucose with additional non-essential amino acids (NEAA) as well as IL-6 for 24 h. After this resting phase, the cells were treated with 2-DG for another 24 h and analysed using flow cytometry. The cell culture supernatant was stored for subsequent analysis with ELISA. In addition to the plasma cell panel shown in figure 12, LAMP-1 (lysosome-associated membrane protein 1) was stained to check for differences in the lysosome assembly or function.

As had been established before, 2-DG reduced the number of plasma cells at the end of the culture (Fig. 13A). The plasma cell numbers decreased strongest in the control group and arguably less strongly when more glucose was added. Since glucose competes with the 2-DG, a certain decrease in efficacy was expected at higher glucose levels. However, adding an identical amount of mannose reduced the effect of 2-DG to such an extend that no difference was detected after treatment. Adding NEAA to check whether 2-DG induced UPR by reducing amino synthesis showed no difference to the control or glucose group. After 24 h treatment with 2-DG, significantly more plasma cells survived in the mannose group than in the control or NEAA group (Fig. 13B). In line with the impact on plasma cell numbers, 2-DG decreased the expression of LAMP-1 in all conditions except for the mannose treated group (Fig. 13C). This finding could indicate a link between 2-DG and lysosome function but LAMP-1 is also known to depend on glycosylation (Kundra and Kornfeld, 1999). Interestingly, only IgM^+ plasma cells seemed to be affected by 2-DG treatment as the number of IgM^- plasma cells was constant across all conditions and treatments (Fig. 13D). This result contradicts the *in vivo* data that showed a clear decrease in IgM^- plasma cells after 2-DG treatment. Since this staining did not include other immunoglobulin classes, IgM^+ plasma cells that lost their IgM expression could not be differentiated from plasma cells expressing different immunoglobulins. Clarification of this issue requires further experiments.

Taken together, mannose, but not glucose or NEAA, was able to counteract the 2-DG-induced decrease in plasma cell numbers as well as the decrease in LAMP-1 expression. In this *in vitro* setting, only IgM^+ plasma cells succumbed to the 2-DG treatment.

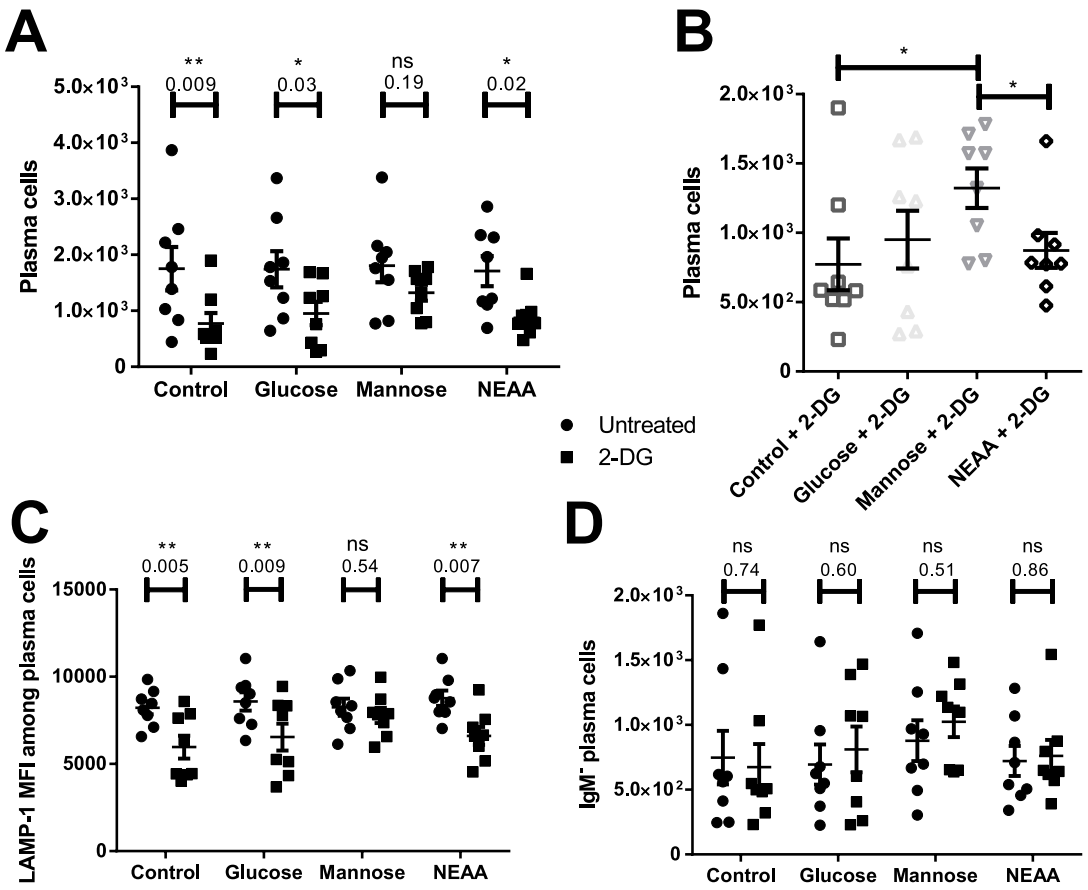

Figure 13: Reduced impact of 2-DG after mannose supplementation. Cells from spleen from C57BL/6 mice were cultivated in the presence of 10 ng/mL IL-6. Samples were cultivated on either a base level of 5 mM glucose (control), 10 mM glucose (glucose), a mixture of 5 mM glucose and 5 mM mannose (mannose) or 5 mM glucose and a mixture of non-essential amino acids (NEAA). After 24 h of culture, cells were treated with 1 mM 2-DG for another 24 h before flow cytometric analysis. The gating strategy was identical to that in figure 12A. A) Comparison of the number of plasma cells between all conditions. B) Number of plasma cells within the 2-DG treated groups. C) LAMP-1 expression levels in plasma cells. D) Number of IgM^- plasma cells. Paired t-tests (A, C and D) and one-way repeated measures ANOVA followed by Dunnett's multiple comparison test (B) were used to check for statistical significance. *: $p < 0.05$; **: $p < 0.01$; ns: not significant. Mean values and SEM are shown ($n = 8$).

3.10 2-DG affects the generation and secretion of different immunoglobulin classes

To understand which immunoglobulin classes were affected by 2-DG treatment, cell culture supernatant from the previous experiment was tested for IgM, IgG and IgA using ELISA. The supernatants had been collected at the end of the 48 h culture. It needs to be noted that the supernatant had not been exchanged before the 2-DG treatment meaning that this analysis also encompasses all antibodies produced during the first 24 h (the resting phase / pre-treatment) of the experiment. This may limit the sensitivity of the analysis. With this in mind, differences in the supernatant caused by the treatment were likely more pronounced than this analysis suggests.

In line with the flow cytometric analysis, the IgM concentration decreased in the 2-DG treated group compared to the control (Fig. 14A). Contrasting the flow cytometry data, mannose did not have an obvious reversing effect on the IgM concentration. This finding suggests that there is another mechanism by which 2-DG reduces antibody concentrations in addition to plasma cell killing. This suggestion was reinforced by both IgG (Fig. 14B) and IgA (Fig. 14C) concentrations being significantly lower after 2-DG treatment. Although the corresponding plasma cells appeared to be unaffected in the previous experiment (Fig. 13D), the antibody synthesis and/or secretion was decreased by 2-DG. While the impact of the different sugar conditions was less clear than in the flow cytometric analysis, the p-value was lowest in the mannose group across all antibody isotypes.

In conclusion, IgM^+ plasma cells may be the only ones which's survival was decreased by 2-DG treatment but antibody concentrations were decreased across all isotypes. This finding suggests that, beyond decreasing plasma cell survival, there must be another mechanism by which 2-DG hampers with antibody synthesis or secretion.

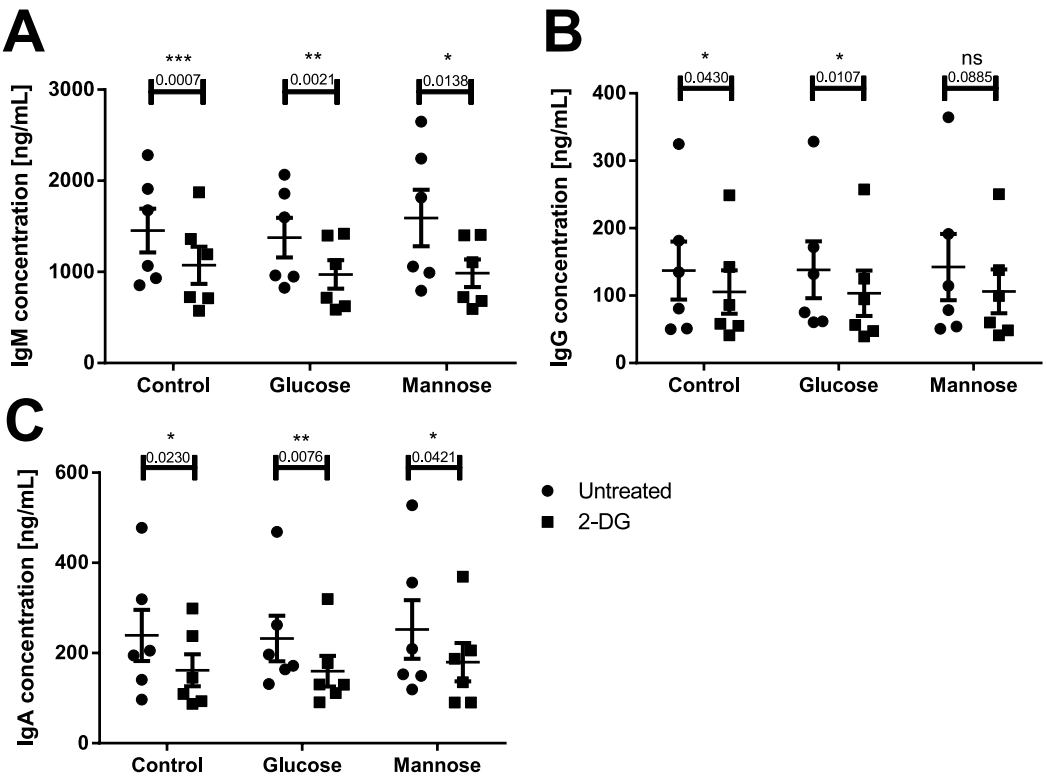

Figure 14: Immunoglobulin concentration in the supernatant of 2-DG treated spleen cells. Cell culture supernatants from the experiment in figure 13 were collected and used in ELISA to determine the concentration of different immunoglobulin classes. The concentrations of A) IgM antibodies, B) IgG antibodies and C) IgA antibodies in the supernatant were assessed. Paired t-tests were used to check for statistical significance. *: $p < 0.05$; **: $p < 0.01$; ***: $p < 0.001$; ns: not significant. Mean values and SEM are shown ($n = 6$).

3.11 2-DG affects Igκ light chain expression in plasma cells that survive treatment

Next, we aimed to get a deeper, more differentiated understanding of the impact of 2-DG on plasma cells expressing different antibody isotypes and to test whether different mouse strains used for previous *in vivo* and *in vitro* experiments reacted similarly to the 2-DG treatment. To achieve these goals, another 48 h whole spleen cell culture was utilised using BcN mice instead of C57BL/6J. As before, cells from spleen were cultivated in medium containing 5 mM glucose (control), 10 mM glucose (glucose) or 5 mM glucose and 5 mM mannose (mannose). After 24 h, samples were treated with 2-DG or vehicle control for another 24 h. At the end of the culture, the expression of IgM, IgA, IgG, Igκ and XBP-1s in plasma cells was determined.

In line with the data from C57BL/6J mice, 2-DG reduced numbers of IgM^+ plasma cells by a factor of 2 from 1.4×10^4 to 0.67×10^4 in the control group. This effect was less pronounced in the presence of mannose or higher levels of glucose (Fig. 15A). In

IgM^+ plasma cells, the expression level of Igκ light chain was not altered after treatment, regardless of the sugar concentrations (Fig. 15B). Numbers of IgA^+ and IgG^+ plasma cells were not affected by 2-DG treatment (Fig. 15C and E). However, the Igκ expression level in individual IgA^+ and IgG^+, but not IgM^+ plasma cells was increased after treatment (Fig. 15D and F). In IgA^+ $Ig\kappa^+$ plasma cells, the Igκ expression increased by 26.5 % after 2-DG treatment in the control group, while no difference was found in the glucose or mannose groups. In IgG^+ $Ig\kappa^+$ plasma cells, the Igκ expression increased by 34.5 % after 2-DG treatment in the control group and 28.6 % in the glucose group, while no difference was found in the mannose group. No such differences were found in IgA^+ $Ig\kappa^+$ plasma cells. This data suggests that the immunoglobulin synthesis still takes place in the presence of 2-DG. In addition to the amount of antibodies present in the cells, XBP-1s levels were measured to detect UPR activation. In IgM^+ plasma cells, the control group showed a 20 % decrease in XBP-1s expression after treatment with 2-DG while the other sugar conditions were not affected (Fig. 15G). Unlike in IgM^+ plasma cells, XBP-1s levels in IgG^+ plasma cells increased by 25 % after treatment in all sugar conditions (Fig. 15H). In IgA^+ plasma cells, only the control condition showed a similar increase after treatment but barely failed the criteria for statistical significance with a p-value of 0.088 (data not shown).

Taken together, 2-DG treatment increased the amount of Igκ light chain present in IgA^+ and IgG^+, but not IgM^+ plasma cells. While IgM^+ plasma cells did not show changes in Igκ levels, their numbers were decreased after treatment. IgA^+ and IgG^+ plasma cell numbers were unaffected by the 2-DG treatment but showed higher XBP-1s levels.

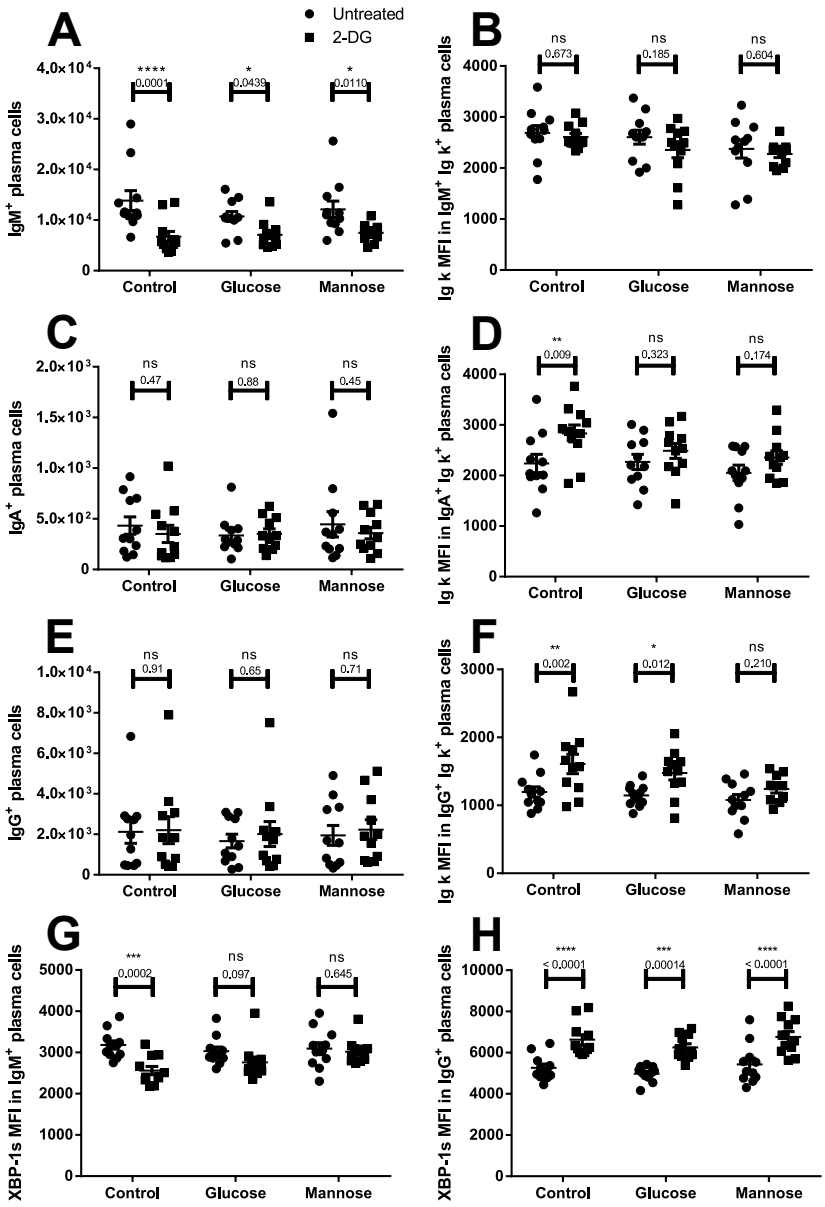

Figure 15: Impact of 2-DG and mannose treatment on plasma cells with distinct immunoglobulin classes. Cells from spleen from BcN mice were cultivated in the presence of 10 ng/mL IL-6 and either a base level of 5 mM glucose (control), 10 mM glucose (glucose) or a mixture of 5 mM glucose and 5 mM mannose (mannose) for 24 h. Afterwards, cells were treated with 1 mM 2-DG for another 24 h and analysed by flow cytometry as shown in figure 12A. A) Number of IgM^+ plasma cells and B) Igκ expression in $Ig\kappa^+$ IgM^+ plasma cells. C) Number of IgA^+ plasma cells and D) Igκ expression in $Ig\kappa^+$ IgA^+ plasma cells. E) Number of IgG^+ plasma cells and F) Igκ expression in $Ig\kappa^+$ IgG^+ plasma cells. Comparison of XBP-1s expression in G) IgM^+ and H) IgG^+ plasma cells. Paired t-tests were used to check for statistical significance. *: $p < 0.05$; **: $p < 0.01$; ***: $p < 0.001$; ****: $p < 0.0001$; ns: not significant. Mean values and SEM are shown ($n = 11$). The experiment was performed once.

3.12 Mannose reduces the effect of 2-DG, but not 2-FDG

Since my previous experiments and literature (Kurtoglu, Gao, *et al.*, 2007) suggested that the mode of action of 2-DG might be linked to posttranslational modifications rather than impared translation, 2-FDG - another glycolysis inhibitor - was used to compare the impact mannose has on both substances. Unlike 2-DG, 2-FDG substitutes the oxygen at the C2 atom with fluorine. The resulting structure is chemically more similar to glucose than 2-DG which is closer to mannose. Therefore, 2-FDG is a stronger glycolysis inhibitor than 2-DG (Lampidis *et al.*, 2006). As in previous experiments, whole spleen cells from C57BL/6J mice were cultured for 48 h with different sugar conditions. Here, cells were cultured in either 10 mM glucose (Glucose) or 5 mM glucose and 5 mM mannose (Mannose). Additionally, cells were treated with 1 mM 2-DG, 1 mM 2-FDG or PBS as vehicle control.

As has been established before, 2-DG treatment reduced the number of plasma cells by around two-fold in the glucose condition (Fig. 16A). Cultivating the cells in mannose during the 2-DG treatment increased the number of plasma cells by approximately factor two compared to the glucose condition. However, the difference between the glucose and mannose conditions barely fell short of the significance threshold with a p-value of 0.057. The difference between the glucose and mannose conditions was missing entirely in the 2-FDG treated group ($p = 0.501$). As found in my previous experiments, 2-DG drastically decreased the frequency of IgM^+ cells but this effect could be diminished by adding mannose (Fig. 16B). Interestingly, 2-FDG decreased the frequency of IgM^+ cells to a similar degree as 2-DG. Unlike the effect of 2-DG, however, the impact of 2-FDG was not diminished by supplementation of mannose at all. Lastly, LAMP-1 expression was analysed in the most affected cell type, IgM^+ plasma cells. Treating the cells with 2-DG showed no impact on the LAMP-1 expression in plasma cells cultivated in mannose, while plasma cells in glucose medium showed a 37 % decrease in LAMP-1 expression (Fig. 16C). Using 2-FDG did not affect the LAMP-1 expression regardless of the sugar condition.

Taken together, although 2-DG and 2-FDG are structurally similar, there seems to be a different mechanism by which these glucose analogues exert their effect on plasma cells. While there is some overlap between the action of the two inhibitors, e.g. the strong reduction in IgM^+ cells, only the effect of 2-DG was reduced or prevented by the addition of mannose to the culture medium. This was not the case for changes induced by 2-FDG, suggesting that glycolysis inhibition might not be the main cause for the effects induced by 2-DG.

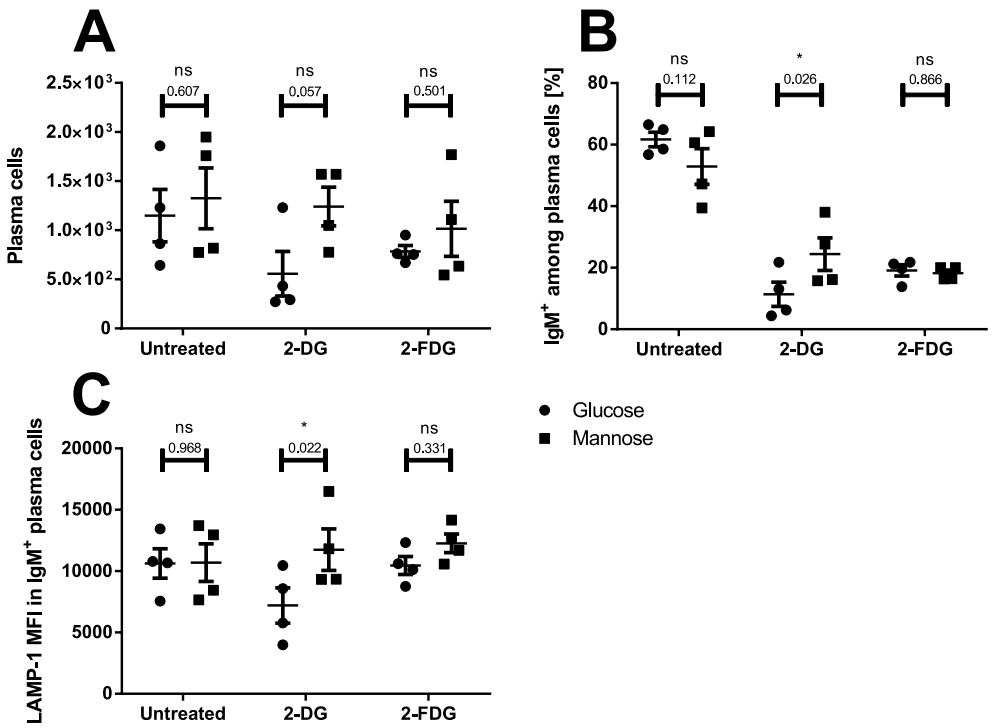

Figure 16: Comparing the impact of 2-DG and 2-FDG on plasma cells. Total cells from spleen of C57BL/6 mice were cultivated in the presence of 10 ng/mL IL-6 for 24 h together with either 10 mM glucose (glucose) or a mixture of 5 mM glucose and 5 mM mannose (mannose). Afterwards, cells were treated with 1 mM 2-DG or 1 mM 2-FDG and cultivated for another 24 h. Subsequently, cells were analysed by flow cytometry as shown in figure 12A. A) Number of plasma cells. B) Frequency of IgM^+ cells among the plasma cells. C) LAMP-1 expression in plasma cells. Paired t-tests were used to check for statistical significance. *: $p < 0.05$; ns: not significant. Mean values and SEM are shown ($n = 4$).

3.13 Hexokinase, but not phosphofructokinase, inhibitors hinder the generation of plasmablasts

Since the previous experiment revealed differences even between the closely related inhibitors 2-DG and 2-FDG (Fig. 16), further inside into the effects of different glycolysis inhibitors was needed. For this reason, in addition to the hexokinase inhibitors 2-DG and 2-FDG used in the previous experiment, 3PO, a 6-phosphofructo-2-kinase/fructose-2,6-biphosphatase 3 (PFKFB3) inhibitor, was used to assess the impact of blocking glycolysis further downstream of the hexokinase reaction. For this experiment, isolated B cells from spleen from C57BL/6J mice were stimulated with 10 µg/mL LPS for 5 days. This setup was chosen again due the high sensitivity towards 2-DG treatment it displayed in previous experiments. In addition to LPS, the glycolysis inhibitors 2-DG, 2-FDG and 3PO were added at day 0. This dataset was generated by bachelor student Sandra Hilberath under my supervision. Both the experimental design and the final

analysis presented in this thesis was done by myself.

For the analysis, dead cells were excluded and plasmablasts and B cells separated based on their CD138 expression (Fig. 17A). Adding 200 µM 2-DG to the culture reduced the number of plasmablasts by a factor of approximately 9. Simultaneously, the number of B cells decreased by a factor of 1.2 which was not strong enough to be statistically significant (Fig. 17B). Similar to 2-DG, adding 2-FDG resulted in a 6-fold decrease in plasmablast numbers (Fig. 17C). In contrast, median B cell numbers decreased by a factor of 1.5, which did not suffice for statistical significance. Unlike the hexokinase inhibitors 2-DG and 2-FDG, 3PO reduced both the numbers of plasmablasts and B cells by a factor of 32 and 23, respectively (Fig. 17D). The impact of 3PO on plasmablast formation and/or survival was therefore far stronger than that of 2-DG or 2-FDG. However, it also eradicated the B cells, lacking the specificity of the hexokinase inhibitors. While the lack of specificity seen in this experiment could be due to an excessively high concentration of 3PO, the same concentration had no effect when used for only the last 24 h or in a different B cell culture system.

Taken together, strong glycolysis inhibition seems to be lethal for both plasmablasts and B cells alike as shown by 3PO treatment. Using the hexokinase inhibitors, however, plasmablasts are much more affected than the B cells. This data suggests that the glycolytic metabolites between the hexokinase and the phosphofructokinase, glucose-6-phosphate and fructose-6-phosphate, are vital for plasmablasts, but not B cells. However, as shown in figure 16, while treatment with the hexokinase inhibitors 2-DG and 2-FDG show mostly similar results, 2-DG appears to have an additional mode of action by which it affects plasma cells. This additional effect could be reduced by adding mannose.

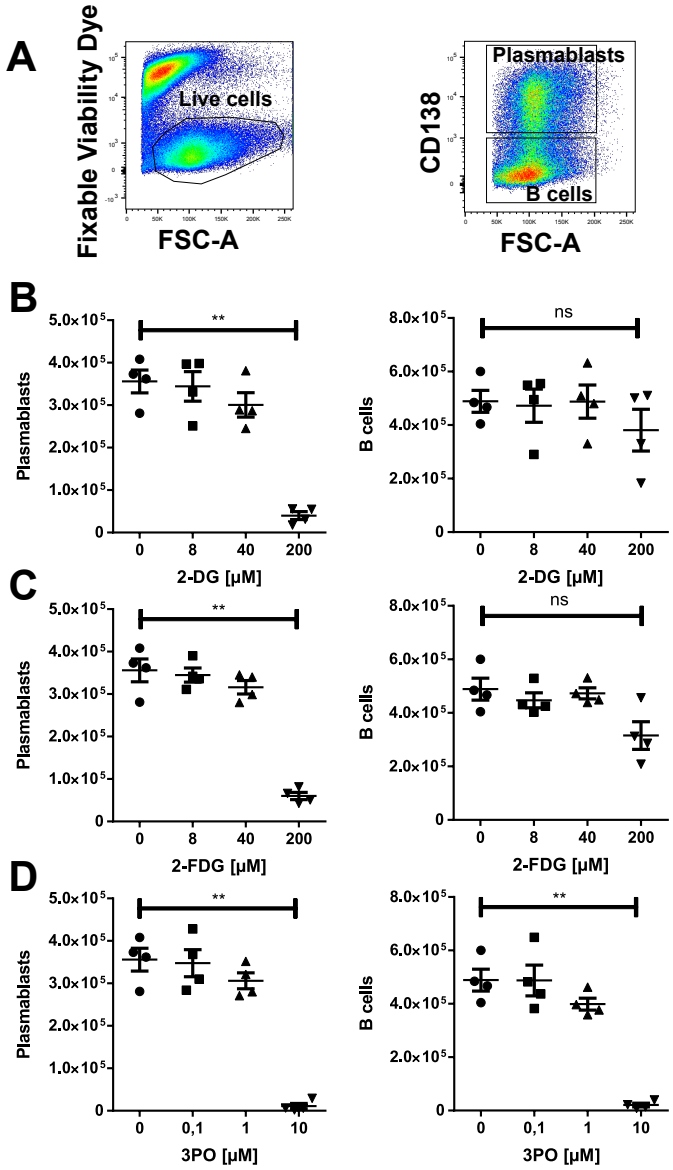

Figure 17: Comparing the impact of hexokinase and phosphofructokinase inhibitors on B cells and plasmablasts. Two different enzymes of the glycolytic pathway were targeted with inhibitors to further understand whether the effect of 2-DG was due to blocking glycolysis or its involvement in other processes. B cells were isolated from spleen of C57BL/6J mice and cultivated in RPMI 1640 medium with 11 mM glucose and different concentrations of inhibitors. 8 µM to 200 µM 2-DG and 2-FDG were used to target hexokinase activity. The phosphofructokinase inhibitor 3PO was used at concentrations from 0.1 µM to 10 µM to assess the impact on glycolysis. After cultivation for 5 days, cells were harvested and analysed using flow cytometry. A) Dead cells were excluded and divided into $CD138^+$ plasmablasts and $CD138^-$ B cells. The numbers of both cell populations were analysed after treatment with B) 2-DG, C) 2-FDG and D) 3PO. Repeated measures one-way ANOVA was used to check for statistical significance. ns: not significant; **: $p < 0.01$. Mean values and SEM are shown ($n = 4$).

3.14 Glycosylation inhibition and 2-DG treatment result in similar plasma cell numbers, LAMP-1 and XBP-1s expression

To get another angle on the mechanism of 2-DG, it was used in combination with tunicamycin. This reagent blocks N-linked glycosylation by inhibiting N-acetylhexosamine phosphotransferases, part of which are essential for the glycosylation of proteins (Elbein, 1987; Kornfeld, 1978). Whole spleen cells from C57BL/6J mice were cultivated for 48 h in the presence of IL-6 but without further stimulant. For the last 24 h, cells were treated with 1 mM 2-DG, 0.5 µg/mL tunicamycin or a combination of both. Afterwards, cells were analysed by flow cytometry as shown in figure 12A.

After 24 h treatment, 2-DG treatment led to an approximately two-fold decrease in plasma cell numbers (Fig. 18A). Treating the sample with tunicamycin led to similar plasma cell numbers as the 2-DG treatment, but combining both treatments did not decrease plasma cell numbers further. Similarly, the expression of the lysosome marker LAMP-1 was decreased by 25 % after 2-DG treatment (Fig. 18B). Again, the tunicamycin treatment resulted in a similar LAMP-1 expression as the 2-DG treatment. Combining tunicamycin and 2-DG did not decrease the LAMP-1 exression further. Unlike the other parameters, the XBP-1s expression was not affected by either 2-DG or tunicamycin treatment (Fig. 18C). The combination of both drugs, however, led to a 13 % increase in XBP-1s expression in plasma cells. This could indicate a certain level of synergy between the two drugs.

In conclusion, treatments with 2-DG and the glycsoylation inhibitor tunicamycin result in similar plasma cell numbers, LAMP-1 expression and XBP-1s levels. Combining them does not reduce the plasma cell numbers or the LAMP-1 expression any further but induces a stronger UPR response as indicated by the increased XBP-1s expression. These results show a similar impact of the glycosylation inhibitor tunicamycin and 2-DG, further supporting the notion that the mechanism behind 2-DG is not limited to glycolysis.

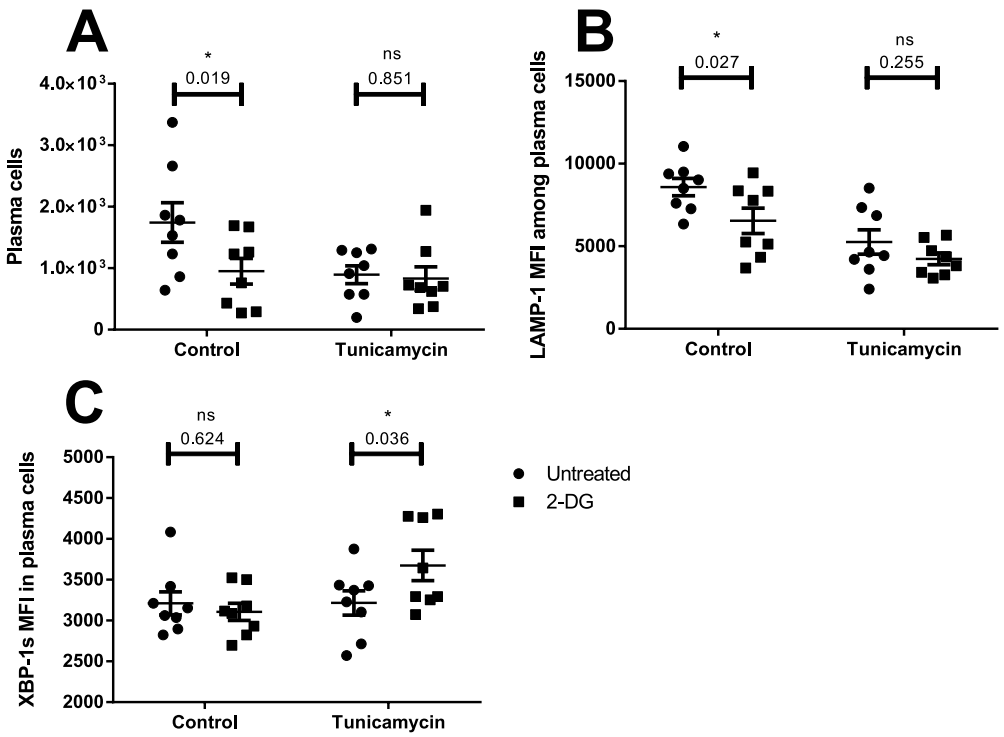

Figure 18: Impact of 2-DG treatment and glycosylation inhibition with tunicamycin on spleen plasma cells. Total spleen cells from C57BL/6 mice were cultivated in the presence of 10 ng/mL IL-6 and 5 mM glucose for 24 h. Afterwards, cells were treated with (1 mM 2-DG or PBS as a vehicle control for another 24 h and analysed by flow cytometry as shown in figure 12A. A) Number of plasma cells. B) Expression level of LAMP-1 in plasma cells. C) Expression level of XBP-1s in plasma cells. Paired t-tests were used to check for statistical significance. *: $p < 0.05$; ns: not significant. Mean values and SEM are shown ($n = 8$). This experiment was performed once.

4 Discussion

The metabolism of immune cells has been of keen interest in the past decade. While the metabolic profiles of a variety of different immune cells had already been investigated, little was known about the B cell lineage when this thesis was started in 2017. Alongside this thesis, research started to focus on the metabolism of B cells and plasma cells. This thesis provides evidence that glucose metabolism is of major importance for plasma cell function and survival, making glucose a promising target for therapeutic approaches in autoimmune diseases. Interestingly, glucose metabolism appears to be essential not only due to energy generation via glycolysis but also due to its importance for the glycosylation of antibodies.

4.1 Plasma cells show high glucose uptake while having low mitochondrial mass

Determining the glucose uptake and mitochondrial mass of B cells and plasma cells under homoeostatic conditions revealed an inverse correlation between the two parameters. B cells showed high levels of mitochondrial mass indicative of mitochondrial activity but comparatively low glucose uptake. On the contrary, $CD138^{high}$ plasma cells were characterised by excessive glucose uptake but lower mitochondrial mass than the much smaller B cells (see section 3.1E and F). A closer analysis of the plasma cells revealed two distinct subpopulations, one with intermediate (2-$NBDG^{int}$) and one with high (2-$NBDG^{high}$) glucose uptake (see section 3.1A). Comparing plasma cells from spleen and bone marrow showed that these subpopulations were present in both organs but varied in distribution with 2-$NBDG^{high}$ plasma cells being more common in bone marrow than in spleen.

The high levels of glucose uptake found in plasma cells suggest a high demand for glucose in these cells. Since plasma cells show high activity due to the synthesis of enormous amounts of antibodies, glucose could be necessary both for energy generation via glycolysis and oxphos as well as anabolic processes providing amino acids for protein biosynthesis or modified sugars for glycosylation. Unlike plasma cells, B cells should have a distinctly lower demand for both energy as well as precursor molecules for protein synthesis which would explain the lower glucose uptake of the B cells. This idea is supported by the group led by Prof. Deepta Bhattacharya, showing that human LLPCs use approximately 90 % of cellular glucose for antibody glycosylation instead of energy generation (Lam, Becker, *et al.*, 2016). Similar to the results shown in this thesis, Lam, Becker, *et al.* (2016) found two distinct subpopulations of plasma cells, differing in their glucose uptake. Even the distribution of 2-$NBDG^{high}$ cells in spleen and bone marrow was close to that found in this thesis (here: 50 % in spleen and 75 % in bone marrow

vs. 50 % and 80 % in Lam, Becker, *et al.* (2016)). The group found that 2-NBDG^{low} plasma cells secreted 5-fold fewer antibodies than their 2-NBDG^{high} counterparts, linking glucose and protein biosynthesis. Assuming a similar use of glucose, B cells would not require the same amount of glucose as their plasma cell counterparts, since they do not secrete antibodies (Tellier and Nutt, 2018).

Since the glucose uptake correlated with the antibody secretion, the plasma cells in spleen and bone marrow could possibly differ in antibody secretion. In addition to that, I hypothesised that glucose uptake could influence the longevity of plasma cells, since the 2-NBDG^{high} population was dominant in the bone marrow which is known to be enriched with LLPCs (Manz, Thiel, and Radbruch, 1997; Slifka, Matloubian, and Ahmed, 1995). This notion was supported in a follow-up study of the 2016 paper, showing that higher 2-NBDG uptake does in fact correlate with an increased plasma cell half-life based on BrdU feeding experiments (Lam, Jash, *et al.*, 2018). Furthermore, after immunisation the number of NP-specific plasma cells decreased more slowly in 2-NBDG^{high} compared to 2-NBDG^{int} cells, suggesting a longer retention of 2-NBDG^{high} cells. In addition to correlating the glucose uptake with longevity and antibody secretion, 2-NBDG^{high} cells were also associated with increased levels of autophagy, further increasing the metabolic robustness of these plasma cells (Lam, Jash, *et al.*, 2018).

While the glucose uptake of plasma cells exceeded that of B cells, mitochondrial mass was distributed inversely. A paper focussing on the role of mitochondria in B cells showed that B cells with high mitochondrial were prone to undergo class-switch recombination, while B cells with low mitochondrial mass were primed for plasma cell differentiation (Jang *et al.*, 2015). The mitchondrial bias during differentiation might lead to the selection of plasma cells with low mitochondrial mass. However, high mitochondrial mass seems to be advantageous for B cells during activation. Shortly after activation, B cells increase their mitochondrial mass (Jang *et al.*, 2015). The increase in mitochondrial activity after BCR ligation is so strong that the resulting calcium signalling becomes lethal after several hours. Secondary signals via TLR9 or from T helper cells are necessary to prevent apoptosis (Akkaya *et al.*, 2018).

Taken together, B cells appear to depend on high mitochondrial mass during activation, proliferation and class-switch recombination, while plasma cells depend on large amounts of glucose for protein biosynthesis. Nonetheless, even plasma cells make use of oxidative phosphorylation, with LLPCs showing higher oxphos activity than SLPCs making them more resistant to metabolic stress (Lam, Jash, *et al.*, 2018).

4.2 Glycolysis and mTORC1 inhibition drastically reduce the ability to generate plasmablasts *in vitro*

Assessing the impact of glycolysis and mTORC1 inhibition on *in vitro*-generated plasmablasts using 2-DG and rapamycin revealed that the number of plasmablasts, but not B cells, was severely decreased by both drugs (see section 3.2A and B). Among the surviving cells, rapamycin induced IL-10 expression in both plasmablasts and B cells (see section 3.2C). On the other hand, 2-DG lead to increased IL-10 expression in B cells but

reduced expression in plasmablasts.

mTORC1 is one of the main signalling hubs integrating metabolism and various cellular processes like proliferation and cell growth. Using isolated spleen B cells and stimulating them with LPS for 5 d is likely to activate MZB instead of FOB cells, inducing a T cell-independent B cell response. A paper from 2017 showed that mTOR activity in MZBs induces proliferation and class switching as well as plasmablast differentiation (Sintes *et al.*, 2017). Using rapamycin treatment or B cells with conditional mTOR deficiency resulted in abrogated NF-κB signalling, reducing the antibody production. Interestingly, B cell survival was not affected by blockade of mTOR signalling. A recent paper focussing on the impact of mTORs antagonist AMPK showed that loss of AMPK activity and resulting increased mTOR activity limited the recall response of memory B cells but strengthened the primary immune response (Brookens *et al.*, 2020). These findings are in line with the data presented in this thesis with rapamycin hampering with the plasma cell differentiation but not altering the B cell numbers after treatment.

Surprisingly, rapamycin treatment led to a striking increase in IL-10$^+$ cells among both plasmablasts and B cells. In a variety of different immune cells, mTOR activity has been shown to increase IL-10 expression via NF-κB-signalling as well as increased lactate production following aerobic glycolysis (Weichhart, Hengstschläger, and Linke, 2015). In contrast, AMPK activation and subsequent decrease in mTOR signalling in myeloid cells has been shown to reduce the expresion of IL-10 (Kovarik *et al.*, 2017). However, IL-10 expression in this thesis was only measured qualitatively using an eGFP-reporter system and not quantified. It cannot be excluded, that the IL-10$^+$ cells did express lower quantities of IL-10 after rapamycin treatment. The increase in frequency might be caused by an increased protection against apoptosis due to IL-10 expression, selecting the fitter IL-10$^+$ cells over the IL-10$^-$ ones (Itoh and Hirohata, 1995; Zeng *et al.*, 2010). Additionally, IL-10 promotes mitophagy, eliminating dysfunctional mitochondria from the cell (Ip *et al.*, 2017). This effect would further increase the survival of IL-10$^+$ cells over the IL-10$^-$ ones.

Using the glycolysis inhibitor 2-DG resulted in plasmablast numbers that were very similar to the rapamycin treated group. Since one of the main consequences of mTOR activity is the induction of aerobic glycolysis, blocking glycolysis directly is likely to have a outcome similar to mTOR inhibition. As overall lymphocyte numbers were not affected at all, glycolysis appears to be essential for plasma cell differentiation, but less important for B cell survival. This notion is supported by the large amounts of glucose plasma cells were shown to take up (see section 3.1). 2-DG could also be shown to activate AMPK and reduce mTOR activity in tumour cells (Liu *et al.*, 2013). Since the inhibitor 2-DG closely resembles glucose, cells with high glucose uptake are likely to take up equivalent amounts of 2-DG as well, making plasmablasts and plasma cells prime targets to 2-DG treatment. Taking into account that 90 % of glucose in plasma cells is used for glycosylation, the low plasmablast numbers might be caused by blocking glycosylation and not hampering with energy generation via glycolysis (Lam, Jash, *et al.*, 2018). In this case, B cells would be less affected due to their lower rate of protein synthesis and glycosylation compared to plasma cells.

Interestingly, 2-DG treatment increased the frequency of IL-10$^+$ among B cells but reduced the frequency among plasmablasts (see section 3.2C). Similar to the situation in the rapamycin treated group, IL-10 might have a beneficial effect on the B cells, increasing their mitochondrial fitness (Itoh and Hirohata, 1995; Zeng *et al.*, 2010). However, this hypothesis fails to explain the decrease in IL-10$^+$ plasmablasts. It is possible that 2-DG affects different plasmablast subsets to different degrees, leading to the decrease in IL-10$^+$ plasmablast.

In conclusion, mTOR signalling is essential for the plasma cell differentiation of MZBs with rapamycin treatment resulting in drastically reduced numbers of plasmablasts. 2-DG treatment drastically reduces the number of plasmablasts as well, although it is unclear whether blockade of glycolysis or glycosylation is the direct cause of this outcome. The impact of both drugs on IL-10 expression is severely contradictory and requires further experiments.

4.3 2-DG eliminates terminally differentiated plasma cells

Assessing the impact of 2-DG on primary lymphocytes from spleen showed a high susceptibility of plasma cells but a lower susceptibility of B cells and other non-B lymphocytes (see section 3.3). The effect of 2-DG on plasma cells was dose-dependent.

Adding to the data discussed above showing that 2-DG prevents the generation of plasmablasts *in vitro*, this finding reveals that 2-DG does not necessarily inhibit the B cells ability to differentiate, but acts on primary plasma cells directly as well. As shown before, plasma cells take up large amounts of glucose (see section 3.1). While 2-DG treatment is able to reduce ATP levels, suggesting decreased glycolytic activity, inhibition of glycolysis alone appears to be insufficient to explain the toxicity level of 2-DG (Kurtoglu, Gao, *et al.*, 2007). Since plasma cells use around 90 % of glucose for glycosylation (Lam, Becker, *et al.*, 2016) and have a high demand for glycoslyation due to their outstanding level of protein synthesis, hampering with this process would make plasma cells highly susceptible, while B cells and other lymphocytes used in this experiment would be much less affected. In 1979, a first article was published dealing with the impact of 2-DG on precursor molecules for glycosylation, showing that 2-DG reduced the incorporation of radio-labelled sugars into LLOs (Datema and Schwarz, 1979). Kurtoglu, Gao, *et al.* (2007) provided similar results showing that 2-DG interferes with N-linked glycosylation due to 2-DG being incorporated into LLOs instead of mannose. These incorrectly synthesised LLOs induced the UPR, leading to a higher toxicity of 2-DG compared to the stronger glycolysis inhibitor 2-FDG (Kurtoglu, Maher, and Lampidis, 2007). In addition to triggering the UPR, dysfunctional glycosylation caused by 2-DG treatment was able to attenuate inflammation in several mouse models by inhibiting pro-inflammatory signalling molecules like IL-6, TNF-α, IL-1β and IFN-γ (Uehara *et al.*, 2022). Blocking IL-6 signalling is especially interesting in the context of this thesis, as it is known to be important for plasma cell differentiation as well as survival (Cassese *et al.*, 2003). This finding further supports the idea that hampering with glycosylation, not glycolysis, is the cause for the high susceptibility of plasma cells to 2-DG treatment.

4.4 Combining 2-DG and bortezomib leads to a synergistic decrease in plasma cell frequencies *in vitro*

To understand whether plasma cells experience elevated levels of ER stress during 2-DG treatment due to dysfunctional glycosylation, primary plasma cells from spleen were treated with proteasome inhibitor bortezomib in addition to 2-DG. At the concentrations used, both drugs killed around 50 % of plasma cells when used on their own, but an additional 65 % of cells were killed when both drugs were combined (see section 3.4).

Bortezomib has been shown to induce UPR components that lead to apoptosis (Obeng *et al.*, 2006). Due to their high protein synthesis acitivity, bortezomib treatment is especially effective in depleting multiple myeloma and primary plasma cells (Obeng *et al.*, 2006; Neubert *et al.*, 2008). Its impact on plasma cells can be seen in this thesis as well. Starting from the idea discussed above that 2-DG might lead to large amounts of misfolded proteins in plasma cells, a synergy between 2-DG and a proteasome inhibitor like bortezomib seemed likely. The significant reduction in plasma cell numbers after combined treatment compared to single treatments clearly supports this hypothesis. Xi, Kurtoglu, Liu, *et al.* (2010) showed that 2-DG treatment upregulates autophagy, lowers ATP levels and increases ER stress. When autophagy was blocked by siRNA, the cells became more susceptible to 2-DG treatment, revealing that autophagy is at least partially used to deal with the increased ER stress. Since the ubiquitin pathway, leading to the protein degradation in the proteasome, is the other common option to relieve ER stress by degrading the misfolded proteins, adding bortezomib is likely to increase susceptibility to 2-DG as well. A paper from 2009 showed that interfering with glycosylation strongly reduced the amount of protein found in the cells (Nakagawa *et al.*, 2009). When a proteasome inhibitor was added, higher levels of the misfolded protein were found in the cells. The inability to deal with the misfolded protein induces long-lasting ER stress that culminates in apoptosis. This mechanism links 2-DG to bortezomib and fits the data presented here nicely.

4.5 2-DG decreases the number of germinal centre B cells and plasma cells *in vivo*

When assessing the impact of 2-DG in BcN mice developing lupus-like symptoms, B cells were affected more distinctly than other cells present in the spleen (see section 3.5). Within the B cell lineage, plasma cell and GCB numbers were reduced the most after 2-DG treatment followed by class-switched B cells. Overall B cell numbers were reduced as well, but to a much lower extend. The surviving plasma cells showed an increased CD19 expression and a higher frequency of IgM expression on the surface.

In line with the data presented here, a 1994 study concluded that 2-DG was not cytotoxic to normal T cells *in vitro* (Miller *et al.*, 1994). While the impact of 2-DG on the expression of cytokines like IL-6 has already been mentioned above, extremely high concentrations of 2-DG were often necessary to see an impact on T cells (up to 50 mM

compared to the 0.2 mM to 5 mM used here) (Cham *et al.*, 2008). These results support the finding that B cells were more affected than other immune cells of the spleen, a large part of which are T cells. The different levels of susceptibility to 2-DG within the B cell lineage could be due to their different levels of protein synthesis. The overall number of B cells includes many resting and naive B cells with low protein synthesis and low need for glycosylation which would reduce the impact of glycosylation inhibition by 2-DG. During class switch, B cells proliferate and therefore need to sustain a higher level of protein synthesis than resting B cells, making them more susceptible to 2-DG. As a consequence of the lower level of class switch, plasma cells would be more likely to express IgM, as can be seen in the data presented. Similar to class-switched B cells, GCB undergo constant changes, bursts of clonal expansion and are rigorously selected based on their BCR affinity during the germinal centre reaction, suggesting an increased susceptibility to 2-DG, as well (De Silva and Klein, 2015). Furthermore, the inhibition of pro-inflammatory cytokine signals like IL-6, TNF-α, IL-1β and IFN-γ could severely limit the cellular interaction, restricting the germinal centre reaction (Uehara *et al.*, 2022). This mechanism would also affect the maturation of the plasma cells, likely blocking their terminal differentiation and full maturation. The increase in CD19 expression among plasma cells shown in this thesis, fits this narrative. As described above, the high ER stress caused by 2-DG treatment is likely to induce apoptosis in plasma cells decreasing the plasma cell number. Additionally, a breakdown of the germinal centre reaction due to inhibiting main signalling pathways would also impact the plasma cell differentiation, decreasing their numbers indirectly. The decrease in GCB numbers is in line with data from Jellusova, Cato, *et al.* (2017), showing high protein synthesis activity in the GCB population. The breakdown of the germinal centre reaction could also result in a more dominant role of the extrafollicular B cell reaction. Since the extrafollicular response yields fewer memory B cells and LLPCs, which, in addition, show a lesser degree of affinity maturation, the composition of the B cell compartment in general and the plasma cells in specific would change after 2-DG treatment (Chu and Berek, 2013; Jenks *et al.*, 2019).

4.6 Bone marrow plasma cells survive 2-DG treatment *in vivo* but show phenotypical changes

Unlike in spleen, treating BcN mice with 2-DG had very little impact on immune cells in the bone marrow (see section 3.6). The numbers of overall B cells, immature, mature, pre, pro and pre-pro B cells were unaffected. While the number of plasma cells was not altered by 2-DG treatment, glucose uptake decreased and CD19 expression increased in these cells, showing that they were affected but survived. Comparing the plasma cell populations in spleen and bone marrow, the susceptibility to 2-DG correlated inversely with the level of TACI expression.

As has been discussed before, 2-DG treatment interferes with N-linked glycosylation, resulting in increased toxicity of 2-DG compared to glycolysis inhibitor 2-FDG due to upregulation of the UPR (Kurtoglu, Maher, and Lampidis, 2007). While long-term

activation of the UPR leads to apoptosis, pro-apopototic signals are integrated with anti-apoptotic signals (Grootjans *et al.*, 2016; Hu *et al.*, 2019). The bone marrow niche is known to provide large amounts of cytokines that increase the survival of plasma cells, like IL-6 or APRIL (Chu and Berek, 2013). It seems likely that the supply of anti-apoptotic signals in the bone marrow could hinder the induction of apoptosis. This idea is supported by the finding that both the glucose uptake and CD19 expression in plasma cells changed after 2-DG treatment. 2-DG reduces glucose uptake by reducing its correct metabolisation, which results in elevated levels of cellular stress, which in turn leads to apoptosis. To display a significant decrease in glucose uptake, the cell needs to be able to endure the impact of the 2-DG treatment. Across all experiments, 2-DG treatment showed tendencies of reducing glucose uptake (data not shown), but the effect was rarely strong enough to be statistically significant. This pattern could be explained by a negative correlation between glucose uptake and induction of apoptosis. Furthermore, BM plasma cells showed a stronger increase in CD19 expression than plasma cells from spleen, showing the full effect of 2-DG treatment in the BM plasma cells. Of note, the glucose uptake of plasma cells in the BM was more than 3-fold higher than that of plasma cells in the spleen (MFI: BM 20 000 vs. SP 6000), resulting in the same glycolytic rate, but higher absolute glucose available for use in BM plasma cells.

In addition to the high external supply of anti-apoptotic signals in the BM niche, plasma cells in the BM were characterised by a high expression of TACI, one of the receptors for BAFF and APRIL, proteins responsible for survival and maturation of B cells and plasma cells (Vincent *et al.*, 2013). The TACI expression was lowest in IgM^- plasma cells from the spleen (4-fold lower than in BM), followed by IgM^+ plasma cells in spleen (2-fold lower than in BM). This pattern was reflected in their susceptibility to 2-DG, further supporting the notion that anti-apoptotic signalling (due to high levels of ligand or high expression of the corresponding receptors) prevented the elimination of plasma cells in BM.

4.7 Combining 2-DG and bortezomib does not improve drug efficacy *in vivo*

Seeing its synergy *in vitro*, a combined treatment of 2-DG and bortezomib was applied in the BcN mouse model *in vivo*. While the numbers of class-switched B cells, GCB and plasma cells were similar after treatment with either bortezomib or 2-DG, no additional effect was observed after combining 2-DG and bortezomib (see section 3.7).

The synergy between 2-DG and bortezomib in inducing apoptosis *in vitro* was confirmed in a recent paper working on tumour cells (Hashimoto *et al.*, 2020). The authors used higher concentrations of both agents (3 mM 2-DG instead of 1 mM and 10 nM bortezomib instead of 2.6 nM (1.5 ng/mL)), which might be due to the possibly higher resistance of tumour cells compared to primary plasma cells. However, the synergy seen between the two drugs in their *in vitro* experiments were even stronger than the one presented in this thesis. When testing the drugs *in vivo*, they used 2- to 3-fold higher concentrations but detected a clear synergistic effect on tumour growth. Aside from the

higher drug dosage, the treatment was performed over 14 d instead of 4 d. These two major differences in the experimental protocol used in this thesis may limit the ability to detect any synergy between 2-DG and bortezomib. When testing for synergy between 2-DG and bortezomib *in vitro* in this thesis, both drugs had to be titrated thoroughly to find the most effective concentrations, supporting the idea that the differences to literature are due to different experimental protocols.

Interestingly, Hashimoto *et al.* (2020) trace the impact of 2-DG back to HK activity, since no synergy was present in HK-knockdown cells. This finding is in accordance with data showing that bortezomib is able to shift cellular metabolism towards aerobic glycolysis, making it susceptible to glycolysis inhibition (Ludman and Melemedjian, 2019). However, HK is responsible for the generation of glucose-6-phosphate, which is used for both glycolysis and glycosylation.

4.8 2-DG induces an unfolded protein response and reduces TACI expression

Since it was unclear whether the effect of 2-DG on plasma cells was due to its impact on glycolysis or glycosylation, spleen cells were treated with 2-DG for 4 h or 24 h and stained for XBP-1s to measure UPR activity. After 4 h, increased XBP-1s levels and decreased TACI expression were detected in plasma cells, but not in B cells and $B220^-$ cells. After 24 h, XBP-1s expression was increased even at low concentrations of 2-DG, while TACI levels were not affected by 2-DG treatment but were 2-fold lower compared to the 4 h time point overall (see section 3.8).

The increase in XBP-1s expression directly links 2-DG treatment with increased UPR activity in plasma cells. This observation supports the reoccurring idea that the impact of 2-DG on plasma cells is at least in part caused by hampering with glycosylation (Kurtoglu, Maher, and Lampidis, 2007; Kurtoglu, Gao, *et al.*, 2007). The strong increase in XBP-1s expression after 4 h using 5 mM 2-DG likely represents the immediate response to accumulating misfolded protein. After 24 h, the remaining plasma cells still show increased XBP-1s levels but since high UPR activity either reduces ER-stress or induces apoptosis, the expression levels are overall lower than at the 4 h time point (Karagöz, Acosta-Alvear, and Walter, 2019; Hetz and Papa, 2018). Increased XBP-1s expression due to 2-DG treatment was found only in plasma cells, suggesting that these cells are much more susceptible to ER-stress.

Since TACI expression is regulated by the activation of the BCR or PRRs, a decrease in TACI levels after 24 h is likely due to the lack of stimulation and activation of these receptors during the cell culture (Zhang *et al.*, 2015). The impact of 2-DG on TACI expression after 4 h could depend on the BCR signalling as well. Since the signalling activity of the BCR is linked to its sialylation, hampering with glycosylation could reduce the signalling strength, thereby downregulating TACI expression (Ilić *et al.*, 2008). As mentioned before, 2-DG inhibits the responses to the inflammatory cytokines IL-6, TNF-α, IL-1β and IFN-γ (Uehara *et al.*, 2022). The same mechanism could also inhibit the BAFF and APRIL signalling via TACI.

4.9 Mannose decreases the impact of 2-DG on plasma cell survival *in vitro*

A 2007 paper showed that the effect of 2-DG on tumour cells was due to its impact on the mannose metabolism (Kurtoglu, Gao, *et al.*, 2007). When testing this finding in plasma cells, mannose was in fact able to prevent most of the 2-DG-induced death in plasma cells, while adding glucose or NEAA were not (see section 3.9). Simultaneously, 2-DG induced a decrease in LAMP-1 expression in plasma cells which could be prevented completely by adding mannose. Contradicting the results of the *in vivo* experiments, only IgM^+ plasma cells were affected by 2-DG.

As discussed before, 2-DG could be shown to interfere with N-linked glycosylation due to the incorporation of 2-DG into LLOs instead of mannose (Datema and Schwarz, 1979; Kurtoglu, Maher, and Lampidis, 2007). Its impact on the mannose metabolism is based on the similar structure of 2-DG and mannose. Glucose and mannose differ only in the orientation of the hydroxy group at the C2 atom. Since 2-DG has lost the defining oxygen atom, it is similar to both sugars, arguably even closer to mannose than glucose (Kurtoglu, Gao, *et al.*, 2007). Since addition of mannose, but not glucose or NEAA, was able to prevent most of the 2-DG-induced cell death, hampering with mannose metabolism appears to be the main cause of apoptotic signals in plasma cells. As mannose plays a major role in the glycosylation of proteins, this pathway seems to be targeted in plasma cells as well, similar to the mechanism discovered in the tumour cells (Kurtoglu, Gao, *et al.*, 2007; Ahadova *et al.*, 2015). Mannose also acts as a label to transport enzymes like hydrolases to lysosomes to ensure their function (Coutinho, Prata, and Alves, 2012). Phosphorylated 2-DG (2-DG-6P) could compete with mannose-6P for the use as a hydrolase tag. However, 2-DG-6P has no affinity to the mannose-6P receptor, blocking the integration of hydrolases into lysosomes and thereby inhibiting the acidification of lysosomes (Gary-Bobo *et al.*, 2007). Since lysosomes are one of two major pathways to alleviate ER stress by degrading misfolded proteins, their correct function is essential to plasma cells (Cenci, 2014). As one of the main components of the lysosome membrane, the protein LAMP-1 serves as a lysosome marker (Eskelinen, 2006). The decrease in LAMP-1 expression after 2-DG treatment could indicate a decrease in the number of lysosomes, possibly by hampering with the M6P tags used to transport hydrolases to the lysosome membrane (Coutinho, Prata, and Alves, 2012). However, the stability of LAMP-1 is closely linked to its glycosylation, which could be directly impaired by 2-DG treatment (Kundra and Kornfeld, 1999). Both of these effects could be prevented by adding mannose, which is in line with the data showing no decrease in LAMP-1 levels if mannose was added to the culture. Surprisingly, the number of IgM^- plasma cells was unaffected by the 2-DG, suggesting that these cells are more resistant to the treatment than IgM^+ plasma cells. This finding contradicts the results from the *in vivo* experiments, where IgM^- plasma cells were more affected than the IgM^+ ones. However, unlike the 24 h *in vitro* experiments, the 4 d *in vivo* experiment took place during an active immune response where new plasma cells are constantly generated, but class switch appears to be impaired due to treatment. In recent years, a population

of IgM^+ LLPCs was found in spleen that develop in the absence of germinal centres (Bohannon *et al.*, 2016). The existence of these cells could explain the large amount of IgM found in NZB/W mice (Hoyer *et al.*, 2004; Brynjolfsson *et al.*, 2018).

4.10 2-DG affects the generation and secretion of different immunoglobulin classes

Since the impact of 2-DG on plasma cells differed depending on their immunoglobulin class, the concentration of different antibody isotypes was determined in cell culture supernatant. Similar to the flow cytometric data, 2-DG lead to a decrease in the concentration of IgM antibodies (see section 3.10). Contrary to the flow cytometric data, the concentrations of IgG and IgA were decreased as well, although the number of IgM^- plasma cells was previously shown to be unaffected by 2-DG.

The decrease in IgM levels in the supernatant is in line with the decrease in numbers of IgM^+ plasma cells. Since the supernatant encompasses 24 h of treatment as well as the 24 h before the treatment, its sensitivity is limited. A decrease in cell number of 50 % as shown before would lead to a decrease of only 25 % in antibody concentration. These ratios fit nicely to the presented data, indicating that the 2-DG-induced cell death in plasma cells is the main cause for the decrease in IgM levels. However, this effect does not explain the decrease in IgG and IgA concentration as the number of IgM^- plasma cells remained stable during treatment *in vitro*. This finding suggests that, in addition to inducing cell death, 2-DG impairs the synthesis or secretion of antibodies. These two processes again point to problems with glycosylation (Ahadova *et al.*, 2015; Y. H. Kim *et al.*, 2016). While mannose was able to prevent most of the 2-DG-induced cell death, the effect is less clear at the level of the secreted antibodies.

The mannose groups show the highest p-values between 2-DG treated and untreated conditions across all isotypes, indicating the lowest degree of certainty that there is a non-random difference between the conditions. However, there is no clear difference between the 2-DG treated conditions, which could be due to the limited sensitivity of the experiment. It is also plausible that mannose is able to prevent cell death but not the impaired cellular function.

4.11 2-DG affects Igκ light chain expression in plasma cells that survive treatment

While 2-DG led to a decrease in the number of IgM^+ plasma cells that was prevented by adding mannose, numbers of IgG^+ and IgA^+ plasma cells were unaffected (see section 3.11). Looking at the Igκ expression, a marker for the amount of antibody within the cell, IgG^+ and IgA^+, but not IgM^+, plasma cells showed increased levels of antibodies after 2-DG treatment that could be prevented by adding mannose. XBP-1s staining revealed an increase in UPR activity after 2-DG treatment in IgG^+ plasma cells, while XBP-1s expression in IgM^+ plasma cells was reduced and normalised by adding mannose.

The impact of 2-DG on IgM^+ plasma cells nicely reproduces results discussed before. Combing the flow cytometry and ELISA data, the IgM concentration in the supernatant likely decreased due to the 2-DG induced death of the IgM^+ cells since the amount of Igκ light chain inside the cells was not affected by 2-DG. Since the numbers of IgG^+ and IgA^+ plasma cells were not affected by 2-DG, the decrease in concentration of these isotypes in the supernatant could not be explained with 2-DG induced cell death. However, plasma cells of both isotypes show elevated levels of Igκ retained inside the cells which could account for the decrease in secreted antibodies. This finding suggests that, while IgG^+ and IgA^+ are able to survive the 2-DG treatment, their protein synthesis or secretion (and therefore their function) is impaired. As discussed before, both protein synthesis and secretion are linked to glycosylation, supporting the hypothesis that plasma cells suffer not only from inhibition of glycolysis but glycosylation after 2-DG treatment (Ahadova *et al.*, 2015; Y. H. Kim *et al.*, 2016). This is further supported by the finding that IgG^+ plasma cells showed a strong increase in XBP-1s expression after 2-DG treatment. Since one of XBP-1s functions is to reduce the amount of protein that enters the secretory pathway, the high XBP-1s expression seen in IgG^+ plasma cells could explain the large amount of antibodies found inside of these cells (Hollien and Weissman, 2006; Grootjans *et al.*, 2016). In contrast to that, IgM^+ plasma cells showed decreased XBP-1s expression after treatment. Since prolonged ER stress leads to promotion of apoptosis, IgM^+ plasma cells appear to be less resistant to the increase in pro-apoptotic signals than their IgG^+ counterparts, resulting in the survival of IgM^+ plasma cells with lower XBP-1s expression (Ghosh *et al.*, 2014; Grootjans *et al.*, 2016).

In most cases, the effects of the 2-DG treatment could be attenuated or prevented by adding mannose. The impact of mannose was clear on the number and the XBP-1s expression of IgM^+ plasma cells as well as on the Igκ expression of IgG^+ and IgA^+ plasma cells, suggesting that these parameters were influenced by glycosylation or lysosome activity. However, the increase in XBP-1s expression in IgG^+ plasma cells after 2-DG treatment could not be attenuated by adding mannose. Since the assumed cause of the increase in XBP-1s expression, the increased amount of Igκ within the cell, could be attenuated by mannose, another mechanism must exist that induces XBP-1s expression in IgG^+ plasma cells.

4.12 Mannose reduces the effect of 2-DG, but not 2-FDG

Since mannose was able to prevent many of the effects of 2-DG, its impact on the structurally similar glycolysis inhibitor 2-FDG was tested. While similar, the minute difference in structure makes 2-FDG a stronger glycolysis and weaker glycosylation inhibitor (Kurtoglu, Maher, and Lampidis, 2007). As shown before, 2-DG reduced the number of plasma cells, the frequency of IgM expression among the plasma cells and the LAMP-1 expression (see section 3.12). All of these effect could be prevented or at least attenuated by the addition of mannose. Treatment with 2-FDG resulted in a similar decrease in IgM frequency, but had little to no effect on the number of plasma cells or their LAMP-1 expression. Furthermore, adding mannose had no effect on 2-FDG treatment.

As discussed before, 2-DG was able to reduce the number of plasma cells, an effect that could be prevented by mannose. Interestingly, the plasma cell number after 2-FDG treatment appears to be in between the untreated and the 2-DG treated group. This would suggest that, while glycolysis inhibition via 2-FDG has an effect on the survival of plasma cells, it is not as strong as the impact of 2-DG, which acts on glycosylation. Similar results have been obtained from groups working on tumour cells (Liu *et al.*, 2013; Kurtoglu, Maher, and Lampidis, 2007). However, due to the small sample size, the differences in plasma cell number between 2-FDG and either untreated or 2-DG conditions fall short of the significance threshold of $p > 0.05$. Adding mannose to the 2-FDG treatment had no impact on the plasma cells survial, indicating that mannose metabolism is not affected by 2-FDG. As mentioned before, this idea is in line with literature showing that 2-FDG has a stronger impact on glycolysis, but a weaker influence on glycosylation than 2-DG (Kurtoglu, Maher, and Lampidis, 2007). Looking at the frequency of IgM^+ plasma cells, both 2-DG and 2-FDG clearly reduced IgM expression, indicating that hampering with glucose metabolism affects IgM expression. While no clear difference between 2-DG and 2-FDG could be found, addition of mannose was able to attenuate the impact of 2-DG, but had no impact on 2-FDG treatment. The fact that mannose had only a minor effect on 2-DG treatment reinforces the idea that hampering with glucose, but not mannose, metabolism is the main cause for the drop in IgM expression in plasma cells. In contrast to the IgM expression, LAMP-1 expression was decreased by 2-DG, but not 2-FDG treatment. The impact of 2-DG was completely preventable by adding mannose, showing that the decrease in LAMP-1 expression was caused by hampering with mannose instead of glucose metabolism. These findings illustrate that some parameters of plasma cell function are linked to correct use of glucose, while others depend on flawless mannose metabolism. In the end, the mixture of these parameters determines the viability of the cell.

4.13 Hexokinase, but not phosphofructokinase, inhibitors hinder the generation of plasmablasts

Since 2-DG and 2-FDG revealed distinct effects on plasma cells due to their different affinity towards inhibiting glycolysis or glycosylation, the phosphofructokinase inhibitor 3PO was used *in vitro* to assess the impact of glycolysis inhibition further downstream. While both 2-DG, 2-FDG and 3PO all led to a sharp decrease in plasmablast numbers, only 3PO had a significant impact on the B cell numbers as well. The decrease in plasmablast and B cells numbers was 9-fold and 1.2-fold for 2-DG, 6-fold and 1.5-fold for 2-FDG and 32-fold and 23-fold for 3PO, respectively.

Comparing the three inhibitors, 2-DG showed the highest specificity towards plasmablasts since it decreased the number of plasmablasts 7.5 times stronger than the B cells ($9/1.2 = 7.5$). 2-FDG showed the second highest specificity towards plasmablasts with a value of 4 ($6/1.5 = 4$), followed by 3PO with a value of 1.39 ($32/23 = 1.39$). As mentioned before, 2-DG has a stronger impact on the assembly of LLOs and therefore on glycosylation (Kurtoglu, Gao, *et al.*, 2007), while 2-FDG is a more potent glycol-

ysis inhibitor (Kurtoglu, Maher, and Lampidis, 2007). However, both of these drugs inhibit hexokinase to different degrees. Hexokinase generates glucose-6P which is the main source of mannose in the cell. Therefore, while 2-FDG does not directly compete with mannose, it still hampers with the generation of mannose, affecting its metabolism (Sharma, Ichikawa, and Freeze, 2014). Due to its downstream target, 3PO does not interfere with mannose generation, making it the purest glycolysis inhibitor of the three drugs. Combining these different modes of action with the specificity towards plasmablast shows that the stronger the impact on glycolysis is, the weaker is the impact on plasmablasts. Inversely, the stronger the impact on mannose metabolism, the stronger the impact on plasmablasts. This pattern further underlines the notion that inhibition of glycosylation is the main cause of death in plasma cells or plasmablasts, while the effect of glycolysis inhibition is comparatively small. This reflects the fact that approximately 90 % of glucose in plasma cells is used for glycosylation (Lam, Becker, *et al.*, 2016).

4.14 Glycosylation inhibition and 2-DG treatment result in similar plasma cell numbers, LAMP-1 and XBP-1s expression

To assess the impact of glycosylation inhibition on plasma cells, N-linked glycosylation inhibitor tunicamycin was used *in vitro* and compared to 2-DG. Interestingly, both tunicamycin and 2-DG were able to reduce the number of plasma cells as well as their LAMP-1 expression, while combining the two drugs had no additional effect (see section 3.14). Contrary to previous data, neither 2-DG nor tunicamycin had an impact on the XBP-1s expression in plasma cells. However, the combination of both drugs led to an increase in XBP-1s expression.

In line with previous data, 2-DG led to a decrease in plasma cell number by factor 2. Interestingly, tuncamycin had a very similar impact on plasma cell numbers, hinting that both drugs could share some similarities. Since the combination of both drugs had no further effect, it seems likely that both drugs target the same mechanism. This finding further supports the idea that many of the effects of 2-DG are linked to glycosylation. The exact same pattern was found in the expression of LAMP-1. As mentioned before, deglycosylation leads to the rapid degradation of LAMP-1 (Kundra and Kornfeld, 1999). Since both tunicamycin and 2-DG reduced the protein level of LAMP-1 in plasma cells, the seem to share the ability to block glycosylation. This is in line with literature, finding that both drugs are able to block surface expression of proteins and induces ER stress due to their impact on glycosylation (Andresen *et al.*, 2012; Xi, Barredo, *et al.*, 2013). The lack of synergy between the two drugs in decreasing LAMP-1 levels further supports the impact of 2-DG on glycosylation. In contrast to the number of plasma cells and the LAMP-1 expression, the XBP-1s levels were not altered by either drug alone, but only when combining both. Previous experiments have shown that induction of XBP-1s is strong after 4 h using a high concentration of 2-DG but weaker after 24 h treatment (see section 3.8). Since the cells in this experiment were cultivated for 48 h and treated for

the last 24 h, the induction of XBP-1s has likely passed its maximum. Furthermore, a lower concentration of 2-DG was used here. Since both 2-DG and tunicamycin were used at concentrations below their maximum potential, combining the drugs could maximise their effect. However, even in these conditions the combined treatment leads to a rather small increase in XBP-1s levels of approximately 10 % compared to 30 % after 4 h and a high concentration of 2-DG.

4.15 Conclusion

This study shows that the sugar metabolism is vital for plasma cells. Plasma cells take up large amounts of glucose, but show a relatively small mitochondrial mass, reminiscent of cells using aerobic glycolysis or warburg metabolism. Blocking glycolysis with the glucose analogue 2-DG induces apoptosis in plasma cells but has little impact on the number of B cells. However, the frequency of IL-10 expression is increased among these B cells. 2-DG seems to act on plasma cells mainly via its effect on glycosylation, hampering with the generation of LLOs, the building blocks for glycosylation, as well as lysosome function. Many of the effects of 2-DG can be prevented by addition of mannose, showing that 2-DG impacts glycosylation by hampering with both glucose and mannose metabolism. Its inhibiting effect on glycolysis seems to be of minor importance. Blocking the generation of regular LLOs and instead incorporating 2-DG-derived LLOs leads to ER stress and induction of the UPR. While the UPR leads to apoptosis in IgM^+ plasma cells, IgG^+ and IgA^+ plasma cells survive the ER stress but show limited functionality. Initial evidence shows that using 2-DG and bortezomib in combination could amplify the impact of 2-DG due to the synergy of both drugs *in vitro*. These experiments highlight both the promising therapeutic potential of 2-DG in autoimmune diseases as well as the necessary research that remains to be done before 2-DG could be used in a therapeutic setting.

5 Outlook

While this thesis describes many aspects of the role of sugar metabolism for B cells and plasma cells, a lot of details are left unclear. To get a more comprehensive view on the metabolic profile of plasma cells and B cell subsets, functional assays like the Agilent Seahorse Analyzer should be used to determine oxygen consumption and glycolytic flow in addition to the glucose uptake and mitochondrial mass. Such experiments have been performed on activated B cells but a detailed differentiation of these cells is still lacking. These analyses could be combined with the IL-10 expression detected in eGFP reporter mice to check for metabolic differences between IL-10^{+} and IL-10^{-} cells. Furthermore, the impact of 2-DG on glycosylation and lysosome function needs to be examined directly. For this purpose, glycosylation patterns of IgM, IgG and IgA antibodies should be analysed after 2-DG treatment using mass spectrometry. To measure lysosome activity, the increase in fluorescence intensity of proteins labelled with an excess of fluorophores leading to self-quenching can be measured during lysosomal degradation. Combining measurements of these direct effects of 2-DG with mRNA and protein levels of other UPR markers like PERK and ATF6 would specify the mechanism underlying the 2-DG-induced cell death. Gaining a deeper understanding of the impact on glycosylation and lysosome function could also provide evidence for the mechanism behind the synergy of 2-DG and bortezomib found *in vitro*. The impact of both drugs *in vivo* needs to be analysed in more detail, titrating the drugs or using different treatment regimens to assess the full therapeutic potential of both 2-DG and bortezomib.

Bibliography

Adekola, Kehinde, Steven T. Rosen, and Mala Shanmugam (2012). "Glucose transporters in cancer metabolism". In: *Current Opinion in Oncology* 24, pp. 650–654.

Agnello, Maria, Giovanni Morici, and Anna Maria Rinaldi (2008). "A method for measuring mitochondrial mass and activity". In: *Cytotechnology* 56.3, pp. 145–149.

Ahadova, Aysel *et al.* (2015). "Dose-dependent effect of 2-deoxy-D-glucose on glycoprotein mannosylation in cancer cells". In: *IUBMB Life* 67.3, pp. 218–226.

Akkaya, Munir *et al.* (2018). "Second signals rescue B cells from activation-induced mitochondrial dysfunction and death". In: *Nature Immunology* 19.8, pp. 871–884.

Akram, M. (2013). "Mini-review on glycolysis and cancer". In: *Journal of Cancer Education* 28.3, pp. 454–457.

Andresen, Lars *et al.* (2012). " 2-Deoxy d-Glucose Prevents Cell Surface Expression of NKG2D Ligands through Inhibition of N -Linked Glycosylation ". In: *The Journal of Immunology* 188.4, pp. 1847–1855.

Bohannon, Caitlin *et al.* (2016). "Long-lived antigen-induced IgM plasma cells demonstrate somatic mutations and contribute to long-Term protection". In: *Nature Communications* 7.May.

Brookens, Shawna K. *et al.* (2020). "AMPKα1 in B Cells Dampens Primary Antibody Responses yet Promotes Mitochondrial Homeostasis and Persistence of B Cell Memory". In: *The Journal of Immunology* 205.11, pp. 3011–3022.

Brynjolfsson, Siggeir F. *et al.* (2018). "Long-lived plasma cells in mice and men". In: *Frontiers in Immunology* 9.NOV, pp. 1–7.

Calder, Philip C, George Dimitriadis, and Philip Newsholme (2007). "Glucose metabolism in lymphoid and inflammatory cells and tissues." In: *Current opinion in clinical nutrition and metabolic care* 10.4, pp. 531–40.

Caro-Maldonado, Alfredo *et al.* (2014). "Metabolic reprogramming is required for antibody production that is suppressed in anergic but exaggerated in chronically BAFF-exposed B cells." In: *Journal of immunology (Baltimore, Md. : 1950)* 192.8, pp. 3626–3636.

Cassese, G. *et al.* (2003). "Plasma Cell Survival Is Mediated by Synergistic Effects of Cytokines and Adhesion-Dependent Signals". In: *The Journal of Immunology* 171.4, pp. 1684–1690.

Castelo-Branco, Camil and Iris Soveral (2014). "The immune system and aging: A review". In: *Gynecological Endocrinology* 30.1, pp. 16–22.

Cenci, Simone (2012). “The Proteasome in Terminal Plasma Cell Differentiation”. In: *Seminars in Hematology* 49.3, pp. 215–222.

– (2014). “Autophagy, a new determinant of plasma cell differentiation and antibody responses”. In: *Molecular Immunology* 62.2, pp. 289–295.

Cham, Candace M. *et al.* (Sept. 2008). “Glucose deprivation inhibits multiple key gene expression events and effector functions in CD8+ T cells”. In: *European Journal of Immunology* 38.9, pp. 2438–2450.

Chaplin, David D. (2010). “Overview of the immune response”. In: *Journal of Allergy and Clinical Immunology* 125.2 SUPPL. 2, S3–S23.

Chazotte, Brad (2011). “Labeling mitochondria with mitotracker dyes”. In: *Cold Spring Harbor Protocols* 6.8, pp. 990–992.

Cho, Judy H. and Marc Feldman (2015). “Heterogeneity of autoimmune diseases: Pathophysiologic insights from genetics and implications for new therapies”. In: *Nature Medicine* 21.7, pp. 730–738.

Choi, Jinyoung, Sang Taek Kim, and Joe Craft (2012). “The pathogenesis of systemic lupus erythematosus-an update”. In: *Current Opinion in Immunology* 24.6, pp. 651–657.

Chu, Van T. and Claudia Berek (2013). “The establishment of the plasma cell survival niche in the bone marrow”. In: *Immunological Reviews* 251.1, pp. 177–188.

Cobb, Brian A. (2020). “The history of IgG glycosylation and where we are now”. In: *Glycobiology* 30.4, pp. 202–213.

Cossarizza, Andrea *et al.* (2019). “Guidelines for the use of flow cytometry and cell sorting in immunological studies (second edition)”. In: *European Journal of Immunology* In press, pp. 1–528.

Coutinho, Maria Francisca, Maria João Prata, and Sandra Alves (2012). “Mannose-6-phosphate pathway: A review on its role in lysosomal function and dysfunction”. In: *Molecular Genetics and Metabolism* 105.4, pp. 542–550.

Datema, Roelf and Ralph T Schwarz (Oct. 1979). “Interference with Glycosylation of Glycoproteins”. In: *Biochem J* 184.1, pp. 113–123.

De Silva, Nilushi S. and Ulf Klein (2015). “Dynamics of B cells in germinal centres”. In: *Nature Reviews Immunology* 15.3, pp. 137–148.

Donnelly, Raymond P. and David K. Finlay (2015). “Glucose, glycolysis and lymphocyte responses”. In: *Molecular Immunology* 68.2, pp. 513–519.

Dufort, Fay J. *et al.* (2014). “Glucose-dependent de novo lipogenesis in B lymphocytes: A requirement for atp-citrate lyase in lipopolysaccharide-induced differentiation”. In: *Journal of Biological Chemistry* 289.10, pp. 7011–7024.

Elbein, A. D. (1987). “Inhibitors of the biosynthesis and processing of N-linked oligosaccharide chains”. In: *Annual Review of Biochemistry* Vol. 56, pp. 497–534.

Eskelinen, Eeva Liisa (2006). "Roles of LAMP-1 and LAMP-2 in lysosome biogenesis and autophagy". In: *Molecular Aspects of Medicine* 27.5-6, pp. 495–502.

Ganeshan, Kirthana and Ajay Chawla (2014). "Metabolic Regulation of Immune Responses". In: *The Journal of Clinical Investigation* 32.1, pp. 609–634.

Gary-Bobo, M. *et al.* (2007). "Mannose 6-Phosphate Receptor Targeting and its Applications in Human Diseases". In: *Current Medicinal Chemistry* 14.28, pp. 2945–2953.

Ghia, Paolo *et al.* (1996). "Ordering of human bone marrow B lymphocyte precursors by single-cell polymerase chain reaction analyses of the rearrangement status of the immunoglobulin H and L chain gene loci". In: *Journal of Experimental Medicine* 184.6, pp. 2217–2229.

Ghosh, Rajarshi *et al.* (2014). "Allosteric inhibition of the IRE1α RNase preserves cell viability and function during endoplasmic reticulum stress". In: *Cell* 158.3, pp. 534–548.

Grootjans, Joep *et al.* (2016). "The unfolded protein response in immunity and inflammation". In: *Nature Reviews Immunology* 16.8, pp. 469–484.

Hashimoto, Eiichi *et al.* (2020). "Enhanced O-GlcNAcylation Mediates Cytoprotection under Proteasome Impairment by Promoting Proteasome Turnover in Cancer Cells". In: *iScience* 23.7, p. 101299.

Hetz, Claudio and Feroz R. Papa (2018). "The Unfolded Protein Response and Cell Fate Control". In: *Molecular Cell* 69.2, pp. 169–181.

Hiepe, Falk *et al.* (2011). "Long-lived autoreactive plasma cells drive persistent autoimmune inflammation". In: *Nature Reviews Rheumatology* 7.3, pp. 170–178.

Hollien, Julie and Jonathan S. Weissman (July 2006). "Decay of Endoplasmic Reticulum-Localized mRNAs During the Unfolded Protein Response". In: *Science* 313.5783, pp. 104–107.

Hoyer, Bimba F. *et al.* (2004). "Short-lived plasmablasts and long-lived plasma cells contribute to chronic humoral autoimmunity in NZB/W mice". In: *Journal of Experimental Medicine* 199.11, pp. 1577–1584.

Hu, Hai *et al.* (2019). "The C/EBP homologous protein (CHOP) transcription factor functions in endoplasmic reticulum stress-induced apoptosis and microbial infection". In: *Frontiers in Immunology* 10.JAN, pp. 1–13.

Ilić, Vesna *et al.* (2008). "Glycosylation of IgG B cell receptor (IgG BCR) in multiple myeloma: Relationship between sialylation and the signal activity of IgG BCR". In: *Glycoconjugate Journal* 25.4, pp. 383–392.

Ionescu, Lavinia and Simon Urschel (2019). "Memory B Cells and Long-lived Plasma Cells". In: *Transplantation* 103.5, pp. 890–898.

Ip, W. K.Eddie *et al.* (2017). "Anti-inflammatory effect of IL-10 mediated by metabolic reprogramming of macrophages". In: *Science* 356.6337, pp. 513–519.

Itoh, K and S Hirohata (1995). "The role of IL-10 in human B cell activation, proliferation, and differentiation." In: *Journal of immunology (Baltimore, Md. : 1950)* 154.9, pp. 4341–50.

Jang, Kyoung-Jin *et al.* (2015). "Mitochondrial function provides instructive signals for activation-induced B-cell fates." In: *Nature communications* 6, pp. 1–13.

Jellusova, Julia, Matthew H Cato, *et al.* (Jan. 2017). "Gsk3 is a metabolic checkpoint regulator in B cells". In: *Nature Immunology* 18.3, pp. 303–312.

Jellusova, Julia and Robert C. Rickert (2016). "The PI3K pathway in B cell metabolism". In: *Critical Reviews in Biochemistry and Molecular Biology* 9238.September, pp. 1–20.

Jenks, Scott A. *et al.* (2019). "Extrafollicular responses in humans and SLE". In: *Immunological Reviews* 288.1, pp. 136–148.

Karagöz, G. Elif, Diego Acosta-Alvear, and Peter Walter (Jan. 2019). "The Unfolded Protein Response: Detecting and Responding to Fluctuations in the Protein-Folding Capacity of the Endoplasmic Reticulum". In: *Cold Spring Harbor Perspectives in Biology*, pp. 1–20.

Kaul, Arvind *et al.* (2016). "Systemic lupus erythematosus". In: *Nature Reviews Disease Primers* 2.June, pp. 1–22.

Kim, Sang Gyun, Gwen R. Buel, and John Blenis (2013). "Nutrient regulation of the mTOR Complex 1 signaling pathway". In: *Molecules and Cells* 35.6, pp. 463–473.

Kim, Young Hun *et al.* (2016). "N-linked glycosylation plays a crucial role in the secretion of HMGB1". In: *Journal of Cell Science* 129.1, pp. 29–38.

Kondo, Motonari *et al.* (2002). "Origins and functions of B-1 cells with notes on the role of CD5". In: *Annual Review of Immunology* 21.1, pp. 759–806.

Kornfeld, S. (1978). "Effect of Tunicamycin on IgM , IgA , and IgG Secretion by Mouse Plasmacytoma Cells". In: *The Journal of Immunology* 121, pp. 990–996.

Kornfeld, S. and I. Mellman (1989). "The biogenesis of lysosomes". In: *Annual Review of Cell Biology* 5, pp. 483–525.

Kovarik, Johannes J. *et al.* (2017). "Fasting metabolism modulates the interleukin-12/interleukin-10 cytokine axis". In: *PLoS ONE* 12.7, pp. 1–16.

Kundra, Robin and S. Kornfeld (1999). "Asparagine-linked oligosaccharides protect Lamp-1 and Lamp-2 from intracellular proteolysis". In: *Journal of Biological Chemistry* 274.43, pp. 31039–31046.

Kurtoglu, Metin, Ningguo Gao, *et al.* (2007). "Under normoxia, 2-deoxy-D-glucose elicits cell death in select tumor types not by inhibition of glycolysis but by interfering with N-linked glycosylation". In: *Molecular Cancer Therapeutics* 6.11, pp. 3049–3058.

Kurtoglu, Metin, Johnathan C. Maher, and Theodore J. Lampidis (2007). "Differential toxic mechanisms of 2-deoxy-D-glucose versus 2-fluorodeoxy-D-glucose in hypoxic and normoxic tumor cells". In: *Antioxidants and Redox Signaling* 9.9, pp. 1383–1390.

Lam, Wing Y., Amy M Becker, *et al.* (2016). “Mitochondrial Pyruvate Import Promotes Long-Term Survival of Antibody-Secreting Plasma Cells.” In: *Immunity* 45.1, pp. 60–73.

Lam, Wing Y. and Deepta Bhattacharya (2018). “Metabolic Links between Plasma Cell Survival, Secretion, and Stress”. In: *Trends in Immunology* 39.1, pp. 19–27.

Lam, Wing Y., Arijita Jash, *et al.* (2018). “Metabolic and Transcriptional Modules Independently Diversify Plasma Cell Lifespan and Function”. In: *Cell Reports* 24.9, pp. 2479–2492.

Lampidis, Theodore J. *et al.* (2006). “Efficacy of 2-halogen substituted D-glucose analogs in blocking glycolysis and killing "hypoxic tumor cells"”. In: *Cancer Chemotherapy and Pharmacology* 58.6, pp. 725–734.

LeBien, Tucker W and Thomas F Tedder (2008). “B lymphocytes : how they develop and function”. In: *The american society of hematology* 112.5, pp. 1570–1580.

Li, Xue Bing, Jun Dong Gu, and Qing Hua Zhou (2015). “Review of aerobic glycolysis and its key enzymes - new targets for lung cancer therapy”. In: *Thoracic Cancer* 6.1, pp. 17–24.

Lightman, Shivana M., Adam Utley, and Kelvin P. Lee (2019). “Survival of long-lived plasma cells (LLPC): Piecing together the puzzle”. In: *Frontiers in Immunology* 10.MAY, pp. 1–12.

Liu, Huaping *et al.* (2013). “Conversion of 2-deoxyglucose-induced growth inhibition to cell death in normoxic tumor cells”. In: *Cancer Chemotherapy and Pharmacology* 72.1, pp. 251–262.

Ludman, Taylor and Ohannes K. Melemedjian (2019). “Bortezomib-induced aerobic glycolysis contributes to chemotherapy-induced painful peripheral neuropathy”. In: *Molecular Pain* 15.

Luu, Van Phi, Monica I. Vazquez, and Albert Zlotnik (2014). “B cells participate in tolerance and autoimmunity through cytokine production”. In: *Autoimmunity* 47.1, pp. 1–12.

Manz, Rudolf A., Sergio Arce, *et al.* (2002). “Humoral immunity and long-lived plasma cells”. In: *Current Opinion in Immunology* 14.4, pp. 517–521.

Manz, Rudolf A., Andreas Thiel, and Andreas Radbruch (1997). “Lifetime of plasma cells in the bone marrow”. In: *Nature* 388.6638, pp. 133–134.

Mariño, Eliana *et al.* (2008). “Marginal-zone B-cells of nonobese diabetic mice expand with diabetes onset, invade the pancreatic lymph nodes, and present autoantigen to diabetogenic T-cells”. In: *Diabetes* 57.2, pp. 395–404.

Matthews, Allysia J. *et al.* (2014). *Regulation of immunoglobulin class-switch recombination: Choreography of noncoding transcription, targeted DNA deamination, and long-range DNA repair*. 1st ed. Vol. 122. Elsevier Inc., pp. 1–57.

Miller, Edwin S. *et al.* (1994). "Inhibition of murine splenic T lymphocyte proliferation by 2-deoxy-D-glucose-induced metabolic stress". In: *Journal of Neuroimmunology* 52.2, pp. 165–173.

Morel, Laurence *et al.* (2000). "Genetic reconstitution of systemic lupus erythematosus immunopathology with polycongenic murine strains". In: *Proceedings of the National Academy of Sciences of the United States of America* 97.12, pp. 6670–6675.

Nakagawa, Hiroshi *et al.* (2009). "Disruption of N-linked glycosylation enhances ubiquitin-mediated proteasomal degradation of the human ATP-binding cassette transporter ABCG2". In: *FEBS Journal* 276.24, pp. 7237–7252.

Neubert, Kirsten *et al.* (2008). "The proteasome inhibitor bortezomib depletes plasma cells and protects mice with lupus-like disease from nephritis". In: *Nature Medicine* 14.7, pp. 748–755.

Nicholson, Lindsay B. (2016). "The immune system". In: *Essays in Biochemistry* 60.3, pp. 275–301.

O'Neil, Roger G., Ling Wu, and Nizar Mullani (2005). "Uptake of a fluorescent deoxyglucose analog (2-NBDG) in tumor cells". In: *Molecular Imaging and Biology* 7.6, pp. 388–392.

Obeng, Esther A *et al.* (June 2006). "Proteasome inhibitors induce a terminal unfolded protein response in multiple myeloma cells". In: *Blood* 107.12, pp. 4907–16.

Parkin, Jacqueline and Bryony Cohen (June 2001). "An overview of the immune system". In: *The Lancet* 357.9270, pp. 1777–1789.

Paulick, Margot G. and Carolyn R. Bertozzi (2008). "The glycosylphosphatidylinositol anchor: A complex membrane-anchoring structure for proteins". In: *Biochemistry* 47.27, pp. 6991–7000.

Pengo, Niccolò *et al.* (2013). "Plasma cells require autophagy for sustainable immunoglobulin production." In: *Nature immunology* 14.3, pp. 298–305.

Pieper, Kathrin, Bodo Grimbacher, and Hermann Eibel (2013). "B-cell biology and development". In: *Journal of Allergy and Clinical Immunology* 131.4, pp. 959–971.

Pillai, Shiv, Hamid Mattoo, and Annaiah Cariappa (2012). "B cells and Autoimmunity". In: *Curr Opin Immunol.* 23.6, pp. 721–731.

Price, Madeline J. *et al.* (2019). "IgM, IgG, and IgA Influenza-Specific Plasma Cells Express Divergent Transcriptomes". In: *The Journal of Immunology* 203.8, pp. 2121–2129.

Schjoldager, Katrine T. *et al.* (2020). "Global view of human protein glycosylation pathways and functions". In: *Nature Reviews Molecular Cell Biology* 21.12, pp. 729–749.

Segarra, A. *et al.* (2020). "Efficacy and safety of bortezomib in refractory lupus nephritis: a single-center experience". In: *Lupus* 29.2, pp. 118–125.

Sharma, Vandana and Hudson H. Freeze (2011). "Mannose efflux from the cells: A potential source of mannose in blood". In: *Journal of Biological Chemistry* 286.12, pp. 10193–10200.

Sharma, Vandana, Mie Ichikawa, and Hudson H. Freeze (2014). "Mannose metabolism: More than meets the eye". In: *Biochemical and Biophysical Research Communications* 453.2, pp. 220–228.

Shi, Wei *et al.* (2015). "Transcriptional profiling of mouse B cell terminal differentiation defines a signature for antibody-secreting plasma cells." In: *Nature immunology* 16.6, pp. 663–73.

Sintes, Jordi *et al.* (2017). "mTOR intersects antibody-inducing signals from TACI in marginal zone B cells". In: *Nature Communications* 8.1.

Slifka, M K, M Matloubian, and R Ahmed (1995). "Bone marrow is a major site of long-term antibody production after acute viral infection". In: *Journal of Virology* 69.3, pp. 1895–1902.

Soto-Heredero, Gonzalo *et al.* (2020). "Glycolysis – a key player in the inflammatory response". In: *FEBS Journal* 287.16, pp. 3350–3369.

Tellier, Julie and Stephen L Nutt (Oct. 2018). "Plasma cells: The programming of an antibody-secreting machine". In: *European Journal of Immunology*, pp. 1–8.

Teslaa, Tara and Michael A. Teitell (2014). "Techniques to monitor glycolysis". In: *Methods in Enzymology* 542, pp. 91–114.

Thorens, Bernard and Mike Mueckler (Feb. 2010). "Glucose transporters in the 21st Century". In: *American Journal of Physiology-Endocrinology and Metabolism* 298.2, E141–E145.

Uehara, Ikuno *et al.* (2022). "2-Deoxy-d-glucose induces deglycosylation of proinflammatory cytokine receptors and strongly reduces immunological responses in mouse models of inflammation". In: *Pharmacology Research and Perspectives* 10.2, pp. 1–16.

Vincent, Fabien B. *et al.* (2013). "The BAFF/APRIL system: Emerging functions beyond B cell biology and autoimmunity". In: *Cytokine and Growth Factor Reviews* 24.3, pp. 203–215.

Vos, Q. *et al.* (2000). "B-cell activation by T-cell-independent type 2 antigens as an integral part of the humoral immune response to pathogenic microorganisms". In: *Immunological Reviews* 176, pp. 154–170.

Wang, Lifeng, Fu Sheng Wang, and M. Eric Gershwin (2015). "Human autoimmune diseases: A comprehensive update". In: *Journal of Internal Medicine* 278.4, pp. 369–395.

Warburg, Otto, Karl Posener, and Erwin Negelein (1924). "Über den Stoffwechsel von Carcinomzellen". In: *Biochem. Z.* 152, pp. 309–344.

Weichhart, Thomas, Markus Hengstschläger, and Monika Linke (2015). "Regulation of innate immune cell function by mTOR". In: *Nature Reviews Immunology* 15.10, pp. 599–614.

Windt, Gerritje J W van der and Erika L. Pearce (2012). "Metabolic switching and fuel choice during T-cell differentiation and memory development". In: *Immunological Reviews* 249.1, pp. 27–42.

Xi, Haibin, Julio C. Barredo, *et al.* (2013). "Endoplasmic reticulum stress induced by 2-deoxyglucose but not glucose starvation activates AMPK through CaMKKβ leading to autophagy". In: *Biochemical Pharmacology* 85.10, pp. 1463–1477.

Xi, Haibin, Metin Kurtoglu, and Theodore J. Lampidis (2014). "The wonders of 2-deoxy-d-glucose". In: *IUBMB Life* 66.2, pp. 110–121.

Xi, Haibin, Metin Kurtoglu, Huaping Liu, *et al.* (2010). "2-Deoxy-d-glucose activates autophagy via endoplasmic reticulum stress rather than ATP depletion". In: *Cancer Chemotherapy and Pharmacology* 67.4, pp. 899–910.

Xu, Xiaojin *et al.* (2012). "MTOR, linking metabolism and immunity". In: *Seminars in Immunology* 24.6, pp. 429–435.

Zeng, Li *et al.* (2010). "IL-10 promotes resistance to apoptosis and metastatic potential in lung tumor cell lines". In: *Cytokine* 49.3, pp. 294–302.

Zhang, Yi *et al.* (2015). "Effect of TACI signaling on humoral immunity and autoimmune diseases". In: *Journal of Immunology Research* 2015.Cvid.

List of Figures

1 Schematic overview of the glycolytic pathway 9
2 Complete breakdown of glucose from glycolysis to oxidative phosphorylation 10
3 Metabolic pathways of mannose 12
4 Role of metabolism during inflammation and resolution 13

5 Glucose uptake and mitochondrial mass of spleen and bone marrow cells . 30
6 Glycolysis and mTOR inhibition in LPS stimulated B cell culture 32
7 Impact of 2-DG on terminally differentiated plasma cells 34
8 Synergistic effect of 2-DG and bortezomib on splenic plasma cells 36
9 Impact of 2-DG treatment on B lineage cells in the spleen of BcN mice . . 38
10 Impact of 2-DG treatment on B lineage cells in the bone marrow of BcN mice 40
11 Combination of 2-DG and bortezomib on B lineage cells in spleen and bone marrow of BcN mice 42
12 Impact of 4 h and 24 h 2-DG treatment on plasma cells, B cells and non-B lineage cells 44
13 Reduced impact of 2-DG after mannose supplementation 46
14 Immunoglobulin concentration in the supernatant of 2-DG treated spleen cells 48
15 Impact of 2-DG and mannose treatment on plasma cells with distinct immunoglobulin classes 50
16 Comparing the impact of 2-DG and 2-FDG on plasma cells 52
17 Comparing the impact of hexokinase and phosphofructokinase inhibitors on B cells and plasmablasts 54
18 Impact of 2-DG treatment and glycosylation inhibition with tunicamycin on spleen plasma cells 56

Abbreviations

αKG	α-ketoglutarate
2-DG	2-deoxyglucose
2-FDG	2-fluorodeoxyglucose
2-NBDG	2-(N-(7-nitrobenz-2-oxa-1,3-diazol-4-yl)amino)-2-desoxyglucose
A405	Alexa Fluor 405
A488	Alexa Fluor 488
A647	Alexa Fluor 647
Acetyl-CoA	acetyl coenzyme A
ADP	adenosine diphosphate
AMPK	adenosine monophosphate-activated protein kinase
APC	antigen-presenting cell
APC	allophycocyanin
APC-Cy7	allophycocyanin-cyanine 7
APRIL	a proliferation inducing agent
ATP	adenosine triphosphate
B220	Protein tyrosine phosphatase receptor type C 220 kDa isoform
BAFF	B cell activating factor
BCMA	B cell maturation antigen
BcN	B6.NZM-Sle1$^{NZM2410/Aeg}$ Sle2$^{NZM2410/Aeg}$ Sle3$^{NZM2410/Aeg}$/Lmoj
BCR	B cell receptor
BL6	C57BL/6
BLIMP-1	B lymphocyte-induced maturation protein-1
BM	bone marrow
BSA	bovine serum albumin
BV421	Brillant Violet 421
BV510	Brillant Violet 510
BV605	Brillant Violet 605
BV711	Brillant Violet 711
BV785	Brillant Violet 785
CD	cluster of differentiation

CD138	syndecan-1
CD19	B-lymphocyte antigen
CD40L	CD40-ligand
CD43	leukosialin
CD95	Fas receptor
CTL	cytotoxic T lymphocyte
DB	dilution buffer
DC	dendritic cell
DMSO	dimethyl sulfoxide
EDTA	ethylenediaminetetraacetic acid
eGFP	enhanced green fluorescent protein
ELISA	Enzyme-linked Immunosorbent Assay
ETC	electron transport chain
FACS	fluorescences-activated cell sorting
FAD+/FADH	oxidised/reduced flavin adenine dinucleotide
FasL	Fas ligand
FcγR	Fcγ-receptor
FCS	fetal calf serum
FITC	fluorescein isothiocyanate
FOB	follicular B cell
FSC	forward scatter
G6P	glucose-6-phosphate
GAPDH	glyceraldehyde 3 phosphate dehydrogenase
GCB	germinal centre B cell
GDP	guanosine diphosphate
GlcNAc	N-acetylglucosamine
GLUT	glucose transporter
GPI	glycosylphosphatidylinositol
HK	hexokinase
HRP	horseradish peroxidase
i.p.	intraperitoneal
IgA	immunoglobulin A
IgD	immunoglobulin D
IgG	immunoglobulin G
IgM	immunoglobulin M

IL-10	interleukin 10
IL-4	interleukin 4
IL-6	interleukin 6
LAMP-1	lysosome-associated membrane protein 1
LLO	lipid-linked oligosaccheride
LLPC	long-lived plasma cell
LPS	lipopolysaccheride
M6P	mannose-6-phosphate
MACS	magnetic activated cell sorting
MHC	major histocompatibility complex
MPR	mannose-6-phosphate receptor
MTG	MitoTracker Green
mTOR	mammalian target of rapamycin
mTORC1	mTOR complex 1
MZB	marginal zone B cell
NAD+/NADH	oxidised / reduced nicotinamide adenine dinucleotide
NK	natural killer cell
Oxphos	oxidative phosphorylation
PAMP	pathogen-associated molecular patterns
PBS	phosphate-buffered saline
PE	phycoerythrin
PE-Cy7	phycoerythrin-cyanine 7
PFK	phosphofructokinase
PGI	phosphoglucose isomerase
PGK	phosphoglycerate kinase
PGM	phosphoglycerate mutase
PI3K	phosphoinositide 3-kinases
PK	pyruvate kinase
PRR	pattern recognition receptor
QTL	quantitative trait loci
ROS	reactive oxygen species
RT	room temperature
RPMI	Rosweel Park Memorial Institute
SLE	systemic lupus erythematosus
SLPC	short-lived plasma cell

SPF	special-pathogen-free
SSC	sideward scatter
TACI	Transmembrane activator and CAML interactor
TCA	tricarboxylic acid cycle
TCR	T cell receptor
Th1	Type 1 T helper cell
Th17	Type 17 T helper cell
TLR	Toll-like receptor
TP isomerase	triosephosphate isomerase
UDP	uracil-diphosphate
UPR	unfolded protein response
WB	washing buffer
XBP-1	X-box binding protein 1